Effect of chronic, low dose TCDD exposure on glucose homostasis and beta cell function in wild type and *Cyp1a1/1a2* systemic knock-out adult mice

by

Geronimo Parodi-Matteo

A thesis submitted to the Faculty of Graduate and Postdoctoral Affairs in partial fulfillment of the requirements for the degree of

Master of Science

in

Biology

Carleton University

Ottawa, Ontario

Abstract

Exposure to persistent organic pollutants (POPs) is associated with increased diabetic pathology. The goal of my thesis was to understand how chronic, low dose exposure to a model POP, 2,3,7,8-tetracholorodibenzo-*p*-dioxin (TCDD), promotes diabetic pathology in C57BL/6 mice and the role of Cyp1a1/1a2 enzymes during exposure. My first aim was to determine the effect of chronic, low dose TCDD exposure in wild type and systemic *Cyp1a1/1a2* knock-out mice on glucose homeostasis and β-cell function. My second aim was to determine the effects of direct, low dose TCDD exposure in isolated pancreatic islets with and without *Cyp1a1/1a2* gene deletion. My third aim was to determine the effect of concurrent high-fat diet (HFD) and TCDD exposure in wild type mice on glucose homeostasis and β-cell function. I found sex differences in the role of Cyp1a1/1a2 in insulin secretion during TCDD exposure *in vitro* and during concurrent TCDD exposure and HFD-feeding *in vivo*.

Acknowledgements

I dedicate my MSc thesis to my mother and hero, Maria Magdalena. To my father Stan and my brothers Diego and Alfredo, only through your love has this been possible.

To my friends Mutasem, Marcus, Eric, Ben, Menad, Lucas, Andrew, Phira, Simon, Anthony, Maryse, Rodrigo, Stephanie, thank you for always being there for me. To angel in heaven, Kristina, thank you for watching over me.

To my lover, Lina, who I found stealing NaCl from my lab one Saturday morning, you stole my heart. Thank you for your love, patience and support.

To all the professors who believed in me: Dr. Buist, Dr. Manthorpe, Dr. Smith, Dr. Hellemans, and Mrs. Munteanu. Thank you for inspiring me.

To all the members of the Bruin Lab past and present including Myriam, Erin, Noa, and Kayleigh, I could never thank you enough. You were there for me every time. A special thank you to my Morty, Salar, because Rick and Morty for 100 years.

To my thesis committee, Dr. Abizaid and Dr. Trudeau, thank for your insight and support which has guided me to this point. To my thesis supervisor and mentor, Jenny Bruin, thank you for constant guidance, patience, and always believing in me. I am forever grateful for this opportunity.

To all the animals who sacrificed their lives to make this research possible, thank you.

Table of Contents

List of Figures

List of Tables

List of Acronyms

AhR: Aryl hydrocarbon receptor

ANOVA: Analysis of variance

ATP: Adenosine triphosphate

AUC: Area under the curve

Ca^{2+}: Calcium

CO: Corn oil

CO_2: Carbon dioxide

CYP1A1: Cytochrome P450 1A1

ddH_2O: Double distilled water

ELISA: Enzyme-linked immunosorbent assay

ER: Endoplasmic reticulum

ERα: Estrogen receptor alpha

GCK: Glucokinase

GLUT: Glucose transporter

GSIS: Glucose stimulated insulin secretion

HFD: High-fat diet

IP_3: Inositol 1,4,5-trisphosphate

IRS: Insulin responsive substrate

ITT: Insulin tolerance test

K^+: Potassium

K_{ATP}: ATP-sensitive potassium channel

KO: Knock-out

mM: Millimolar

PBS: Phosphate buffered solution

PFA: Paraformaldehyde

PIP: Phosphatidylinositol 4-phosphate

PIP_2: Phosphatidylinositol 4,5-bisphophate

PIP_3: Phosphatidylinositol 3,4,5-trisphosphate

PKA: Protein kinase A

PLA_2: Phospholipase A_2

PLC: Phospholipase C

POP: Persistent organic pollutant

RIPE: Rat insulin promoter element

RR: Relative risk

SEM: Standard error of the mean

T1D: Type 1 diabetes

T2D: Type 2 diabetes

TCDD: 2,3,7,8-Tetrachlorodibenzo-*p*-dioxin

VGCC: Voltage gated calcium channel

WT: Wild type

XRE: Xenobiotic response element

CHAPTER 1: Introduction

1.1 Pancreatic β-cells

1.1.1 *β-cells & Insulin*

The pancreas is an organ of the digestive system composed of four major cell types: exocrine, endocrine, ductal, and connective cells (In't Veld & Marichal, 2010). Exocrine cells, the most numerous, are organized into acini (lobules) that secrete digestive enzymes into the pancreatic duct, which is joined with the bile duct to empty into the duodenum. Endocrine cells, including α-, β-, δ-, ε-, and pancreatic polypeptide-cells, assemble into clusters known as islets of Langerhans that secrete hormones in response to nutrient levels and metabolic needs. Pre-prandially, α-cells secrete glucagon, the primary catabolic peptide of the endocrine pancreas. Comprising the bulk of the islet, β-cells post-prandially release the main anabolic peptide, insulin. The *insulin* gene encodes for a 110-amino acid precursor, preproinsulin, that translocates from the rough endoplasmic reticulum (ER) membrane to the ER lumen. Rodents have two copies of the *insulin* gene (*Ins1* and *Ins2*) differing in number of introns and location on the chromosome while humans maintain one copy (Shiao et al, 2008). In the lumen, preproinsulin is cleaved to proinsulin (Patzelt et al, 1978), folded into a tertiary structure (Huang and Arvan 1995), and packaged into vesicles termed 'granules' (Rhodes and Halban 1987). Granules require acidification (Orci et al, 1986) and cleavage of proinsulin into insulin and C-peptide (Davidson et al, 1987) with insulin granules occupying roughly 10% of the β-cell (Dean 1973). Insulin monomers oligomerize into hexamers by coordinating with two Zn^{2+} atoms to afford mature insulin (Smith et al, 2003).

Following an increase in blood glucose and intracellular β-cell glucose, insulin is secreted into the blood, dissociating into its active monomeric due to diffusion and electrostatic repulsion (Fu et al, 2013). Insulin binds to its receptor, the insulin receptor, that acts as an intracellular tyrosine kinase to phosphorylate insulin responsive substrates 1 (IRS1) and 2. IRS proteins are kinases that phosphorylate a host of enzymes including phosphatidylinositol 3-kinase to produce phosphatidylinositol 3,4,5-trisphosphate (PIP_3) to account for the mitogenic effects of insulin in skeletal muscle and glycogenesis in the liver (Copps and White, 2012). As a result of chronic hyperglycemia phenotypic of diabetes, there is a compensatory increase in insulin secretion (Del Prato and Tiengo, 2001). Over time, insulin receptor expression is upregulated leading to a decrease of insulin action at target tissues, namely skeletal muscle and the liver, termed insulin resistance. With insulin resistance, β-cell mass increases to produce more insulin as a final method of compensation.

1.1.2 *β-Cell Transcription Factors*

Transcription factors that regulate insulin synthesis and secretion bind to discrete sequences elements, A, C, E, Z, and CRE, spanning the insulin gene promoter region (Hay and Docherty, 2006). Exclusively expressed in β-cells, *Pdx-1* binds to A elements to regulate insulin gene expression and determine pancreatic fate (Ohlsson et al, 1993). Mice lacking *Pdx-1* have arrested pancreatic development at the early post-bud stage (Jonsson et al, 1994) and mutations to the *PDX-1* gene in humans is associated with type 2 diabetes (T2D) (Staffers et al, 1997). *PAX-6* is expressed in all endocrine cells and binds to the C elements of the insulin promoter region to transactivate insulin, glucagon,

and somatostatin (Zhao et al, 2005). Genetic ablation of *Pax-6* in mice leads to decreased islet numbers and α-cell mass (Sander et al, 1997) while heterozygous mutations in humans are associated with eye abnormalities and glucose intolerance (Yasuda et al, 2002). Another element that binds to C elements is *MafA* which is part of a heteromeric protein complex, rat insulin promoter element 3b1 (RIPE3b1) and RIBE3b2, which is necessary for β-cell differentiation and maturation (Khattabi and Sharma, 2015). Homozygous MAFA KO mice are hyperglycemic at fasting and have severely impaired insulin secretion to glucose and non-glucose secretagogues both *in vivo* and *ex vivo* but have normal total insulin content (Zhang et al, 2005).

NKX6.1 is a repressor on the glucagon promoter and is necessary for adequate glucose-stimulated insulin secretion (GSIS) along with β-cell maturation (Schisler et al, 2005). In cooperation with *Pdx-1*, *Nkx6.1* inhibits β- to α-cell conversion (Schaffer et al, 2013). Functional *Nkx6.1* KO mice developed hyperglycemia and hypoinsulinemia, had impaired GSIS, and developed markers of δ-cell identity (Taylor et al, 2013a) and variants to *NKX6.1* were associated with increased T2D incidence in one human cohort (Yokoi et al, 2006). BETA2, also known as NEUROD1, is expressed in enteroendocrine cells as well as α- and β-cells and binds to the E element to regulate insulin expression (Naya et al, 1997). *Beta2* is necessary for islet maturation and maintaining adequate insulin levels as mice with homozygous mutations to the gene had underdeveloped islets, decreased β-cells, were severely diabetic and died perinatally (Naya et al, 1997). In line with these data, heterozygous mutations to *BETA2* in humans is associated with T2D (Malecki et al, 1999).

1.2 Mechanisms of Nutrient-Stimulated Insulin Secretion

1.2.1 *Glucose-Stimulated Insulin Secretion*

Post-prandially, glucose is taken in to pancreatic β-cells by glucose transporters, GLUT-1 in humans and GLUT-2 in rodents. Glucose is subsequently phosphorylated by glucokinase (GCK), a subtype of hexokinase, the low affinity rate-limiting enzyme in β-cell glucose utilization (Meglasson and Matschinsky, 1986). Phosphorylation of glucose by GCK inhibits the molecule from exiting the cell thereby committing it to being metabolized. Passing through the glycolytic, citric acid cycle and mitochondrial oxidative phosphorylation pathways, glucose influx increases the cytoplasmic ATP:ADP ratio, prompting the closure of ATP-sensitive K^+ channels (K_{ATP}) and leading to membrane depolarization (Ashcroft et al, 1984). Pancreatic β-cells accommodate approximately 60 different ion channels with the majority situated on the membrane and some intracellular (Yang et al, 2014). The resting potential, approximately -70 mV (Ashcroft and Rorsman, 1989), of β-cells is maintained by K_{ATP}-channel mediated K^+ efflux (Aguilar-Bryan and Bryan, 1999). The β-cell K_{ATP}-channel is activated by plasma membrane phospholipids such as phosphatidylinositol 4-phosphate (PIP), phosphatidylinositol 4,5-bisphophate (PIP_2), and PIP_3 (Fan and Makielski, 1997; Hilgemann and Ball, 1996; Krauter et al, 2001). That is, the presence of these phospholipids aid in stabilizing the open state of the K_{ATP}-channel by physically adhering to a distinct binding site (Stansfeld et al, 2009) as well as counteracting the closing effects of ATP. The closure of K_{ATP}-channels is the first step in initiating GSIS.

During development, insulin secretion is monophasic whereas adult β-cells secrete insulin in a biphasic manner in response to an increase in glucose concentration

(Newshome et al, 2010). That is, fetal β-cells present only one response to changes to glucose concentrations whereas adult β-cells have a multiphasic response with a 'first-phase' and 'second-phase' insulin secretion. The predominating notion is that the 'first-phase' response is K_{ATP}-dependent while 'second-phase' is a K_{ATP}-independent pathway (Straub and Sharp, 2002). First-phase insulin occurs 1-2 minutes after intravenous glucose injection and lasts approximately 10 minutes. This is followed by a second-phase insulin secretion that can lasts up to 120 minutes or the duration of the hyperglycemia (Pfeifer et al, 1981). First-phase insulin secretion is not affected by basal, pre-stimulus glucose levels while second-phase is (Pfeifer et al, 1981). In this way, the higher the pre-stimulus glucose concentration, the stronger the second-phase insulin response. First-phase insulin release is dependent on a readily-releasable pool of insulin granules that account for approximately 5% of all insulin granules in the 'reserve' pool whereby the rest is sequestered for the sustain second-phase insulin response (Rorsman and Renström 2003).

Following the closure of β-cell K_{ATP}-channels, the change in membrane potential opens voltage-gated Ca^{2+} channels (VGCC) increasing intracellular Ca^{2+} influx. VGCCs account for the depolarization phase of the action potential and Ca^{2+} acts as a secondary messenger to trigger insulin secretion. VGCCs are positively regulated by protein kinases including protein kinase A (PKA) (Hall et al, 2007; Sang et al, 2016) and their density and activity are modulated by growth factors through tyrosine kinase receptors (Rosenbaum et al, 2001; 2002). Equally important as extracellular Ca^{2+} influx during GSIS is intracellular release of the cation from the ER stores (Gilon et al, 2002). Activated by the increase in intracellular Ca^{2+}, phospholipase C (PLC) hydrolyzes PIP_2 into inositol 1,4,5-

trisphosphate (IP_3) and diacylglycerol. The former will bind to IP_3 receptors (IP_3Rs) on the ER to release intracellular Ca^{2+} into the cytoplasm and the latter activates PKC (Zawalich and Zawalich, 1996). The PLC/PKC pathway is tied second-phase insulin secretion by increasing PIP_2 hydrolysis and promoting PKC translocation from the cytosol (Ganesan et al, 1990; 1992). Parallel to the IP_3Rs, ryanodine receptors are also present in the β-cell ER and are activated by increases in intracellular Ca^{2+} (Ca^{2+}-induced Ca^{2+} release) to release further intracellular stores of Ca^{2+} into the ER. To mediate exocytosis of insulin granules, β-cell VGCCs physically associate with exocytotic proteins including syntaxin 1A (Yang et al, 1999), SNAP-25, and synaptotagmin (Wiser et al, 1999). In this way, VGCCs in β-cells serve to couple changes in intracellular Ca^{2+} concentrations to insulin granule exocytosis.

Bringing about the hyperpolarization phase of the action potential are $K_v2.1$ channel-mediating a K^+ efflux (Jacobson and Philipson, 2007). Genetic ablation of the channel in mice results in significantly lower fasting blood glucose combined with heightened GSIS (Jacobson et al, 2007a). Furthermore, this channel may be regulated by the phospholipase A_2 (PLA_2) pathway. Mice genetically overexpressing PLA_2 not only display lower fasting blood glucose, higher basal insulin, heightened insulin secretion following an *in vivo* or *ex vivo* glucose challenge, but also an attenuated $K_v2.1$ current (Bao et al, 2008). Moreover, micromolar quantities of arachidonic acid has been shown to decrease $K_V2.1$ current in INS-1E cells, HEK cells, along with isolated mouse and human islets while increasing intracellular Ca^{2+} (Jacobson et al, 2007b). These data highlight the role of K^+ channel in acting as the 'brake' during GSIS depolarization event.

1.2.2 *Lipid-Stimulated Insulin Secretion*

While glucose is the primary insulin secretagogue, lipids also modulate GSIS. Concomitant exposure to millimolar quantities of palmitate and glucose (15 mM) potentiates GSIS in isolated female murine islets compared to glucose alone (Olofsson et al, 2004) although results using immortalized β-cells are heterogenous (MIN6 cells: Watson et al, 2011; INS-1E cells: Maris et al, 2012). Cholesterol has also been shown to be involved in GSIS as mouse islets incubated micromolar quantities of a squalene epoxidase inhibitor, an enzyme involved in the biosynthesis of cholesterol (Gill et al, 2011), produced less insulin during high glucose exposure (Xia et al, 2008). This same effect was also observed in INS-1E cells (Hao et al, 2007). Furthermore, linoleic acid has been implicated in stimulating insulin secretion, reducing K_{ATP} channel currents and increasing intracellular Ca^{2+} in MIN6 cells mediated by the GP40 receptor (GPR40) (Feng et al, 2006; Itoh et al, 2003). The GPR40 binds to medium- to long-chain fatty acids, increases intracellular Ca^{2+} following ligand binding (Briscoe et al, 2003), and its inhibition prevents linoleic acid-mediated potentiation of GSIS (Salehi et al, 2005) as well as palmitate (Shapiro et al, 2005). As a result, the action of lipids on GSIS is speculated to be mediated by the GPR40 and have a direct effect in modulating glucose and insulin homeostasis. Indeed, a diet rich in high-fat foods, known as a high-fat diet (HFD), is associated with weight gain, glucose intolerance, insulin resistance and development of T2D in humans (Nagao et al, 2015). In animal models, a HFD typically consists of 35-60% of the total calories being derived from fat. *In vivo*, HFD-fed rodents display similar changes to weight, glucose and insulin sensitivity as humans (Buettner et al, 2007) while data from *ex vivo* (isolated pancreatic islets) is heterogenous (Ahrén et al, 1997; 1999;

Briaud at el, 2002). Taken together, these data indicate that lipids directly affect insulin secretion and an increase in lipid consumption can promote diabetic pathology.

1.3 Diabetes Mellitus

Diabetes mellitus is a group of chronic metabolic diseases characterized by hyperglycemia and insulin resistance, which can lead to eye, kidney, nerve and vascular complications (American Diabetes Association 2010). An estimated 415 million people in the world suffer from diabetes in 2015 and by 2040 that number is expected to reach 642 million (International Diabetes Foundation 2015). In general, insulin secretion and/or action is diminished stemming from (but not limited to) autoimmune destruction of pancreatic β-cells in type 1 diabetes (T1D) or over-nutrition and/or sedentary lifestyle in T2D. As a result, both disorders produce post-prandial hyperglycemia with T1D patients being dependent on chronic insulin administration and T2D on blood glucose management therapies. Accounting for 90% of diabetes incidence, T2D is characterized by one of two phenotypes: compensated noninsulin-dependent diabetes and decompensated noninsulin-dependent diabetes. In the former, the fasting plasma glucose is 115-200 mg/dL with the normal physiologic range of plasma glucose in humans is 80 – 200 mg/dL (Pfeifer et al, 1981). If fasting plasma glucose is above 115 mg/dL during following a bolus of glucose, individuals will typically display impaired first-phase insulin secretion (Brunzell et al, 1976). Individuals with fasting glucose above normal physiological range but below 200 mg/dL will have a normal second-phase insulin response and respond normally to non-glucose insulin secretagogues such as lipids and amino acids (Pfeifer et al, 1981). A fasting plasma blood glucose of 300 mg/dL is

considered decompensated noninsulin-dependent diabetes and is associated with impaired first-phase and second-phase insulin secretion. In early T2D, individuals will initially be hyperinsulinemic as a response to chronic hyperglycemia proceeded by a deficit in first-phase insulin and enhancement of second-phase insulin secretion as the pathology progresses (Del Prato and Tiengo, 2001). In contrast, individuals living with T1D have severely impaired insulin secretion leading to hyperglycemia, proteolysis, lipolysis and ketosis (Atkinson et al, 2015). Global incidence of T1D and T2D is rising dramatically yet the underlying pathogenesis remains to be elucidated. We hypothesize that increased production and exposure to synthetic, organic materials may be a possible culprit for diabetes pathogenesis (Neel and Sargis, 2011).

1.4 TCDD and the AhR Pathway

1.4.1 *POPs & TCDD*

Dioxins are a family of polyaromatic hydrocarbons that include dibenzo dioxins, dibenzo furans and biphenyls, along with their polyhalogenated derivatives (Mandal 2005). This class of synthetic, organic chemicals belong to the persistent organic pollutants (POPs) due to their lipophilicity and ability to resist degradation. As a result, these chemicals accumulate in soils, dust, and may permeate into wildlife and foods. Exposure to polycholorinated dibenzo dioxins (PCDDs) occurs through contaminated vegetables and seafood, accidents involving the manufacture of polychlorophenols, air pollution from waste incineration, as well as natural sources such as volcanoes and forest fires (Chobtang et al, 2011). The most toxic dioxin is 2,3,7,8-tetrachlorodibenzo-*p*-dioxin

(TCDD) owing to its ability to most potently induce transcription of the cytochrome P-450 1A1 (CYP1A1) mRNA (Durrin et al, 1987). TCDD is a by-product of the synthesis of many different polychlorophenols used as herbicides, fungicides, and disinfectants (Poland and Knutson, 1982). Operation Ranch Hand (1961-71) during the Vietnam War employed Agent Orange as a defoliant composed of chlorophenols including 2,4,5-trichlorophenoxyacetic acid and 2,4-dichlorophenoxyacetic acid contaminated with TCDD (Veterans and Agent Orange, 2012). While governments worldwide have taken considerable precautions to reduce production of dioxins and their parent compounds in the last four decades, dioxins remain a concern as they persist in our food supply and environment. TCDD remains a model chemical to study the effects of POPs on mammals.

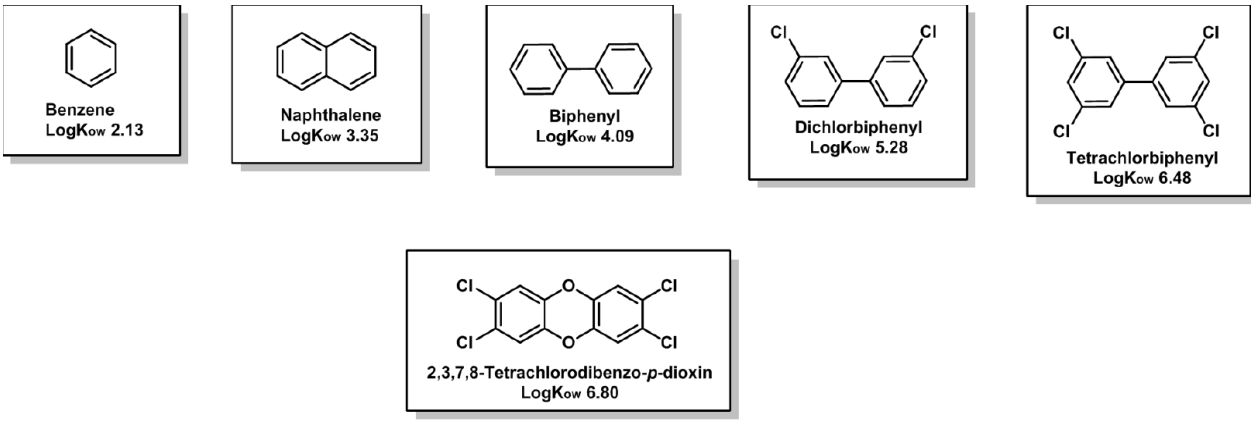

Figure 1.1: Examples of persistent organic pollutants, including TCDD, with associated partitioning coefficient ($LogK_{ow}$).

1.4.2 *Cellular Transport of TCDD*

Owing to its highly lipophilic character ($\log K_{ow}$= 6.8; National Toxicology Program 2006), TCDD is speculated to passively diffuse across the lipid bilayer into the cytosol of mammalian cells. Once in the cytosol, TCDD interacts with the aryl hydrocarbon receptor (AhR; Mimura and Fujii-Kuriyama, 2003). The AhR is part of the basic helix-loop-helix Per, Arnt/AhR, Sim homology gene family (Gu et al, 2000) and, in the absence of a ligand, associates with heat shock protein 90 (Hsp90), hepatitis B virus X-associated protein (XAP2) and p23. When TCDD binds to the AhR, the receptor is sequestered to the nucleus where it dissociates from Hsp90 and heterodimerizes with AhR nuclear translocator (ARNT, also known as hypoxia inducible factor 1β). The AhR/ARNT heterodimer goes on to recognize an enhancer DNA element, the xenobiotic/dioxin response element (XRE or DRE), and promote transcription of CYP450 enzymes including *CYP1A1* and *CYP1A2* (Durrin et al, 1987), transforming growth factor-β (Zaher et al, 1998), interleukin 1-β (IL-1β; Henley et al, 2004), plasminogen activator inhibitor-1 (Son and Rozman, 2002), p27 (Kolluri et al, 1999), and Fos and Jun (Hoffer et al, 1996).

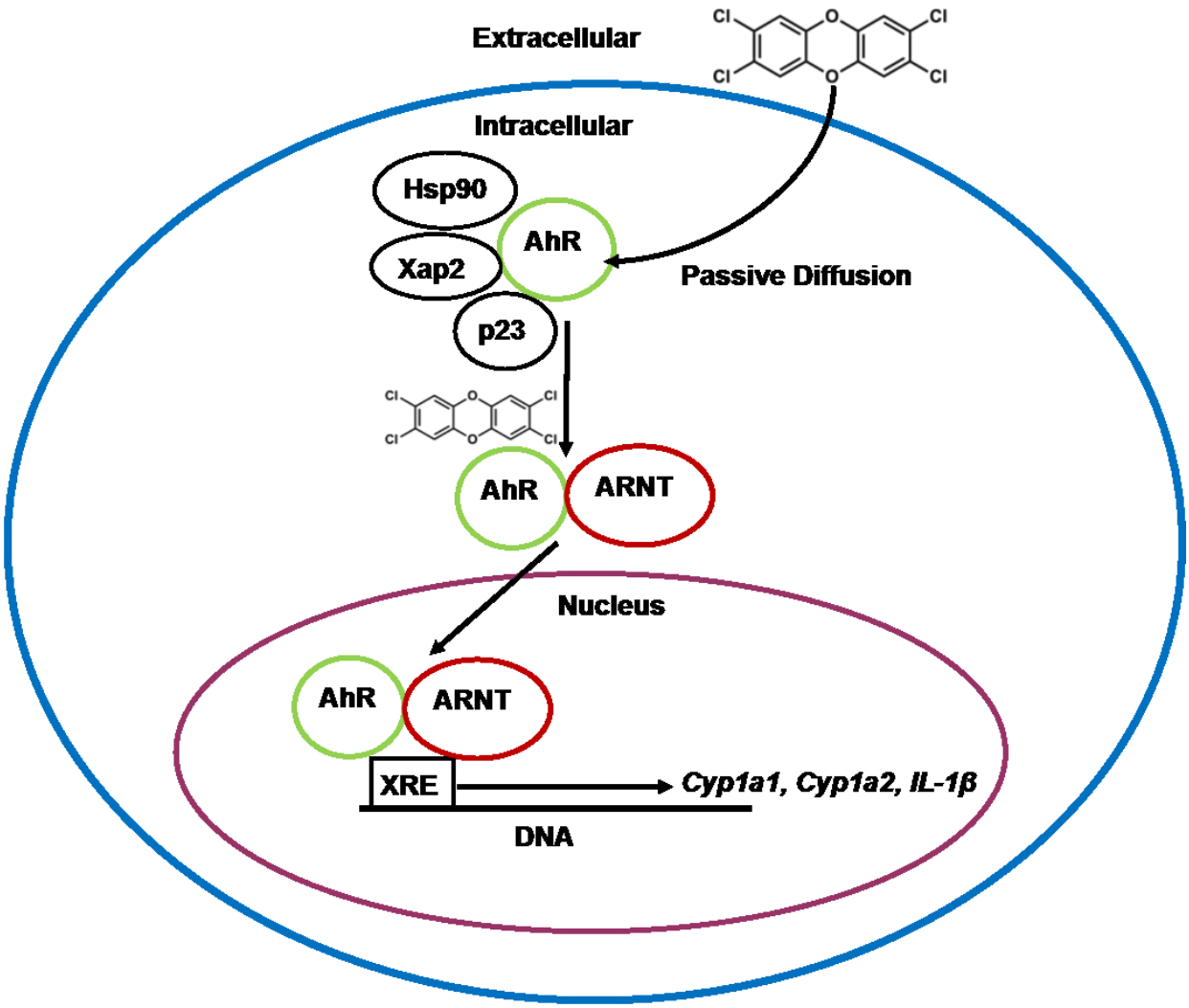

Figure 1.2: Aryl hydrocarbon receptor pathway following TCDD exposure.

1.5 Human TCDD Exposure

1.5.1 *Adsorption, Distribution, Metabolism, and Excretion of TCDD in Humans*

Viktor Yushchenko was poisoned with TCDD-contaminated food in 2004 and the elimination of the compound was studied over three years (Sorg et al, 2009). Sorg and colleagues observed similar first-order decay curves of TCDD between serum lipids and

subcutaneous fat suggesting an equilibrium state between the two compartments. In other words, TCDD was equally distributed across serum lipids and subcutaneous fat and was eliminated approximately in the same amount of time. Over the three years, approximately 250 μg of TCDD was estimated to be eliminated primarily in the feces. Previous data by Poiger and Schlatter (1986) using a 42 year-old volunteer ingesting 105 ng of [^{3}H-TCDD] also support that elimination follows first-order kinetics and occurs almost exclusively via the alimentary route. Furthermore, two metabolites of TCDD were identified in the urine and feces (but not fat or skin) of Viktor Yushchenko: 2,3,7-trichloro-8-hydroxydibenzo-*p*-dioxin and 1,3,7,8-tetrachloro-2-hydroxydibenzo-*p*-dioxin. These findings are line with those of Poiger and colleagues (1982) in rodents supporting the enzymatic epoxidation of TCDD across the 1,2 carbons and subsequent hydroxyl-chlorine rearrangement or chlorine elimination. The metabolites accounted for 38% of the total 250 μg suggesting that the majority of TCDD remained unmetabolized as it was eliminated. The half-life of TCDD was determined to be 15.4 months, which is low with respect to previous reports. The single, low dose exposure experiment by Poiger et al (1986) produced a half-life of 4.5-years whereas chronic, low dose exposure studies involving Operation Ranch Hand veterans (Michalek et al, 1999; Pirke et al, 1989) and the Seveso disaster victims was 7-10 years (Bertazzi et al, 1999). These data support the inverse hypothesis of half-life with tissue distribution such that greater TCDD exposure is associated with a shorter half-life, possibly due to increased metabolism and elimination of TCDD.

1.5.2 *Human TCDD Exposure and Diabetes*

In 1972, the variation in T2D was speculated to be associated with POP disposal (Great Lakes Water Quality Agreement, 1972). In other words, individuals living near sites heavily contaminated with POPs would be more at risk of developing T2D due to their chronic exposure. While this speculation is tempting giving the drastic rise in T2D in North America (International Diabetes Foundation 2015), no mechanism was proposed to explain the how POP exposure led to the development of T2D. Veterans of Operation Ranch Hand, occupationally exposed to low doses of TCDD, had an average relative risk (RR) of 1.5 for T2D (Henriksen et al, 1997; Kang et al, 2006; Michalek et al, 1999; Michalek and Pavuk 2008). These findings are paralleled by those from the population living closest to the disaster site at Seveso, the location of a TCDD spill where approximately 1 kg of the chemical was released into the environment (Bertazzi et al, 1999; Bertazzi and di Domenico 2003; Consonni et al, 2008). In particular, one follow-up study reported that only women who were 12 years old or less at the time, living nearest to the disaster site were at any risk (RR 2.03) to develop T2D (Warner et al, 2013). Data from TCDD exposed polychlorophenol manufacturers (Vena et al, 1998; Calvert et al, 1999), Korean Vietnam War veterans (Joung-Soon et al, 2003), and individuals eating TCDD-contaminated food (Wang et al, 2008) also support a modest yet consistent increased RR to develop T2D associated with dioxin exposure.

Lee and colleagues observed a modest positive dose-dependent response between serum concentration of different POPs and RR for T2D as part of the National Health and Examination Survey from 1999-2002 (Lee et al, 2006), along with some evidence for insulin resistance (Lee et al, 2007). Focusing solely on PCDDs within the same cohort,

Everett et al found that serum levels of dioxins were positively associated with increased risk to develop T2D (Everett et al, 2007). Interestingly, re-analysis of Operation Ranch Hand veterans supports an inverse hypothesis of TCDD exposure. Diabetic pathology is associated with dyslipidemia and the release of lipids from the liver (Ginsberg et al, 2005). Given that TCDD is highly lipophilic, this may promote higher serum dioxin levels as the disease progresses and more TCDD is released from lipid stores (Kerger et al, 2012). This provides a methodological challenge in measuring dioxin concentrations over time in exposed populations as the change in BMI can affect serum concentrations of TCDD. It must be noted that the data surrounding T2D prevalence and dioxin exposure is heterogenous and several studies have found no association between serum dioxin concentration and/or exposure with T2D prevalence (Collins et al, 2009; Karouna-Renier et al, 2007; Steenland et al, 1999; Warner et al 2013). While some of the differences in results are likely to emerge from differences in methodologies, and some contemporary reviews support the association between dioxin exposure and T2D (Magliano et al, 2014; Taylor et al, 2013b), it is modest. At-risk populations considered 'pre-diabetic' (hyperglycemia, high BMI, blood pressure, and blood cholesterol; Bansal 2015) may be more vulnerable to TCDD-elicited metabolic dysfunction. This notion is akin to the second-hit hypothesis whereby an initial insult (in this case, TCDD exposure) may not be sufficient to promote pathology until paired with a secondary insult such as pre-existing disease or deleterious lifestyle choices such as poor diet and remaining sedentary. Therefore, further research into dioxin exposure and effects on key metabolic markers such as blood glucose and insulin in pre-diabetic populations is warranted to accurately establish its propensity to cause diabetes in exposed populations.

1.6 TCDD Exposure in Mammalian Models

1.6.1 *Absorption, Distribution & Excretion of TCDD in Animals*

Allen et al (1975) administered 50 µg of [^{14}C]-TCDD to rodents via gastric intubation and sacrificed animals at different time points up to 21 days following exposure. TCDD-treated rodents had excessive hair loss, hypophagia, lost an average of 37% of their weight, had gross thymic atrophy, and died within 25 days of exposure. Notably, the authors found no changes in blood cell composition, total serum lipids, cholesterol, triglycerides, serum protein, or albumin/globulin ratio. Approximately 75% of the dose was adsorbed via the gastrointestinal tract as the radioactivity of the tissue decreased dramatically after the first day. The liver had the highest distribution with 75% of the administered dose deposited, resulting in a radioactivity 6-7 times greater than other tissues. Specifically, the bulk of the radioactivity was found in the microsomes along with reduced esterase, glucose-6-phosphatase and unspecific CYP450 activity in the microsomal fraction. While other authors have reported that activity of CYP450 enzymes (Lucier et al 1973) increased up to 16 days post-exposure, albeit with smaller doses (0.2-0.5 µg), activity reportedly decreased thereafter. The increase in hepatic metabolic enzymes coincide with the hepatomegaly and steatosis noted after 21 days, suggesting that liver sequesters TCDD, leading to hepatotoxicity. Approximately 25% of the radiolabelled TCDD was excreted in the feces within the first three days followed by 1-2% daily excretion throughout the subsequent 18 days. By day 21, the authors noted that 52% of the initial TCDD radioactivity was excreted. In contrast, only a total of 4.5% of the radioactivity was detected in the urine suggesting that the bulk of the excretion occurs via the alimentary route. Interestingly, the radioactivity of the urine almost doubled (from 0.25% to 0.43%)

by day 21. When all distribution of all tissues was account for, approximately 90% of the administered radiolabelled TCDD was excreted. In line with previous data (Piper et al, 1973), Allen and colleagues reported a half-life of 16.3 days when plotting total radioactivity in the entire body while 21.3 days when considering the amount excreted in the feces, in line with previous reports using oral exposure (Rose et al, 1976). In comparison to human half-life estimates following acute, high TCDD exposure (15 months, see Sorg et al, 2009), rodents have a much shorter half-life indicative of differences in adsorption and excretion.

1.6.2 *TCDD Metabolism in Mammalian Models*

The CYP450 family, including CYPA through CYPF, of enzymes contribute to the bulk of phase I metabolism in mammals and generally oxidize substrates to increase water solubility and excretion (Guengerich 2008). While involved in a variety of endogenous and exogenous small molecule metabolism, members of the CYP450, specifically the CYP1A1, contribute to bioactivation of toxins. For example, the CYP1A1 metabolizes aflatoxin to produce an exo-8,9-epoxidated intermediate that is highly electrophilic and intercalates with DNA to be a potent genotoxin (Kobertz et al, 1997). As previously mentioned, although TCDD produces an epoxidated electrophilic intermediate, there is no evidence to support that it is genotoxic (Giri 1986). Although TCDD exposure increases *Cyp1a1* mRNA transcription, this isoform of the Cyp 450 enzyme is not thought to metabolize TCDD. Indeed, work by Diliberto and colleagues (1997) supports the role of the Cyp1a2 as being causal in liver sequestering. In mice administered 25 μg/kg [^{3}H]-TCDD once orally, the authors noted significantly lower liver/fat concentration of dioxin in

Cyp1a2 KO mice compared to C57BL/6 mice. Based on these data, the authors propose that Cyp1a2 is the TCDD binding protein in the liver.

Poiger and colleagues (1982) administered 5.4 mg (4 times over two weeks) of [^{3}H]-TCDD intraperitoneally to a canine resulting in emesis, anorexia, cachexia, and death two weeks post-initial exposure. Compared to rodents, dogs reach a maximum concentration in the bile within 1-2 days as opposed to 2-7 days. Three days following the last dose of TCDD, radioactivity of the bile was 8% of the amount administered. Given that only 2% was excreted after the first dose, this suggests that TCDD exposure increases its own metabolism inferring an increase in the transcription of metabolic enzymes. A bile sample was used to extract the metabolites of TCDD yielding 50% radioactivity and treatment with glucuronidase or arylsulfatase did not increase extractability suggesting that TCDD does not undergo second-phase metabolism. A major metabolite of TCDD, 1,3,7,8-tetrachloro-2-hydroxy-dibenzo-*p*-dioxin, was identified along with minor metabolites including 2,3,7-trichloro-8-hydroxy-dibenzo-*p*-dioxin. This compound is further metabolized into isomers of trichloro-dimethoxydibenzo-*p*-dioxin via epoxidation and chlorine rearrangement. Alternatively, TCDD can undergo cleavage via epoxidation of one or both ethers to afford a tetrachloro-dimethoxydiphenylether metabolite and 1,2-dichloro-4,5-dimethoxybenzene, respectively. Using isolate rat hepatocytes incubated with radiolabelled TCDD, Sawahata et al (1982) also identified hydroxylated metabolites of TCDD, namely 1-hydroxy-2,3,7,8-tetrachlorodibenzon-*p*-dioxin and 8-hydroxy-2,3,7-trichlorodibenzo-*p*-dioxin, in line with Poiger and colleagues (1982). However, Sawahata and colleagues (1982) employed glucuronidase and found increased radioactivity in the hepatic microsome extract suggesting that TCDD may undergo glucuronate conjugation.

Importantly, the metabolites identified in animals parallel those found in humans, specifically, 1,3,7,8-tetrachloro-2-hydroxy-dibenzo-*p*-dioxin and 2,3,7-trichloro-8-hydroxy-dibenzo-*p*-dioxin. Given that the same hydroxylated metabolites are found across mammals, this indicates animal models of TCDD metabolism are relevant to human exposure and likely involve the similar CYP-mediated metabolism with little evidence to support second-phase metabolism.

1.6.3 *Effects of TCDD on Mammalian Models*

In animal models a single high dose of TCDD, typically 20 – 200 μg/kg (see Poland and Knutson, 1982), produces a wasting syndrome characterized by progressive loss of weight and adipose tissue up to 50% (McConnell 1980). Common symptoms following an acute, high dose of TCDD include hypophagia (Seefeld et al, 1984), hypertriglyceridemia (Swift et al, 1981), hypoinsulinemia (Ebner et al, 1988), reduced adipose lipoprotein lipase activity (Brewster and Matsumura, 1984; Olsen el al, 1998) and decreased fasting blood glucose (Chapman and Schiller, 1985). The death associated with high doses of TCDD is not directly linked to the wasting syndrome as rodents fed by gastric intubation gain weight but still die two weeks post-exposure (Gasiewicz et al, 1980). Rather, it is speculated that the lethality of TCDD in animals stems from its interference with the utilization of nutritional macronutrients (De Tata 2014). TCDD promotes thymic and lymphoid atrophy across several species (Buu-Hoi et al, 1972; Gupta et al, 1973, McConnell et al, 1978a; Vos et al, 1980), hepatomegaly (Kociba et al, 1979; McConnell 1980), gastric lesions in primates (Allen and Norback 1973) but not rodents (McConnell et al, 1978a), chloracne (Inagami et al, 1969; McConnell et al, 1978b), urinary tract

hyperplasia (McConnell et al, 1978a; 1978b) and a variety of neoplasms across different mammals (Kociba et al, 1978). Finally, TCDD increases expression of F4/80, a marker of macrophage activation, in the liver (Fader et al, 2015; 2017) and vascular tissues (Wu et al, 2011), supporting its role in activating the immune system.

If glucose transporter expression is significantly decreased, the sensitivity of the pancreatic β-cell to glucose decreases due to the diminished ability of the cell to intake glucose. As a result, GSIS is compromised as β-cells lose their ability to sense changes in blood glucose levels (Orci et al, 1990; Thorens et al, 1990; Valera et al, 1994). TCDD decreases glucose uptake in adipose, liver, gut, brain, and pancreas (Enan and Matsumura, 1994; Ishida et al, 2005), along with the brain *in vivo* (Liu and Matsumura, 1995) as well as *in vitro* (Liu and Matsumura, 2006; Nagashima and Matsumura 2002; Tonak et al, 2007). Following a single dose of TCDD (1 μg/kg) by intraperitoneal (i.p.) injection, male rats showed no difference in fasting plasma glucose, insulin, triglycerides, or leptin levels, whereas free fatty acids were increased (Novelli et al, 2005). Interestingly, insulin secretion from isolated islets of TCDD-treated rodents was decreased compared to controls and uptake of a non-metabolized radio-labelled glucose analogue, [^{3}H]-2-deoxy-glucose, was also decreased in pancreatic tissue indicating lower glucose absorption. Furthermore, Kurita and colleagues treated male C57BL/6 mice with one dose of TCDD (10 μg/kg, i.p.) and observed a similar impairment of insulin secretion *ex vivo* 60 minutes after incubation in high glucose (Kurita et al, 2009). Moreover, TCDD decreased plasma insulin *in vivo* 60 and 120 minutes following a glucose bolus 24 hours post-TCDD exposure. Unlike wild type littermate controls, TCDD exposure did not impact insulin secretion in AhR KO mice *in vivo* or *in vitro*. These findings support that TCDD exposure

produces hypoinsulinemia and that its action requires a functional AhR signaling pathway to influence insulin secretion in rodents. Taken together, these data warrant further research into the effects of chronic, low dose TCDD exposure akin to that seen in human epidemiological data on blood glucose homeostasis and markers of β-cell function. In this way, the role of TCDD in promoting diabetic pathology can be elucidated.

1.7: Overall Goal and Specific Aims of Thesis

The overarching goal of my thesis is to understand the mechanism by which chronic, low dose TCDD exposure promotes diabetic pathology in C57BL/6 mice and the potential role of the Cyp1a1/1a2 enzymes in mediating this effect. I hypothesize that chronic, low dose TCDD exposure will promote diabetic-like pathology in adult mice. Furthermore, I hypothesize that Cyp1a1/1a2 enzymes are protective during chronic, low dose TCDD exposure.

Specific Aim 1 (CHAPTER 3): Global incidence of T2D is increasing and the cause(s) remain to be elucidated. Exposure to POPs has been associated with an increase in relative risk to develop T2D and TCDD is speculated to be the among the most harmful of the POPs to health in mammals. Exposure to the dioxin is strongly associated with induction of the CYP1A1 metabolic enzymes whose role in the pathogenesis of T2D is unknown. **My first aim is to determine the effect of chronic, low dose TCDD exposure in wild type and systemic *Cyp1a1/1a2* KO mice on glucose homeostasis and β-cell function.**

Specific Aim 2 (CHAPTER 4): The pancreatic islet contains endocrine cells that secrete hormones in response to changes in blood nutrient levels. Specifically, β-cells secrete the anabolic hormone insulin in response to increases in blood glucose and deficits in insulin secretion are central to diabetic pathology. The impact of TCDD exposure to the pancreatic islet and the β-cell are important in determining how the dioxin causes T2D. Furthermore, the role of CYP1A1 in the pancreatic islet both constitutively and during TCDD exposure is not well understood as either protective or deleterious. **My second aim is to determine the effect of direct, low dose exposure on isolated pancreatic islets with and without *Cyp1a1/1a2* deletion.**

Specific Aim 3 (CHAPTER 5): The composition of our diet is integral to blood glucose management. A diet in which fat consumption is in excess with respect to carbohydrates is strongly associated with hyperglycemia and the development of T2D. TCDD exposure is associated with a modest increase in T2D, but the effects of diet in conjunction with dioxin exposure are not known. Termed a 'double hit', the effects of a HFD during dioxin exposure with regard to blood glucose homeostasis and β-cell function are speculated to be more deleterious than either in isolation. **My third aim is to determine the effect of concurrent HFD and chronic, low dose TCDD exposure in wild type mice on glucose homeostasis and β-cell function.**

CHAPTER 2: General Methods

2.1 *Islet Isolation & Pancreatic Dissection*

Mice were anaesthetized with inhalable isoflurane (3-5%, 1 L/min) and euthanized by cervical dislocation. The abdomen was opened to expose the pancreas and bile duct. A clamp (Fine Science Tools, Cat: 18052-01) was used to close the major duodenal papilla. The upper end of the bile duct was gently grasped with forceps and pulled towards the experimenter and 5 mL of collagenase (Sigma-Aldrich, Cat: C7657; 1,000 units/mL) dissolved in Hanks Balanced Salt Solution (HBSS; See Appendix for recipe) without calcium (Ca^{2+}) was slowly injected using a .30 gauge needle. The pancreas was excised and submerged in 2.5 mL of cold HBSS without Ca^{2+}. The tissue was heated at 37°C for 12 minutes to activate the collagenase and shaken up-and-down forcefully 10 times to dissociate the pancreatic tissue. The reaction was then quenched by adding 5 mL of cold HBSS with Ca^{2+}. Pancreas was further dissociated by pipetting up-and-down 3 times with a serological pipette and then HBSS with Ca^{2+} was added to a final volume of 40 mL. The tubes were centrifuged (1000 rpm, 1 minute, 4°C) and the supernatant discarded. The tissue pellet was resuspended in 40 mL of HBSS with Ca^{2+} and centrifuged again. This process was repeated a total of 3 times. After the final centrifugation, the supernatant was discarded and the tissue was resuspended in 30 mL of warm HyClone Ham's Nutrient Mixture F10 (Hams F10, Fisher Scientific, Cat: SH30025.01) with 0.5% bovine serum albumin (BSA; Sigma-Aldrich, Cat: 10775835001) and 1% penicillin and streptomycin (Pen/Strep; Sigma-Aldrich, Cat: P4458). The cell suspension was passed through a 70 µm strainer (Fisher Scientific, Cat: 22363548). The flow through was discarded and contents of the cell strainer were transferred into a 100 mm petri dish (Fisher Scientific,

Cat: 08-757-100D) containing 5 mL of complete HamsF10 media and placed in an incubator (37°C, 5% CO_2) to equilibrate pH (approximately 20-30 minutes). Using a 20 µL pipette with filtered tips, islets were hand-picked under a dissecting microscope and transferred into a 60 mm petri dish (VWR, Cat: 10861-588) containing 2.5 mL of complete Hams F10 media. This process was repeated 2-3 times until the final dish contained pure islets that were free of exocrine tissue.

2.2 *Tissue Processing for Histology or RNA Extraction*

To preserve the pancreas, liver, and perirenal adipose for histology, tissues were excised following euthanasia and submerged in cold 4% paraformaldehyde (PFA; Fisher Scientific, Cat: AAJ19943K2). The tissues were stored in 4% PFA for 24 hours at 4°C and then transferred to 70% ethanol for long-term storage at 4°C. All tissues were sent to the University of Ottawa Heart Institute for processing and embedding in paraffin wax blocks.

2.3 *Ex Vivo Glucose Stimulated Insulin Secretion*

Following pancreatic islet isolation, 15 islet-equivalents were suspended in a 1.5 mL microcentrifuge tube containing 500 µL of Krebs-Ringer Bicarbonate Buffer (KRBB; See Appendix for recipe) with 2.8 mM glucose and incubated (37°C, 5% CO_2) for 40 minutes. The tube was then centrifuged (1000 rpm, 1 minute, room temperature) and the supernatant was discarded. The pellet containing the islets was then resuspended in 500 µL KRBB with 2.8 mM glucose and incubated (37°C, 5% CO_2) for 1 hour. The sample was then centrifuged, and the supernatant was stored at -30°C. The islets were then

resuspended in 500 µL KRBB with 16.7 mM glucose and incubated (37°C, 5% CO_2) for 1 hour. After the high glucose incubation, the supernatant was stored at -30°C. The islets were resuspended in 500 µL acid-ethanol (1.5% HCl in 70% ethanol) and stored at 4°C overnight. The next day, the sample was centrifuged and the supernatant was collected and neutralized with equivalent amount of Tris Base (Fisher BioReagents, Cat: BP1521) and stored at -30°C. Samples were assayed for insulin by using an enzyme-linked immunosorbent assay (ELISA) kit (Mouse Insulin ELISA, ALPCO, Cat: 80-INSMS-E01) according to manufacturers instructions.

2.4 *DNA Isolation & Genotyping*

All animals in the transgenic mouse colony reared by our laboratory were ear notched and the tissue sample was utilized to determine genotype. The tissue sample was suspended in 100 µL of Chelex Solution (Bio-Rad, Cat: 1421253; See Appendix for recipe) and incubated at 55°C for 1 hour, then 95°C for 15 minutes. After heating, the samples were centrifuged (10,000 rcf, 4°C, 1 minute), and the supernatant was transferred to a tube. DNA quality was assessed by nanodrop. MasterMix-Primer Solution (See Appendix for recipe) was mixed with 1 µL of the extracted DNA sample and placed in a thermocycler (Bio-Rad T100 Thermal Cycler, Serial: 621BR28468) for 1 hour (See Appendix for thermocycler protocol) to undergo DNA amplification. After amplification, 5 µL of DNA ladder (see below) was added to a well in an agarose gel (2% agarose; Bio-Rad, Cat: 1613101) containing a fluorescent dye (Thermo-Fisher, Cat: S33102) and 20 µL of each DNA sample (suspended in MasterMix-Primer Solution) was added to the

other wells. The gel was run at constant voltage (130 V) for 40 minutes and subsequently visualized using a fluorescence imager (Vilber Fusion FX5-XT, Serial: 15200012).

2.5 *RNA Extraction from Pancreatic Islets*

Pancreatic islets collected for RNA extraction were stored in approximately 250 µL RNAlater (Qiagen, Cat: 76106) at 4°C overnight then at -30°C. For RNA extraction, a modified protocol of the Qiagen RNeasy Micro Kit (Cat: 74004) was followed. Samples in RNAlater were thawed and 7 times the volume of RNAlater (approximately 1750 µL) of Buffer RLT-DTT mixture (containing 20 µL of DTT for 1 mL Buffer RLT; Qiagen, Cat: 79216) was added to each sample. Furthermore, the equivalent volume of Buffer RLT-DTT of 70% ethanol was added to each sample for a total of 1750 µL Buffer RLT-DTT and 1750 µL 70% ethanol added. Approximately 700 µL of the suspended sample was pipetted into a RNeasy MinElute column in 2 mL collection tube, centrifuged (8000 rcf, 1 minute, 22°C), and the flow through was discarded. This process was repeated until the entirety of each sample was transferred into the RNeasy MinElute column. After the final flow through was discarded, 350 µL of RW1 was added, the column centrifuged at the same settings, the flow through was discarded and this step was repeated a second time. The RNeasy MinElute column was then transferred into a new 2 mL collection tube and 500 µL of Buffer RPE was pipetted into the column, centrifuged at the same settings and the flow through was discarded. Afterward, 500 µL of 80% ethanol was added to the column, centrifuged (8000 rcf, 2 minutes, 22°C), the flow through was discarded and the RNeasy MinElute was transferred to a new 2 mL collection tube. The lid of the RNeasy MinElute column was opened, centrifuged (full speed, 5 minutes, 22°C) and any flow

through was discarded. The column was transferred into a sterile 1.5 mL collection tube, 14 µL RNase-free water was added and the column was incubated at room temperature for 10 minutes. Following the incubation, the column was centrifuged (full speed, 1 minute, 22°C) and the flow through was stored at -80°C. This step was repeated another time to retrieve two 14 µL aliquots of RNA.

2.6 *DNase Treatment and cDNA Synthesis*

To remove genomic DNA, extracted RNA from pancreatic islets and RNase-free water were mixed in a sterile tube to give an RNA concentration of 17.86 ng/µL (250 ng RNA in 14 µL of water). For a total of 16 µL of RNA, 2 µL of DNase MasterMix (Bio-Rad, Cat: 1725035, See Appendix for recipe) was added. Samples were incubated in a thermocycler (Bio-Rad T100 Thermal Cycler; Serial: 621BR28468) for approximately 10 minutes: 25°C for 5 minutes (DNA digest), 75°C for 5 minutes (DNase inactivation) and kept on ice until proceeding to cDNA Reverse Transcription.

To the RNA sample, 4 µL of iScript Reverse Transcription Supermix (Bio-Rad, Cat: 1708841) were added to give a total of 20 µL. To prepare the No-RT control, 4 µL of iScript No-RT Control Supermix (Bio-Rad, Cat: 1708841) was added. The samples were resuspended and incubated in a thermocycler for approximately 40 minutes: 25°C for 5 minutes (priming), 42°C for 30 minutes (reverse transcription), 85°C for 5 minutes (reverse transcription inactivation), 4°C hold. Samples were stored at -80°C and thawed on ice when ready to use.

2.7 *Quantitative Polymerase Chain Reaction*

Samples, primers (See Appendix for list), and Supermix (SensiFAST SYBR No-ROX, Bioline, Cat: BIO-980050; Sso Advanced Universal SYBR Green Supermix, Bio-Rad, Cat: 1725271) were thawed on ice. Ran in duplicates, 1 µL of cDNA was added to the appropriate wells and 9 µL of the corresponding qPCR MasterMix (See Appendix for recipe) was added into each well including the no-reverse transcriptase (NRT) control sample as well as the no-template control (NTC) sample. The plate was sealed with an optical sealer and transferred to a CFX machine (Bio-Rad CFX 384 C1000 Touch ThermoCycler, Serial: 786BRO5205). The following amplification protocol was used: 95°C for 1 minute, 95°C for 5 seconds, 60°C for 20 minutes, 65°C for 5 seconds, 95°C for 50 seconds, and 4°C hold. Housekeeping genes were hypoxanthine-guanine phosphoribosyltransferase (*HPRT*) and peptidylprolyl isomerase A (*PPIA*). The delta delta CT method was used to quantify gene expression. Primers were validated by the Bruin lab for melt curve, amplification, and efficiency (see Supplemental Figure 1 for *Cyp1a1* primer validation data).

CHAPTER 3: The effect of chronic, low dose TCDD exposure in wild type and systemic *Cyp1a1/1a2* KO mice on glucose homeostasis and β-cell function

3.1 Introduction

Global incidence of T2D is increasing and the cause(s) remain to be elucidated. Exposure to POPs has been associated with an increase in relative risk to develop T2D and TCDD is speculated to be the among the most harmful of the POPs to health in mammals. Exposure to the dioxin is strongly associated with induction of the CYP1A1 metabolic enzymes but the role of these enzymes in the pathogenesis of T2D is unknown. My first aim is to determine the effect of chronic, low dose TCDD exposure in wild type (WT) and systemic *Cyp1a1/1a2* knock-out (KO) mice on glucose homeostasis and β-cell function.

CYP1A1 is a phase I metabolism enzyme that oxidizes xenobiotic compounds, including POPs, to increase their water solubility and excretion. Expression of *CYP1A1* is well characterized in hepatic tissue and is increased by the XRE due to a ligand-receptor interaction. Compared to other known CYP1A1 inducers such as 3-methylcholanthrene, TCDD is 10,000 times more potent an AhR agonist (Poland and Glover, 1974). Due to its ability to induce *CYP1A1*, TCDD is speculated to be the most harmful of the POPs in mammals. Classically, CYP1A1 is known for bioactivating benzo[a]pyrene into a carcinogenic metabolite, benzo[a]pyrene-7,8-dihydrodiol-9,10-epoxide (Walsh et al, 2013). However, CYP1A1 does not metabolize TCDD and its role during TCDD exposure is not known. Most of the acute effects of TCDD are likely mediated by the AhR as mice

lacking the receptor are unaffected by doses that are 10-times greater (2000 μg/kg) than the lethal dose (Gonzalez and Fernandez-Salguero, 1998).

Diabetes is characterized by changes to insulin secretion and sensitivity. A single high dose of TCDD (micromolar quantity) decreases insulin secretion following a glucose stimulus and glucose tolerance *in vivo* in mice (Kurita et al, 2009). As exposure to TCDD is associated with a modest increase in relative risk to develop T2D in humans (Henriksen et al, 1997; Kang et al, 2006; Michalek et al, 1999; Michalek and Pavuk 2008), the effects of TCDD on glucose homeostasis are important to understanding diabetic aetiology. However, most animal research has used doses in the micromolar range that is not representative of chronic, low dose TCDD exposure in humans from environmental contamination. As a result, animal research using doses in the nanomolar range will be able to better model physiologically relevant TCDD exposure in order to determine if and how this POP promotes diabetic pathology. Furthermore, the potential role of CYP1A1 in regulating glucose homeostasis following TCDD exposure remains to be elucidated.

3.2 Experimental Approach

To understand the role of *Cyp1a1* induction in glucose homeostasis during chronic, low dose TCDD exposure, systemic *Cyp1a1/1a2* double KO mice were utilized. By knocking out the Cyp1a1 enzyme in mice, we will be able to determine the function of this enzyme as it pertains to glucose tolerance, insulin sensitivity and secretion during TCDD exposure. The dosage utilized is in the nanomolar range and is comparable to chronic, low dose exposure in humans through food and soil and is 10,000 times lower than the

lethal dose in mice. I assessed role of Cyp1a1/1a2 in regulating body weight, fasting glucose levels, glucose tolerance, insulin tolerance, and beta cell function (i.e. GSIS) during chronic, low dose TCDD exposure *in vivo.* I hypothesize that TCDD exposure will promote glucose intolerance, insulin resistance, and decreased insulin secretion in WT mice. Furthermore, I hypothesize that mice lacking Cyp1a1/1a2 will be more glucose intolerant and insulin resistant during TCDD exposure than their WT littermates along with secreting less insulin in response to a glucose stimulus.

3.3 Methods

3.3.1 *Animals*

Both WT mice and those with systemic genetic deletion of *Cyp1a1/1a2* were raised from a colony of transgenic mice bred by the Kieffer Lab at University of British Columbia (UBC). The colony was originally generated by Dr. Daniel Nebert (Dragin et al, 2007) on a C57BL/6J background, and breeding pairs were generously provided by Dr. Frank Gonzalez (University of Cincinnati).

3.3.2 *Experimental Design*

Male (10 KO, 8 WT) and female (6 KO, 11 WT) 6-8 week old mice were treated by subcutaneous injection with either 20 ng/kg TCDD (Sigma-Aldrich, Cat: 48599) dissolved in corn oil (Sigma-Aldrich, Cat: C8267) or corn oil vehicle while under inhalable isoflurane (3-5%, 1L/min) anaesthesia 2 times per week for 4 weeks (7 treatments total). Animals

were kept in a 12 hour light/dark cycle and fed irradiated standard lab chow (2014 Teklad global 14% protein rodent maintenance diet) and water ad-libitum. All experiments were approved by UBC Animal Care Committees and carried out in accordance with Canadian Council on Animal Care guidelines and performed in collaboration with Dr. Tim Kieffer's Lab at UBC.

3.3.3 *Body Weight and Blood Glucose Tracking*

Body weight and blood glucose measurements were performed once per week following a 4 hour fast. Blood was collected from the saphenous vein and measured on a glucometer (Johnson & Johnson OneTouch Verio Flex Glucometer).

3.3.4 *Insulin Tolerance Test*

An insulin tolerance test (ITT) was performed 3 weeks post-exposure using 10 male *Cyp1a1/1a2* KOs (5 TCDD, 5 control), 6 female *Cyp1a1/1a2* KOs (3 TCDD, 3 control), 8 male WT (4 TCDD, 4 control), and 10 female WT (6 TCDD, 4 control) mice. Blood glucose was measured as described above after a 4 hour fast and mice were given a bolus of insulin (0.7 IU/kg) dissolved in PBS (2.0 IU/mL) by i.p. injection. Blood glucose was measured at 10-, 20-, 30-, 60-, 90- and 120-minutes post-insulin injection and all animals received 200 µL of Lactated Ringer's Solution subcutaneously after their final blood glucose measurement.

3.3.5 *Glucose Tolerance Test and Glucose Stimulated Insulin Secretion*

A glucose tolerance test (GTT) and GSIS were performed at 4 weeks after the start of treatments on 10 male *Cyp1a1/1a2* KOs (5 TCDD, 5 control), 5 female *Cyp1a1/1a2* KOs (3 TCDD, 2 control), 8 male WT (4 TCDD, 4 control), and 11 female WT (6 TCDD and 5 control) mice. Following a 6 hour fast, blood glucose was measured and approximately 50 µL of blood was collected in a capillary tube. An i.p. bolus of glucose (2 g/kg) dissolved in distilled water (3 mL of 50% dextrose in 2 mL ddH_2O) was then administered. Blood glucose was measured 15-, 30-, 60-, 90-, and 120-minutes post-glucose bolus and approximately 30 µL of blood was collected at time points 15-, 30-, and 60-minutes post-insulin bolus. All animals received 200 µL of Lactated Ringer's Solution after their final blood glucose measurement. Blood plasma was separated following centrifugation (9000 rcf, 3 minutes, 4°C), and assayed for insulin by using an enzyme-linked immunosorbent assay (ELISA) kit (Mouse Ultrasensitive Insulin ELISA, ALPCO, Cat: 80-INSMSU-E10) according to manufacturers instructions.

3.3.6 *Histology Endpoint*

Animals were anaesthetized at 4 weeks after the beginning of treatment with inhalable isoflurane (3-5%, 1L/min) and transferred to a nose cone plate with inhalable isoflurane (3-5%, 1L/min). To collect cardiac blood, a needle (.30-gauge) treated with heparin (Pfizer) was inserted at a 30-degree angle just below the sternum. Following blood collection, all animals were euthanized by cervical dislocation and whole pancreas and liver were excised as previously described (see General Methods 2.1). The tissues were

stored in 4% PFA for 24 hours at 4°C and then transferred to 70% ethanol for long-term storage at 4°C. Tissues were processed by Wax-it Histology Services (Vancouver, BC) for histology and embedded in paraffin wax blocks (5 µm thickness).

3.3.7 Statistical Analysis

Statistical analysis was performed using GraphPad Prism software (GraphPad Software Inc., La Jolla, CA). Specific statistical tests are indicated in figures legends. For all analyses, $p < 0.05$ was considered statistically significant. Data are either presented as mean +/- SEM (line graphs) or as bar plots with individual data points overlaid.

3.4 Results

3.4.1 *Body Weight and Blood Glucose Tracking*

There were no discernable trends in female body weight regardless of genotype or treatment (Figure 3.1A and 3.1B) while male WT mice exposed to TCDD were heavier than TCDD-exposed KO male mice (Figure 3.1E and 3.1F). Furthermore, TCDD-exposed female KO mice trended towards hyperglycemia compared to control and TCDD-exposed WT female mice (Figure 3.1C and 3.1D) and WT males exposed to TCDD were hypoglycemic compared to all other male mice (Figure 3.1G and 3.1H).

3.4.2 *Glucose Homeostasis and Beta Cell Function at Weeks 3-4*

TCDD-exposed female KO mice were insulin resistant 3 weeks post-initial TCDD exposure compared to their vehicle control KO counterparts (Figure 3.2A and 3.2B) while there were no discernable trends in male mice regardless of genotype or treatment (Figure 3.2C and 3.2D). These data indicate that TCDD exposure promoted insulin resistance in females only if *Cyp1a1/1a2* was absent, suggesting a protective role for Cyp1a1/1a2 in females. At 4 weeks post-initial exposure, there were no effects of TCDD on glucose tolerance in male mice (Figure 3.2G and 3.2H), regardless of treatment or genotype. Notably, due to a technical error, only one TCDD-exposed female KO mouse was utilized for the glucose tolerance test, so we are unable to make conclusions about this group (Figure 3.2E and 3.2F). Finally, there were no clear effects of genotype or treatment in the either female (Figure 3.2I and 3.2J) or male (Figure 3.2K and 3.2L) insulin secretion following a glucose challenge.

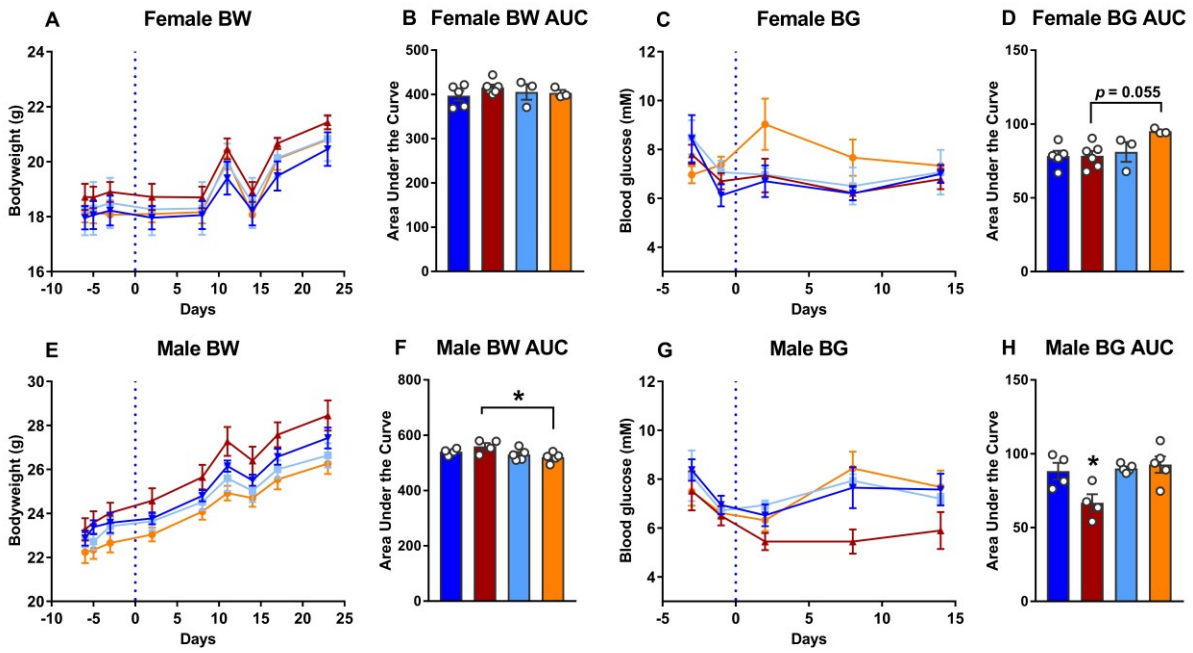

Figure 3.1: Body weight and blood glucose tracking of wild type and *Cyp1a1/1a2* KO mice. A,E) Body weight of female (A) and male (E) mice measured during a combination of either fasted or non-fasted conditions. **B,F)** Area under the curve of female (B) and male (F) body weight tracking. **C,G)** Fasted blood glucose measurements in female (C) and male (G) mice. **D,H)** Area under the curve of female (D) and male (H) fasted blood glucose. # $p < 0.05$, one-way ANOVA with Tukey's post-hoc test for multiple comparisons; see Supplemental Table 1 for detailed ANOVA values. Data are presented as mean +/- SEM.

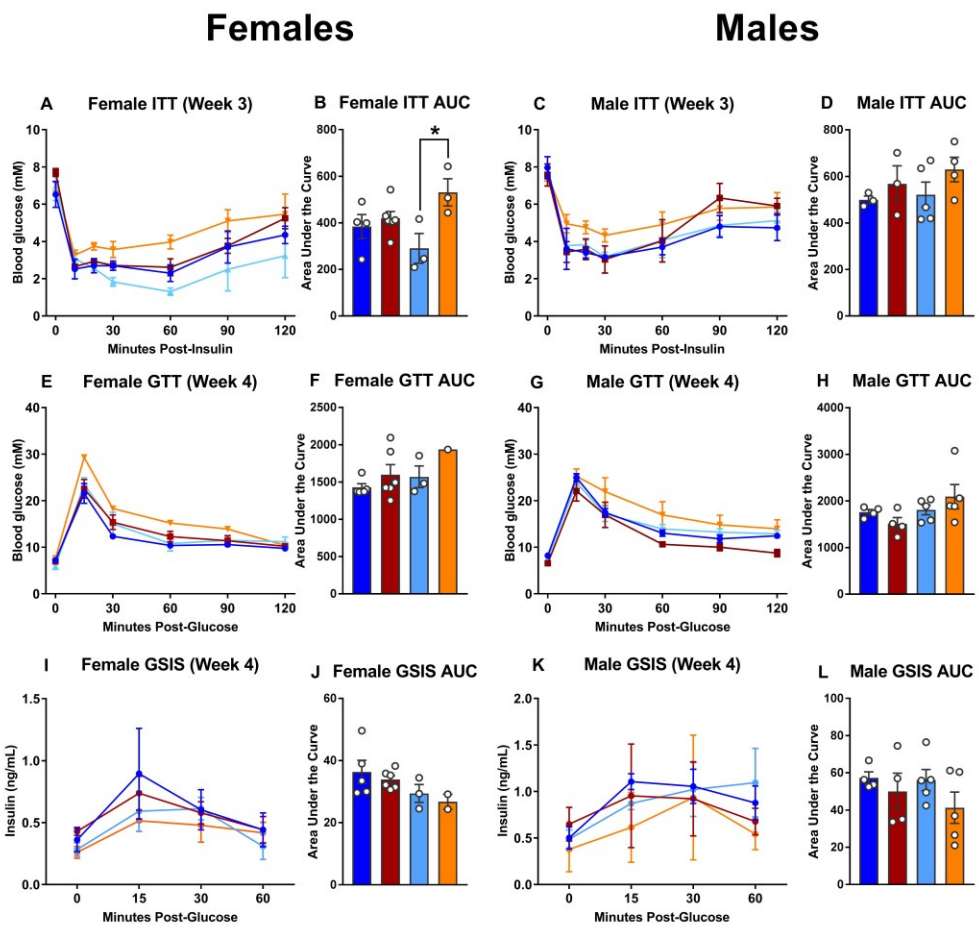

Figure 3.2: *In vivo* metabolic testing in wild type and *Cyp1a1/1a2* KO mice. A,B,C,D) Insulin tolerance test data from female mice (A) and male (C) mice at 3 weeks with associated area under the curve data (female B; male D). **E,F,G,H)** Glucose tolerance test data from female (E) and male (G) mice with associated area under the curve data (female F; male H). **I,J,K,L)** Glucose stimulated insulin secretion data from female (I) and male (K) mice with associated area under the curve data (female I; male L). * $p < 0.05$, one-way ANOVA with Tukey's post-hoc test for multiple comparisons; see Supplemental Table 2 for detailed ANOVA values. Data are presented as mean +/- SEM.

3.5 Discussion

Contrary to my hypotheses, chronic, low dose TCDD exposure, had no significant effect on body weight or fasting blood glucose in mice regardless of sex or genotype. My data demonstrated that TCDD-exposed WT male mice became hypoglycemic with respect to other male mice. However, in the last week of the experiment TCDD-exposed WT male mice seemed to be returning to normoglycemia. Furthermore, mice showed no changes to glucose tolerance or insulin secretion in either female or male mice regardless of chemical treatment or genotype. These data are novel in that we explored the effects of chronic, low dose TCDD exposure at a concentration 100-1000 times lower than previously reported (Kurita et al, 2009; Novelli et al, 2005) in both sexes. In this way, our model is more representative of human TCDD exposure (Eskenazi et al, 2004; Geusau et al, 2001; Neuberger et al, 1991) compared to previous studies. Moreover, our data indicate that Cyp1a1/1a2 does not play a role in modulating body weight or blood glucose homeostasis in mice during chronic, low dose TCDD exposure.

Interestingly, TCDD exposure in female KO mice decreased insulin sensitivity with respect to their vehicle control KO counterparts while there were no differences in male mice regardless of chemical treatment or genotype. These data suggest that under normal conditions, Cyp1a1/1a2 may be protective in female WT mice during chronic, low dose TCDD exposure and as such WT females had no difference in their insulin sensitivity. These findings suggest a possible difference between sexes in the role Cyp1a1/1a2 plays in modulating insulin sensitivity. The biochemical crosstalk between the AhR and the nuclear estrogen receptor α (ERα) has been well established as AhR activation typically has an anti-estrogenic effect (Matthews and Gustafsson 2006). In the

HepG2 cell line expressing ERα, exposure to TCDD decreases estradiol-mediated ERα signalling of ER responsive elements, which was reversed by AhR antagonism (Göttel et al, 2014). That is, in the presence of estradiol, TCDD inhibits the ability of the hormone to recruit ER-responsive DNA elements. Furthermore, other research in immortalized cells demonstrates that concomitant estradiol and TCDD exposure decreases TCDD-mediated *Cyp1a1* induction (Beischlag and Perdew 2005; Kharat and Saatcioglu 1996). Interestingly, CYP enzymes, in particular those associated with the AhR-XRE pathway such as CYP1A1, CYP1A2, and CYP1B1, metabolize estradiol and estrone (Lee et al, 2003). These data indicate that the AhR and ERα pathways overlap and interact to affect downstream targets of the XRE and estrogen metabolites.

One potential explanation for the difference in insulin sensitivity may be that females lacking *Cyp1a1/1a2* may not metabolize estrogens efficiently resulting in constitutive differences in estrogen concentrations. As female sex hormones are well known to modulate insulin sensitivity (for a review, see Gupte et al, 2015), the resulting increase in estrogens in control females lacking *Cyp1a1/1a2*, particularly in the liver, may increase insulin sensitivity. That is, KO females are speculated to be more insulin sensitive due to the decrease in estrogen metabolism and therefore higher concentration of native estrogens. By unknown mechanism(s), this effect is lost following exposure to TCDD in KO female mice leading to insulin resistance. In the future, the role of Cyp1a1/1a2 in metabolizing estrogens can be explored by comparing estrogen-related genes between WT and KO female mice as well measuring circulating estrogens. As both pathways are well integrated, it is speculated that constitutive changes to *Cyp1a1/1a2* expression will result in genetic changes to estrogen-related genes.

For future investigations, a longer experimental timeframe (8-12 weeks) may provide more insight into the development of diabetic pathology. Due to the low concentration of TCDD used with respect to previous research, a longer experiment would allow for greater accumulation of the dioxin and possibly increase metabolic disruption. Combined with a longer experimental timeframe, utilizing a larger sample size (8 per group as opposed to 4-5) would strengthen our data by decreasing variability and help determine if TCDD-exposed WT male mice remain hypoglycemic. As human epidemiological data suggests that young females are particularly at risk during TCDD exposure (Eskenazi et al, 2004; Warner et al, 2013), future investigation could incorporate early-life TCDD exposure into an experimental paradigm that tracks glucose tolerance and insulin sensitivity throughout maturity.

Overall, these data suggest that Cyp1a1/1a2 does not play a role in body weight, fasting blood glucose, or glucose tolerance during chronic, low dose TCDD exposure, contrary to my original hypothesis. This experiment revealed that compared to their control KO counterparts, TCDD-exposed female KO mice were insulin resistant in line with my original hypothesis.

CHAPTER 4: Effects of direct, low dose TCDD exposure on isolated pancreatic islets with and without *Cyp1a1/1a2* gene deletion.

4.1 Introduction

The pancreatic islet contains endocrine cells that secrete hormones in response to changes in blood nutrient levels. The impact of TCDD exposure to the pancreatic islet and the β-cell are important in determining how the dioxin causes T2D. Furthermore, the role of CYP1A1 in the pancreatic islet both constitutively and during TCDD exposure is not well understood as either protective or deleterious. My second aim is to determine the effect of direct, low dose exposure on isolated pancreatic islets with and without *Cyp1a1/1a2* deletion.

The pancreatic islet acts as the regulatory unit of metabolism during T2D. Pancreatic islets maintain blood glucose homeostasis by releasing a variety of hormones from distinct endocrine cells in their cluster. As described in section 1.21, β-cells sense changes in blood glucose post-prandially and in response secrete insulin into the blood stream. Disruption to β-cell survival along with insulin secretion contributes to the inability to maintain blood glucose homeostasis and ultimately lead to T2D (Chen et al, 2017). During T2D, chronic hyperglycemia promotes β-cell apoptosis leading to an inability to secrete enough insulin to manage blood glucose (Maedler et al, 2001). Furthermore, surviving β-cells fail to secrete sufficient insulin post-prandially and perpetuate the chronic hyperglycemia leading to more β-cell loss (Park and Woo, 2019). Previous work by the Bruin lab has shown that TCDD exposure decreases β-cell mass in mice (unpublished

data). Following systemic TCDD exposure, insulin secretion from isolated rodent islets was impaired in high glucose conditions (Novelli et al, 2005) and in INS1-E immortalized β-cells treated directly with TCDD (Piaggi et al, 2007). As a result, evidence suggests that TCDD exposure leads to β-cell death and the inability to have a robust GSIS.

In line with previous reports (Kessova 1998), our lab has shown that *CYP1A1* is induced in human and mouse pancreatic islets following nanomolar TCDD exposure (unpublished data). These preliminary data suggest that the AhR pathway is active in human and murine islets and its activation leads to an increase in *CYP1A1* transcription. Furthermore, our lab has also shown that *Cyp1a1* remains active in mouse islets for up to two weeks after a single, high dose injection of TCDD (unpublished data). Given that TCDD induces *CYP1A1* and previous reports indicate that direct TCDD exposure decreases insulin secretion following a glucose stimulus, it is of interest to investigate if CYP1A1 itself plays a role in regulating insulin secretion from pancreatic islets.

4.2 Experimental Approach

In order to determine the effects of direct, low dose TCDD exposure on pancreatic islets, the cell clusters are physically isolated and incubated in dioxin-treated media. By utilizing pancreatic islets from *Cyp1a1/1a2* KO mice, the effects of direct TCDD exposure on pancreatic islets are observable in the presence and absence of Cyp1a1/1a2 enzymes. In this way, the role of *Cyp1a1* in the pancreatic islet in isolation from external signaling during TCDD exposure will be discernable. I hypothesize that direct TCDD exposure will decrease GSIS in WT pancreatic islets. Furthermore, I hypothesize that *Cyp1a1/1a2*

deletion in conjunction with TCDD exposure will further decrease insulin secretion in isolated islets as TCDD-mediated *Cyp1a1/1a2* induction may be protective.

4.3 Methods

4.3.1 *Animals*

Both WT and systemic *Cyp1a1/1a2* KO mice (see 3.3.1 *Animals)* between 16-24 weeks of age mice were raised from a colony of transgenic mice bred by the Bruin Lab at the University of Ottawa. Animals were kept in a 12 hour light/dark cycle and fed irradiated standard lab chow (2014 Teklad global 14% protein rodent maintenance diet) and water ad-libitum. All experiments were approved by Carleton University Animal Care Committees and carried out in accordance with Canadian Council on Animal Care guidelines.

4.3.2 *Experimental Design*

Pancreatic islets from male (8 KO, 5 WT) and female (8 KO, 6 WT) mice were isolated as described above (see General Methods 2.1). Islets were incubated in complete HamsF10 with TCDD (10 nM) or control media for 48hrs and subsequently underwent a GSIS experiment as described previously (see General Methods 2.3). As well, another cohort of male (5 WT, 5 KO) and female (4 WT, 4 KO) mice were sacrificed for islet isolation. These islets were incubated in TCDD (10 nM) or control media for 48hrs and RNA was isolated as described above (see General Methods 2.5).

4.3.3 *Statistical Analysis*

Statistical analysis was performed using GraphPad Prism software (GraphPad Software Inc., La Jolla, CA). Specific statistical tests are indicated in figures legends. For all analyses, $p < 0.05$ was considered statistically significant. Data are presented as bar plots with individual data points overlaid.

4.4 Results

4.4.1 *Ex Vivo Glucose Stimulated Insulin Secretion*

Regardless of treatment, female KO islets produced more insulin than female WT islets following exposure to high glucose (Figure 4.1A). These data support a genotypic difference in females whereby the ablation of *Cyp1a1/1a2* promotes a more robust insulin secretion following exposure to high glucose. There were no differences in total islet insulin content in female islets regardless of genotype of treatment (Figure 4.1B). Male WT islets incubated in TCDD produced significantly less insulin than WT control islets following a high glucose stimulus (Figure 4.1D) indicating that direct TCDD exposure decreases insulin secretion in isolated male islets. Male KO control islets also secreted less insulin under high glucose conditions compared to WT control islets (Figure 4.1D) demonstrating that *Cyp1a1/1a2* ablation alone decreases GSIS to a level comparable to male WT islets exposed to TCDD. Interestingly, male KO islets exposed to TCDD secreted more insulin than male WT islets exposed to TCDD (Figure 4.1D) suggesting that Cyp1a1/1a2 may be protective in male islets during direct TCDD exposure. Like their female counterparts, there were no differences in islet insulin content of male mice (Figure

XD). Finally, our experimental model was validated by demonstrating that TCDD exposure increased *Cyp1a1* in WT islets and that there was no Cyp1a1 induction in KO islets of both sexes.

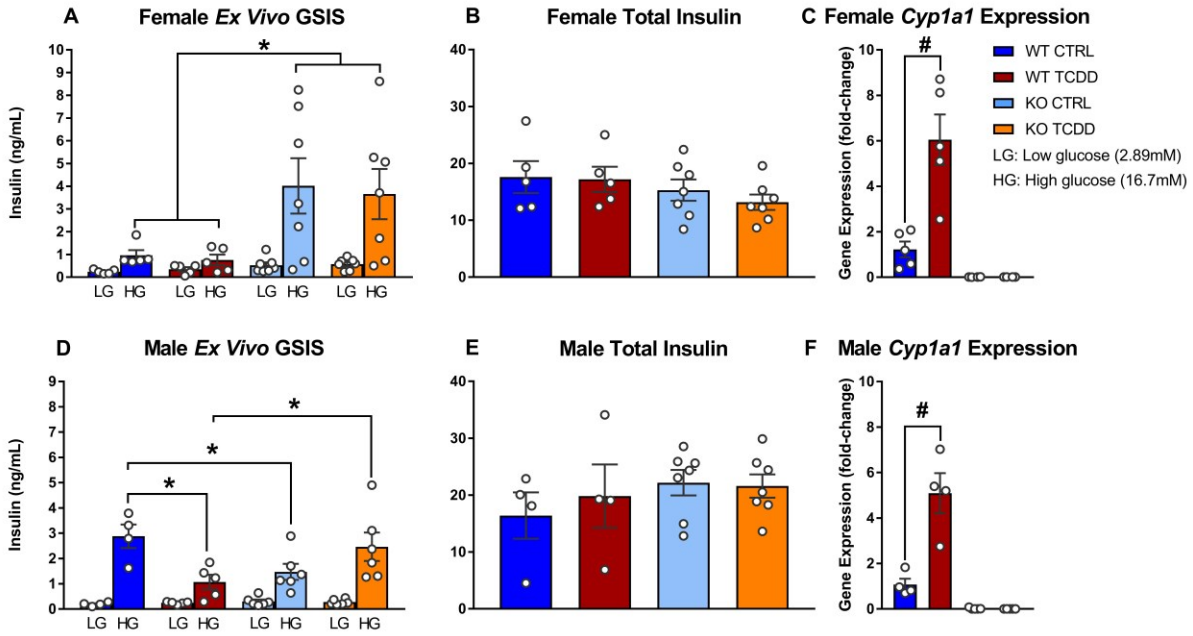

Figure 4.1: *Ex vivo* glucose stimulated insulin secretion in wild type and *Cyp1a1/1a2* KO islets. A,D) Insulin secretion following low glucose and high glucose exposure by islets from female mice (A) and male mice (D). **B,E)** Data from average total insulin content of technical triplicates from female mice (B) and male (E) mice. **C,F)** Average gene expression measured in fold-change relative to WT CTRL of female (C) and male (F) islets for *Cyp1a1*. # $p < 0.05$, one-way ANOVA with Tukey's post-hoc test for multiple comparisons. * $p < 0.05$, two-way ANOVA with Tukey's post-hoc test for multiple comparisons; see Supplemental Table 3 for detailed ANOVA values. Data are

presented as mean +/- SEM and individual data points represent biological replicates (which are an average of three technical replicates).

4.5 Discussion

This *ex vivo* GSIS experiment in isolated pancreatic islets revealed significant sex differences in response to direct exposure to TCDD and the role of Cyp1a1/1a2 during exposure. In line with previous data from isolated murine (Kurita et al, 2009) and rat (Novelli et al, 2005) islets exposed to TCDD *in vivo* and with my hypothesis, exposure to TCDD decreases GSIS in male WT islets. However, unlike Kurita and colleagues (2009), total insulin content was not affected by TCDD exposure. Interestingly, deletion of *Cyp1a1/1a2* in males reduced insulin secretion under high glucose conditions compared to control WT male mice. As there was no difference between the high glucose insulin response between KO male mouse control and TCDD-exposed islets, these data suggest that TCDD-mediated *Cyp1a1/1a2* induction may be deleterious in males, contrary to my hypothesis. This interpretation is furthered by the observation that KO males exposed to TCDD secreted more insulin than their TCDD-exposed WT littermates.

Female mouse islets showed a completely different response to males. Female mice lacking *Cyp1a1/1a2* produced more insulin than their WT counterparts in high glucose conditions regardless of treatment, highlighting a striking genotypic difference in females that was not observed in males. As total insulin content was the same across all females, these data suggest that Cyp1a1/1a2 may have a constitutive role in suppressing insulin secretion following a high glucose stimulus in female islets under non-exposed conditions.

Importantly, these findings must be interpreted with caution as there was much variability in the female KO data. Finally, high glucose conditions only modestly increased insulin secretion in WT female mice and as result, these data await replication. In the future, the *ex vivo* GSIS would be better repeated using a perifusion apparatus to more accurately determine the time course of insulin secretion in isolated islets. These data do not fit with my original hypothesis as TCDD exposure did not affect insulin secretion regardless of genotype in females but highlights a potential role of Cyp1a1/1a2 in modulating insulin secretion in female islets.

In both male and female mice, *Cyp1a1* mRNA is expressed in WT islets under normal conditions, albeit in small quantity. This indicates that *Cyp1a1* may play a constitutive role in pancreatic islets that does not affect total insulin content. This could be tested by comparing key genes involved in insulin synthesis, such as transcription factors (e.g. *Pdx-1*, *Pax-6* and *MafA*), between WT and KO mice. Furthermore, *Cyp1a1* was induced approximately 5-fold after nanomolar TCDD exposure in pancreatic islets of both sexes. Compared to hepatic *Cyp1a1* induction, which is approximately 10 times greater (unpublished data), the changes to *Cyp1a1* in islets are modest but still indicate that TCDD is activating the AhR pathway locally in the endocrine pancreas. In the future, the use of cell sorting to isolate β-cells from other endocrine cells will provide insight into the distribution of TCDD-mediated *Cyp1a1* induction among the different cell types. This will help determine if Cyp1a1 induction is occurring primarily in the β-cell and its role in insulin secretion.

One potential explanation for the decrease in male WT islet insulin secretion following direct TCDD exposure may be due to AhR agonism by TCDD. That is, AhR agonism prior

to a glucose stimulus may decrease insulin secretion in isolated male islets. In order to test this, male pancreatic islets could undergo an *ex vivo* GSIS experiment after concomitant exposure to TCDD and an AhR antagonist such as α-naphthoflavone (Merchant et al, 1990). In other words, the TCDD-mediated agonism of AhR could be blocked by an AhR antagonist in order to elucidate the role of AhR agonism following exposure to a high glucose stimulus. Furthermore, the expression of genes involved in insulin secretion such as *Nkx6.1* and *MafA* can be analyzed to determine the role of AhR agonism in insulin secretion in male mice. In this way, the role of the AhR pathway in modulating GSIS in pancreatic islets during TCDD exposure can be elucidated.

As described earlier (see 3.5 Discussion), the AhR and nuclear ERα pathway overlap to be mutually inhibitory. In isolated mouse cells and in immortalized cells, incubation in millimolar quantities of estradiol increased insulin secretion following a high glucose stimulus greater than glucose itself (Sharma and Prossnitz 2011). As antagonism of the G protein-coupled membrane bound estrogen receptor blocked this increase, the authors determined that the potentiation of insulin secretion was mediated by estrogen (Filardo and Thomas 2012). In my experiment, female *Cyp1a1/1a2* KO islets secreted significantly more insulin than their WT counterparts implicating a role for basal Cyp1a1/1a2 in insulin secretion. Given that female KO mice may have constitutively more estrogen due to the lack of metabolism (as outlined in 3.5 Discussion), it is speculated that unmetabolized estrogens potentiate insulin secretion through one of the estrogen receptors in the presence of a high glucose stimulus. To test this, WT and knock female islets could be incubated with an estrogen receptor antagonist, along with TCDD. In this way, the role of estrogen during insulin secretion can be determined in the absence of Cyp1a1/1a2.

Taken together, these data highlight the role of basal Cyp1a1/1a2 enzymes in female insulin secretion as female mice lacking *Cyp1a1/1a2* secreted significantly more insulin than WT females regardless of chemical exposure. Furthermore, TCDD-mediated *Cyp1a1/1a2* induction may have a deleterious effect in male islets as control male islets lacking *Cyp1a1/1a2* secreted significantly less insulin than WT control male islets.

CHAPTER 5: Effect of concurrent HFD and chronic, low dose TCDD exposure in wild type mice on glucose homeostasis and β-cell function.

5.1 Introduction

The composition of our diet is integral to blood glucose management. Although TCDD exposure is associated with a modest increase in T2D risk in humans, the effects of diet in conjunction with dioxin exposure are not known. Termed a 'double hit', the effects of a HFD during dioxin exposure with regard to blood glucose homeostasis and β-cell function are speculated to be more deleterious than either in isolation. My third aim is to determine the effect of concurrent HFD and chronic, low dose TCDD exposure in WT mice on glucose homeostasis and β-cell function.

Lifestyle factors such as levels of physical activity and diet remain the primary factors in precipitating T2D (Wu et al, 2014). In particular, a diet rich in fat is associated with increased relative risk to develop T2D in humans and death associated with cardiovascular disease (Nagao et al, 2015). In animal models, a HFD is used to induce a diabetic phenotype by promoting hyperglycemia, hyperinsulinemia and eventual insulin

resistance (Liu et al, 2015) along with systemic inflammation due to increased pro-inflammatory cytokines (Nov et al, 2013). In humans, consumption of a HFD causes elevated blood triglyceride levels coupled with low levels of high density lipoprotein C and high low density lipoproteins (Parhofer 2015). An increase in blood lipids increases fat deposition throughout the body as a mechanism to reduce circulating blood lipids. In the liver, increased local lipid storage promotes local inflammation and eventually decreases the sensitivity to insulin's anabolic cellular actions in the liver. As a result, insulin's effects are hindered at the receptor level and glucose metabolism becomes dysregulated resulting in hyperglycemia. In response to the increase in circulating blood glucose, β-cells initially secrete more insulin. Over time, this compensatory mechanism leads to eventual β-cell 'exhaustion' and inability to maintain elevated insulin secretion leading impaired GSIS (Cerf 2013). Finally, lipids themselves are signaling molecules which can modulate pancreatic insulin secretion through the GP40 receptor pathway. Together, these effects contribute to insulin resistance and β-cell dysfunction and accelerate diabetic pathology

As POPs are lipophilic molecules, I predict that HFD-feeding will increase harm done by POPs. This prediction in is in line with the 'double-hit' hypothesis whereby a single biochemical insult is coupled with another to produce a more deleterious effect than either in isolation. Indeed, previous research in C57BL/6 mice demonstrated that concomitant TCDD-exposure in the micromolar range and HFD-feeding (15% fat) resulted in greater liver fat deposition than diet or treatment alone (Angrish et al, 2012). As well, the authors observed a modest increase in intestinal and hepatic lipid transport genes consistent with the notion that TCDD is increasing lipid storage in the liver. In a follow-up, the research

group noted that TCDD-exposure during HFD-feeding decreased serum lipids while increasing the same lipids in the liver (Angrish et al, 2013). Furthermore, TCDD-exposure in the micromolar range has also been shown to promote macrophage migration from the intestinal lining to the liver (Fader et al, 2015; 2017). These data support that concomitant TCDD and HFD exposure is more deleterious than either alone in the liver and it is predicted that these effects extend to the pancreas. As a result, the effects of concurrent TCDD exposure and HFD-feeding on markers of metabolism and β-cell function including glucose tolerance, insulin sensitivity and secretion remain to be elucidated.

5.2 Experimental Approach

To understand the effect of concurrent TCDD exposure and HFD-feeding, male and female WT C57BL/6 mice underwent exposure to either corn oil or TCDD and HFD-feeding for 12 weeks. In this way, the experiment was designed to determine if treatment and diet may converge to accelerate or worsen glucose homeostasis and markers of diabetic pathology in the pancreas. The length of the experiment was designed to model long-term exposure to physiologically relevant TCDD concentrations (as described in Aim 1, Approach 3.2). I hypothesize that concomitant TCDD exposure and HFD-feeding will impair glucose tolerance, insulin sensitivity, and insulin secretion worse than either treatment alone.

5.3 Methods

The same chronic, low dose TCDD exposure protocol utilized in Aim 1 (20 ng/kg/d TCDD dissolved in corn oil or corn oil vehicle control by i.p. injection) was administered twice per week for 12 weeks on 40 male and 40 female 6 week old C57BL/6 WT mice (Charles River Laboratories, USA). Mice were kept a 12-hour day/night cycle and fed either a HFD (45% fat, 35% carbohydrate, 20% protein, Cedarlane, Cat: D12451) or standard lab chow (Chow; 20% fat, 66% carbohydrate, 14% protein) ad-libitum along with access to water. In summary there were 4 treatment groups for both male and female mice (8 groups total): corn oil + chow (CO/Chow), TCDD + chow (TCDD/Chow), corn oil + HFD (CO/HFD), and TCDD + HFD (TCDD/HFD). All experiments were approved by Carleton University Animal Care Committees and carried out in accordance with Canadian Council on Animal Care guidelines.

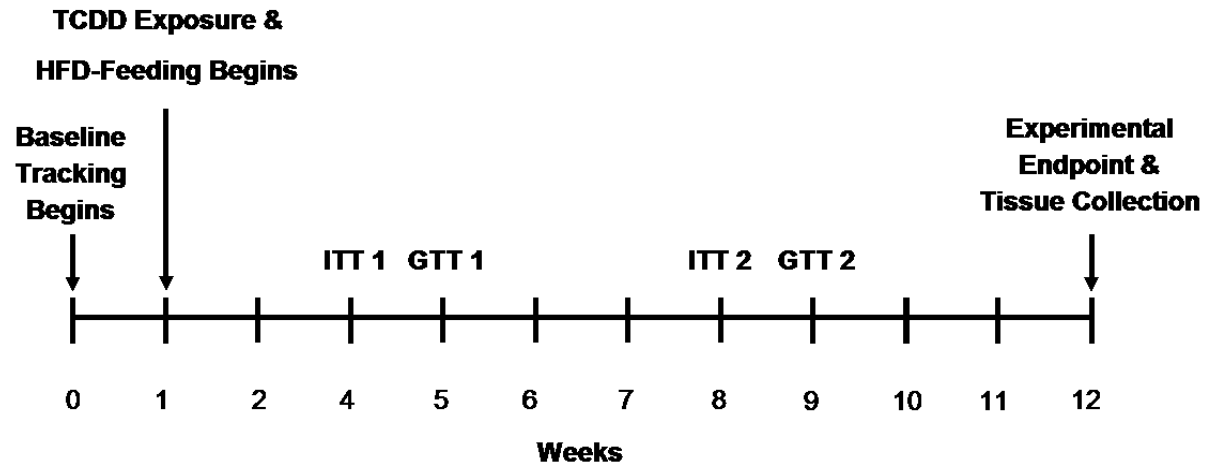

Figure 5.1: Experimental timeline of 'double-hit' HFD-feeding and TCDD exposure experiment of 12 weeks.

5.3.1 *Body Weight and Blood Glucose Tracking*

Body weight and blood glucose were measured as described in Aim 1 (*Body Weight and Blood Glucose Tracking*).

5.3.2 *Insulin Tolerance Test*

At 4 and 8 weeks post-initial TCDD exposure, 30 male (8 TCDD/HFD, 7 TCDD/Chow, 8 CO/Chow, 7 CO/HFD) and 30 female (8 TCDD/HFD, 7 TCDD/Chow, 7 CO/Chow, 8 CO/HFD) mice underwent an ITT as described in Aim 1 (Methods 3.3).

5.3.3 *Glucose Tolerance Test and Glucose Stimulated Insulin Secretion*

At 5 and 9 weeks post-initial TCDD exposure, 32 male (8 TCDD/HFD, 8 TCDD/Chow, 8 CO/Chow, 8 CO/HFD) and 32 female (8 TCDD/HFD, 8 TCDD/Chow, 8 CO/Chow, 8 CO/HFD) mice underwent a GTT and GSIS as previously described in Aim 1 (*Glucose Tolerance Test and Glucose Stimulated Insulin Secretion at Week 4*).

5.3.4 *Tissue Collection for Histology and RNA Extraction Endpoint*

At 12 weeks following the beginning of treatment, 18 male (5 TCDD/HFD, 4 TCDD/Chow, 5 CO/Chow, 4 CO/HFD) and 19 female (5 TCDD/HFD, 4 TCDD/Chow, 5 CO/Chow, 5 CO/HFD) mice were euthanized for collection of pancreas. Half of the pancreas was

stored for histology, as previously described (General Methods 2.2). The other half of the pancreas, right hepatic lobe, and a piece of perirenal fat were excised and placed into 5 mL of RNAlater for RNA extraction as described above (General Methods 2.5).

5.3.5 *Islet Isolation Endpoint*

At 12 weeks following the beginning of treatment, 16 male (5 TCDD/HFD, 3 TCDD/Chow, 4 CO/Chow, 4 CO/HFD) and 18 female (4 TCDD/HFD, 4 TCDD/Chow, 5 CO/Chow, 5 CO/HFD) mice were anaesthetized with inhalable isoflurane (3-5%, 1L/min) and cardiac blood was collected. Pancreatic islets were isolated, as described before (*Islet Isolation & Pancreatic Dissection)* and stored in 250 µL RNA-later for RNA extraction at 4°C overnight, then -30°C long-term. Furthermore, half of the right lobe of the liver was excised for histology as described previously (General Methods 2.2 *Tissue Processing for* Histology) and sent to the University of Ottawa Heart Institute for processing and embedding in paraffin wax blocks. Pancreatic tissue was sectioned into 5 µm slices using a microtome (Thermo Scientific Microm 355S, Serial: S17081604) then mounted on slides to undergo immunohistochemical staining (see below). Each slide contained 2 pancreatic tissue (with spleen attached) sections.

5.3.6 *Immunohistochemical staining*

To prepare pancreatic tissue for immunohistochemical staining, tissue was deparaffinized by washing in xylene (Fisherbrand, Cat: HC-700-1GAL) 3 times, followed by 2 washes of 100% ethanol, then one wash of 95% ethanol and finally one wash with 70% ethanol (5

minutes per wash). Tissues were washed in PBS for 5 minutes on a shaker then underwent heat induced epitope retrieval (10 minutes, 95ºC) in a microwave (Genex EZ-Retriever System, Serial: MW014-MO-1155) in 10 mM citrate buffer (see Appendix for recipe). After epitope retrieval, slides were washed in distilled water for 5 minutes on a shaker followed by a PBS wash. Sections were circled with a hydrophobic pen (Biolnyx, Cat: H-4000) then bathed in a protein block (Agilent Technologies, Cat: X090930-2) for 30 minutes. After the protein block, 100 µL of diluted primary antibodies were applied to both sections of all slides and incubated in a humid chamber overnight at 4ºC. Primary antibodies include: mouse anti-insulin (1:250; New England Biolabs, Cat: 8138S), mouse anti-glucagon (1:1000; Sigma-Aldrich, Cat: G2654), rabbit anti-somatostatin (1:500; Sigma-Aldrich, Cat: HPA019472), and rabbit anti-insulin (1:200; New England Biolabs, Cat: 3014S). The following morning, slides were washed with PBS for 5 minutes on a shaker 3 times, then 100 µL of diluted secondary antibodies were applied and slides were incubated in a humid chamber at room temperature for 1 hour protected from light. Secondary antibodies include: goat anti-mouse AlexaFluor 488 (1:1000; Invitrogen, CAT: A11029), goat anti-rabbit AlexaFluor 594 (1:1000; Invitrogen, Cat: A11037). All antibodies were validated by the Kieffer Lab. Slides were then washed with PBS for 5 minutes on a shaker 3 times, then approximately 50 µL of mounting medium containing DAPI (Biolynx, Cat: H-1500) was applied followed by a cover slip. Imaging was done on 2-5 islets per pancreatic tissue slice using a fluorescence microscope (EVOS FL Cell Imaging System) at 40x magnification. Cell area of α-, β-, and δ-cells was measured using ImageJ software (National Institute of Health) and the average cell area per islet was calculated per mouse.

5.3.7 *Statistical Analysis*

Statistical analysis was performed using GraphPad Prism software (GraphPad Software Inc., La Jolla, CA). Specific statistical tests are indicated in figures legends. For all analyses, $p < 0.05$ was considered statistically significant. Data are either presented as mean +/- SEM (line graphs) or as bar plots with individual data points overlaid.

5.4 Results

5.4.1 *Body Weight and Blood Glucose Tracking*

There was no effect of HFD-feeding and/or TCDD exposure on female body weight (Figure 5.2A and 5.2B). Regardless of chemical exposure, HFD-fed male mice were significantly heavier than chow-fed control male mice from days 73 to 86 (Figure 5.2E and 5.2F). In both female (Figure 5.2C and 5.2D) and male (Figure 5.2G and 5.2H), HFD-feeding caused fasting hyperglycemia in control and TCDD-exposed mice compared to chow-fed control mice.

5.4.2 *Glucose Homeostasis and Beta Cell Function at Week 4 and Insulin Sensitivity at Week 5*

At 4 weeks post-initial exposure, HFD-fed females exposed to TCDD were significantly hyperglycemic 15 and 30 minutes post-glucose bolus compared to their chow-fed counterparts (Figure 5.3A). This effect was driven by TCDD exposure as HFD-fed control

females had an identical response to their chow-fed counterparts. These data indicate that females are prone to glucose intolerance after 4 weeks of HFD feeding, but only when they were simultaneously exposed to chronic low dose TCDD exposure. Furthermore, there was no discernable effect of diet and/or treatment on *in vivo* insulin secretion following a glucose stimulus of female after 4 weeks of diet and treatment (Figure 5.3B and Figure 5.3C).

Interestingly, HFD-fed male mice were significantly hyperglycemic following a glucose stimulus after 4 weeks of exposure, regardless of chemical exposure. In other words, both TCDD-exposed and control males showed a similar response to HFD feeding (Figure 5.3D), unlike the female mice, which only showed hyperglycemia in the presence of TCDD. As in females, there were no discernable effects of diet and/or treatment on *in vivo* insulin secretion of male mice. (Figure 5.3E and 5.3F). At 5 weeks post-initial exposure, there were no effects of diet and/or treatment on female (Figure 5.6A-C) or male (Figure 5.6D-E) insulin sensitivity.

5.4.3 *Glucose Homeostasis and Beta Cell Function at Week 8 and Insulin Sensitivity at Week 9*

Given another 4 weeks of exposure, HFD-fed females exposed to TCDD were significantly hyperglycemic between 15 to 60 minutes post-glucose bolus compared to their chow-fed counterparts (Figure 5.3G). Furthermore, HFD-fed control females were also hyperglycemic at 30-minutes post-glucose bolus compared to their chow-fed counterparts (Figure 5.3F), but the difference in glucose tolerance between HFD-fed and

chow-fed vehicle-exposed groups was not as pronounced as in the TCDD-exposed females. Moreover, HFD-fed control females produced significantly more insulin (2.54-fold increase) during an *in vivo* GSIS than their chow-fed counterparts indicating that HFD-fed females were appropriately compensating for hyperglycemia by producing more insulin (Figure 5.3H and 5.3I). However, HFD-females exposed to TCDD failed to secrete more insulin in response to HFD-feeding like their corn-oil exposed counterparts. This is interesting given that neither HFD-feeding or TCDD exposure had any affect on the ratio of β- to α-cell area or ratio of β- to δ-cell area (Figure 5.4A and 5.4D) suggesting the hyperinsulinemia was not driven by an increase in β-cell area. Finally, there were no differences in insulin sensitivity in female (Figure 5.5G-I) or male (Figure 5.5J-L) mice. Taken together, these data suggest that TCDD exposure accelerated the development of glucose intolerance in female mice after HFD feeding as well as inhibiting compensatory hyperinsulinemia associated with hyperglycemia.

The same effect of HFD feeding seen 4 weeks earlier persisted in TCDD-exposed and control males (Figure 5.3J). These data suggest that HFD-feeding was the primary driver of hyperglycemia in males while TCDD exposure had no discernable effect on glucose tolerance. In line with female GSIS data, HFD-fed control males trended towards hyperinsulinemia during an *in vivo* GSIS compared to their chow-fed counterparts demonstrating a compensatory mechanism for hyperglycemia due to the HFD (Figure 5.3L). Interestingly, HFD-fed males exposed to TCDD also trended towards hyperinsulinemia compared to their chow-fed counterparts unlike HFD-females exposed to TCDD.

5.4.4 *Endocrine Cell Area Analysis*

Chronic, low dose TCDD exposure was associated with greater total islet area in male mice fed a HFD and the same trend was observed in TCDD-exposed male mice fed chow (Figure 5.4J). Diet and/or chemical exposure had no effect on female (Figure 5.4A) or male (Figure 5.4G) percent β-cell area, female (Figure 5.4B) or male (Figure 5.4H) percent α-cell area, female (Figure 5.4C) or male (Figure 5.4I) percent δ-cell area, female total islet cell area (Figure 5.4D), female (Figure 5.4E) or male (Figure 5.4K) ratio of β- to α-cell area, and female (Figure 5.4F) or male (Figure 5.4L) ratio of β- to δ-cell area. Representative images of female and male pancreatic islets are shown in Figure 5.5.

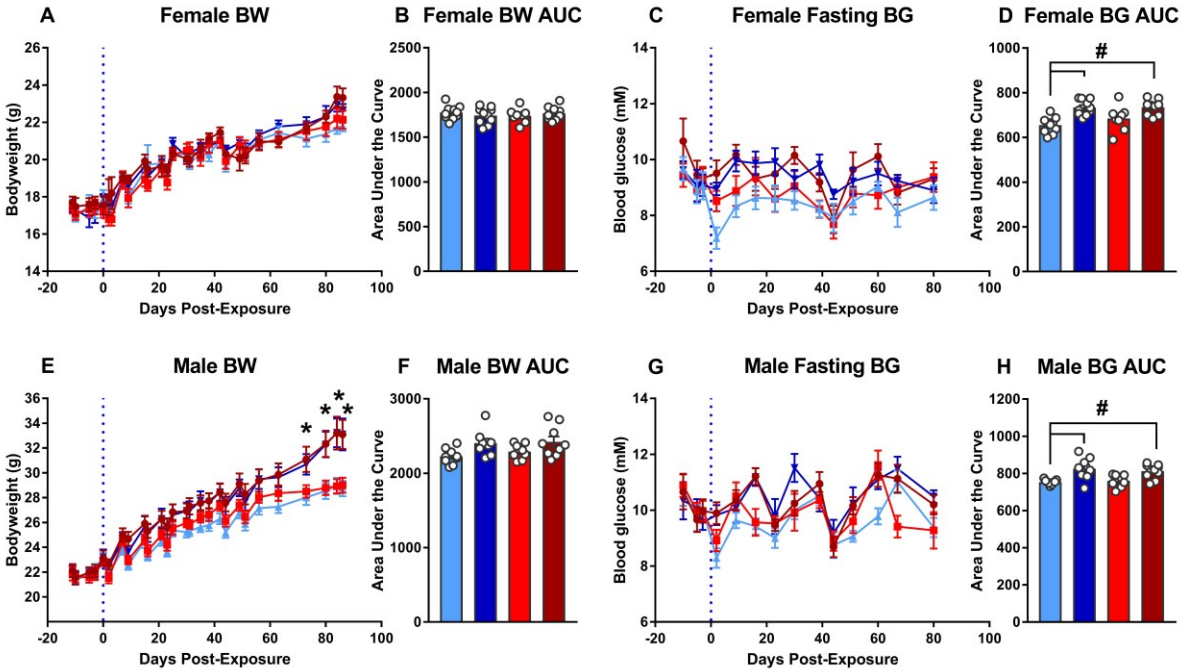

Figure 5.2: Body weight and fasting blood glucose tracking during 'double-hit' experiment. A,E) Body weight of female (A) and male (E) mice compiled from fasted

and non-fasted measurements. **B,F)** Area under the curve of female (B) and male (F) body weight. **C,G)** Blood glucose female (C) and male (G) mice from fasted measurements. **D,H)** Area under the curve of female (D) and male (H) blood glucose. Blue dotted line indicates the beginning of TCDD or corn oil vehicle exposure. # $p < 0.05$, one-way ANOVA with Tukey's post-hoc test for multiple comparisons. * $p < 0.05$, two-way ANOVA with Tukey's post-hoc test for multiple comparisons indicating significant difference between HFD-fed male mice and chow-fed control male mice; see Supplemental Table 4 for detailed ANOVA values. Data are presented as mean +/- SEM.

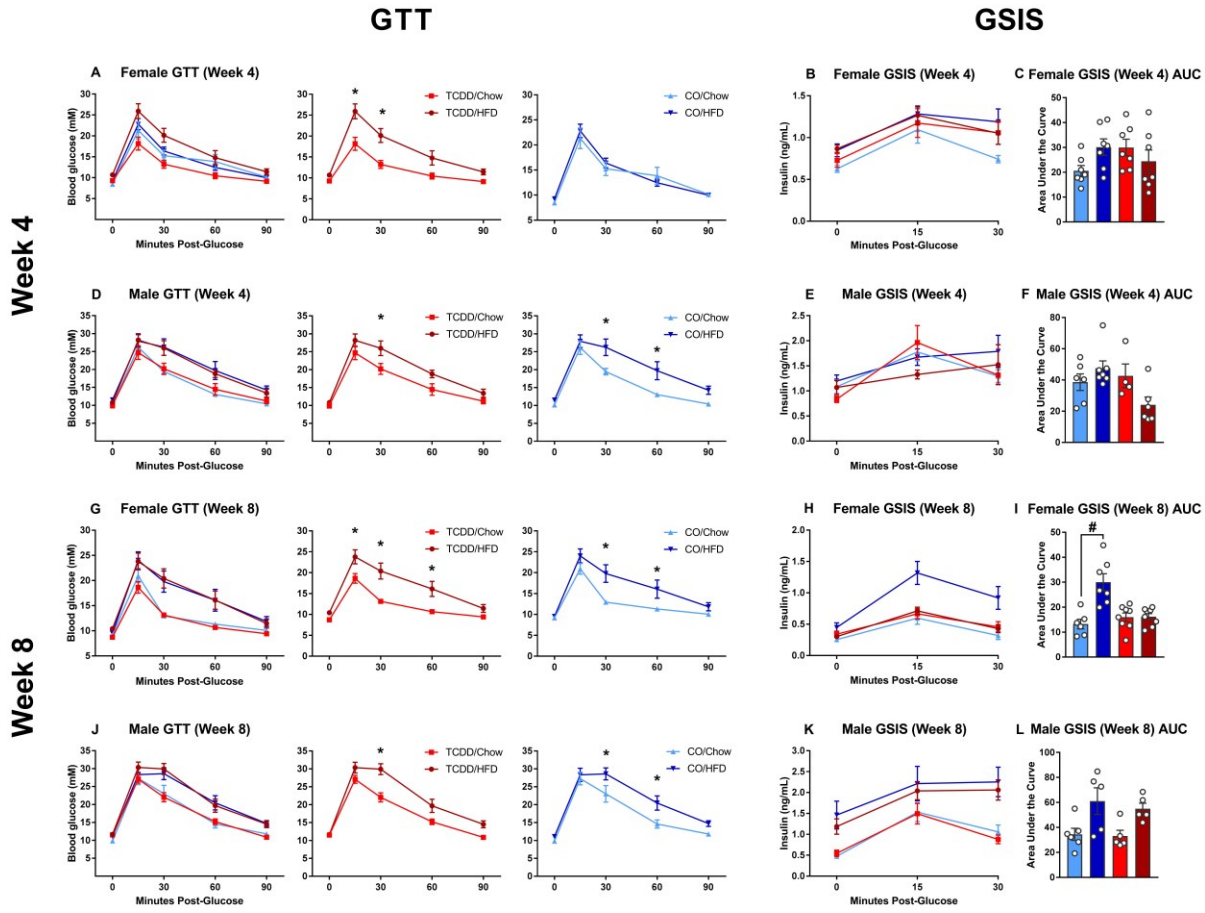

Figure 5.3: *In vivo* metabolic testing during 'double-hit' experiment at 4 and 8 weeks post-initial exposure. A,D) Glucose tolerance test data from female (A) and male (D) mice at 4 weeks post-initial exposure. **B,E)** Glucose stimulated insulin secretion data from female (B) and male (E) mice at 4 weeks post-initial exposure. **C,F)** Area under the curve for glucose stimulated insulin secretion from female (C) and male (F) mice. **G,J)** Glucose tolerance test data from female (G) and male (J) mice at 8 weeks post-initial exposure. **H,K)** Glucose stimulated insulin secretion data from female (H) and male (K) mice at 8 weeks post-initial exposure. **I,L)** Area under the curve for glucose stimulated insulin secretion from female (I) and male (L) mice. * $p < 0.05$, two-way repeated-measures ANOVA with Tukey's post-hoc test for multiple comparisons; see Supplemental Table 5 for detailed ANOVA values. Data are presented as mean +/- SEM.

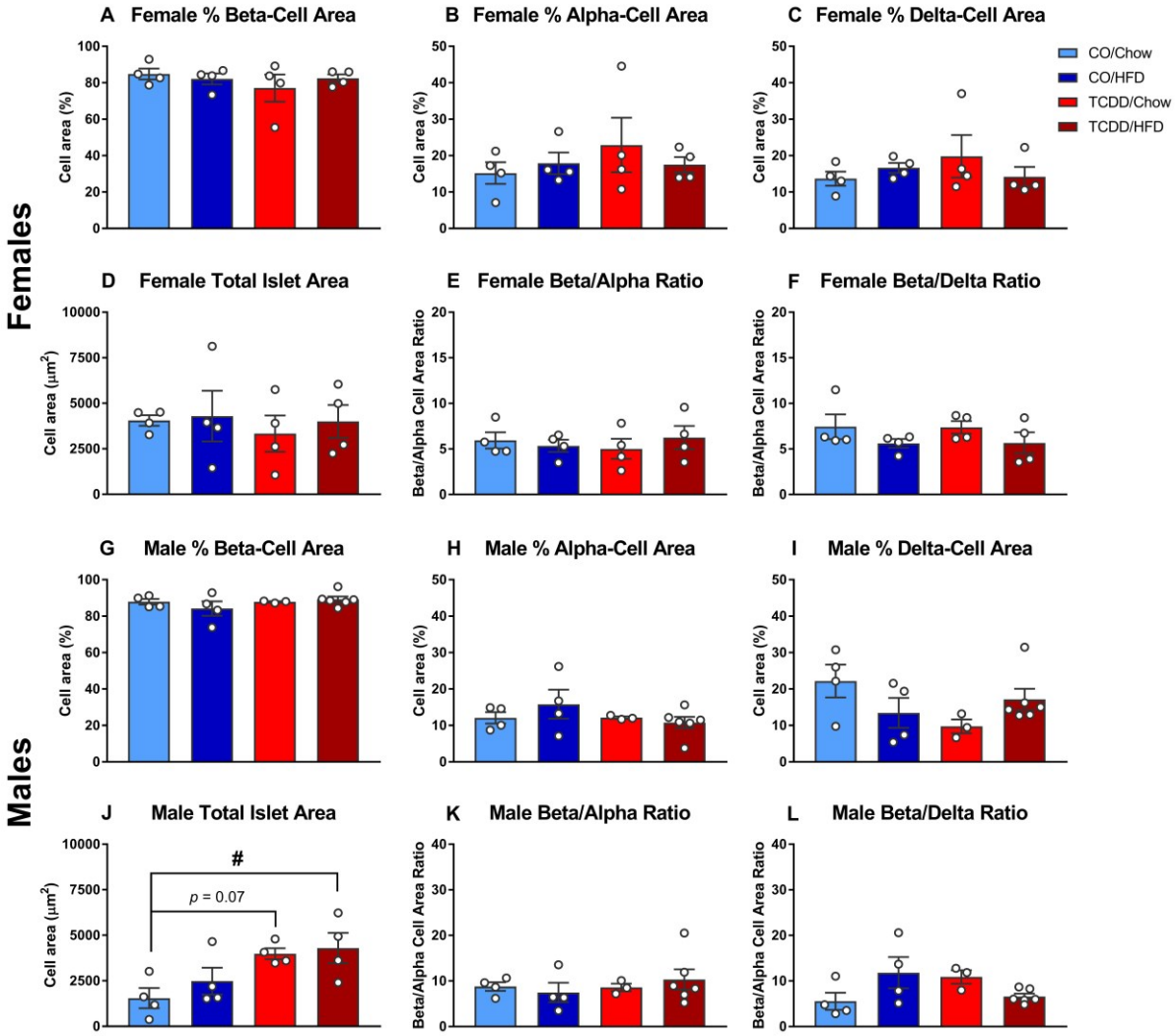

Figure 5.4: Endocrine cell area and ratio of beta/alpha- and beta/delta-cell area from 'double-hit' experiment 12 weeks post-initial exposure. A,G) Beta-cell area of female (A) and male (G) mice. **B,H)** Alpha-cell area of female (B) and male (H) mice. **C,I)** Delta-cell area of female (C) and male (I) mice. **D,J)** Total cell area of female (D) and male (J) mouse islets. **E,K)** Ratio of beta- to alpha-cells in female (E) and male (K) mouse islets. **I,L)** Ratio of beta- to delta-cells in female (I) and male (L) mouse islets. # $p < 0.05$, one-way repeated-measures ANOVA with Tukey's post-hoc test for multiple comparisons; see Supplemental Table 6 for detailed ANOVA values. Data are presented as mean +/- SEM.

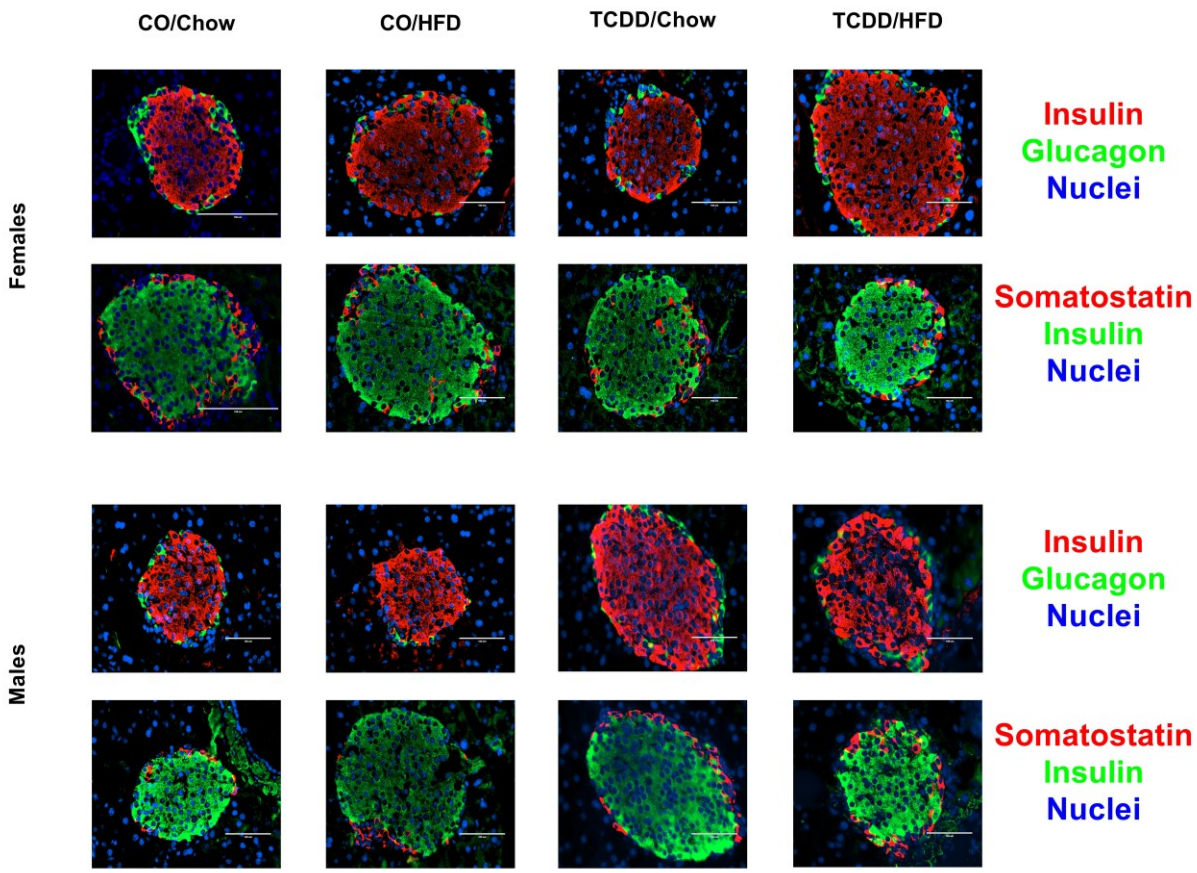

Figure 5.5: Representative images of female and male pancreatic islets from 'double-hit' experiment 12 weeks post-initial exposure. Top row for each sex is co-stained with insulin and glucagon with a DAPI nuclear stain while the bottom row is co-stained with insulin and somatostatin with a DAPI nuclear stain. Scale bar = 100 μm.

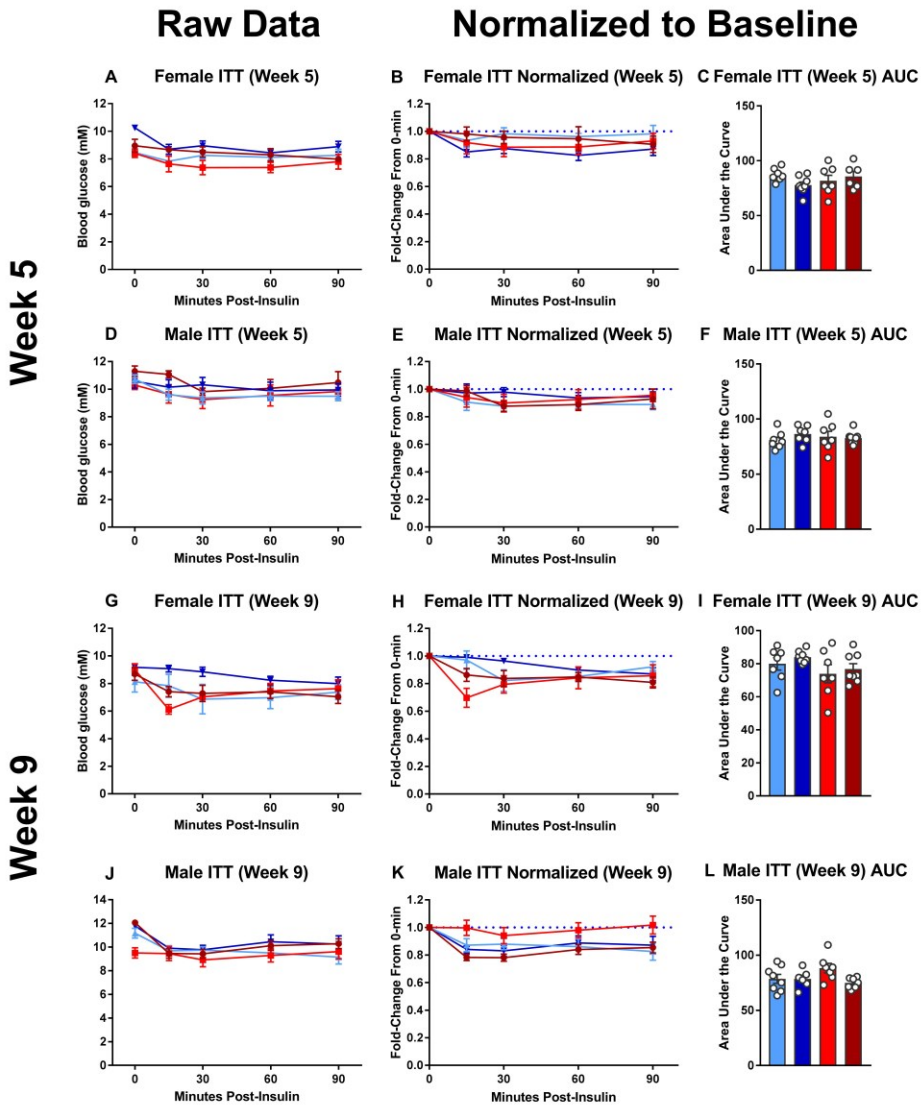

Figure 5.6: Insulin tolerance test during 'double-hit' experiment at 5 and 9 weeks post-initial exposure. A,D) Insulin tolerance test data from female (A) and male (D) mice 5 weeks post-initial exposure. **B,E)** Insulin tolerance test data normalized to baseline from female (B) and male (E) mice. **C,F)** Area under the curve for female (C) and male (F) normalized insulin tolerance test data. **G,J)** Insulin tolerance test data from female (G) and male (J) mice 9 weeks post-initial exposure. **H,K)** Insulin tolerance test data normalized to baseline from female (H) and male (K) mice. **I,L)** Area under the curve for

female (I) and male (L) normalized insulin tolerance test data; see Supplemental Table 7 for detailed ANOVA values. Data are presented as mean +/- SEM.

5.5 Discussion

In female mice, chronic low dose TCDD exposure in conjunction with HFD-feeding accelerated hyperglycemia compared to control females fed chow. Indeed, HFD-fed females exposed to TCDD became hyperglycemic after only 4 weeks compared to their chow-fed counterparts, which remained normoglycemic in response to HFD feeding at 4 weeks. Importantly, HFD-fed control females only became hyperglycemic compared to chow-fed control females after 8 weeks of HFD-feeding. In line with my hypothesis, these data suggest that concomitant TCDD exposure and HFD feeding accelerated the onset of hyperglycemia in female mice. On the contrary, males fed a HFD were hyperglycemic at 4 and 8 weeks compared to their chow-fed counterparts, in line with previous HFD-feeding data (Kim et al, 2014; Liu et al, 2015; Sims et al, 2013) regardless of chemical exposure. As a result, these data indicate that female mice were particularly susceptible to our 'double-hit' model while the hyperglycemia in males was driven by diet.

As previously described (5.1 Introduction), an increase in blood glucose levels promotes increased insulin secretion to return to normoglycemia. Indeed, HFD-fed control females compensated for their hyperglycemia by secreting 2.5 times more insulin than chow-fed control females 8 weeks post initial exposure. Interestingly, HFD-fed females exposed to TCDD did not secrete significantly more insulin than their chow-fed counterparts. This suggests that TCDD exposure in combination with HFD-feeding inhibited the

compensatory hyperinsulinemia in HFD-fed females. This stands in contrast with males as both HFD-fed control males and those exposed to TCDD trended towards hyperinsulinemia with respect to their chow-fed counterparts. This increase in insulin secretion driven by a HFD was not paralleled by an increase in β-cell mass however TCDD exposure increased islet area in male mice regardless of diet. In line with the glucose tolerance data, these data indicate that HFD-fed female mice exposed to TCDD were particularly susceptible to the 'double-hit' model as they failed to compensate for the hyperglycemia. My data demonstrates that the compensatory hyperinsulinemia of HFD-fed control females was not driven by an increase in β-cell mass suggesting that the β-cells of these female mice were secreting more insulin. In the future, gene analysis of transcription factors associated with insulin including *Ins1* and *Ins2* along with insulin secretion such as *Nkx6.1* and *MafA* (as described in 1.1.2 *β-Cell Transcription Factors*) will provide insight into HFD-driven changes to insulin synthesis and secretion in female mice.

HFD-feeding had no effect on female body weight in line with previous reports (Pettersson et al, 2012; Yang et al, 2014) regardless of chemical exposure. However, the HFD caused fasting hyperglycemia in female mice, in line with previous data (Oliveira et al, 2015; Winzel and Ahrén, 2004) in the presence or absence of TCDD exposure. Not all researchers have found that HFD-feeding promoted fasting hyperglycemia in female mice (for example, see Pettersson et al, 2012), likely due to environmental differences in the experimental facility such as animal housing and handling frequency. Importantly, HFD-fed male mice became significantly heavier than chow-fed mice after 73 days of HFD-feeding in line with previous research (Kim et al, 2014; Liu et al, 2015; Sims et al, 2013)

whereby HFD-feeding caused males to gain weight regardless of chemical exposure. Given than that HFD-fed male mice only became heavier than their chow-fed counterparts after 73 days of HFD-feeding, it is predicted that a longer experimental timeframe would exacerbate the trend in HFD-fed male body weight to become significantly heavier than their chow-fed counterparts. Furthermore, males fed a HFD had elevated fasting blood glucose in line with previous research (Kim et al, 2014). In sum, HFD-feeding only promoted weight gain in male mice, but not females, whereas it caused fasting hyperglycemia in both sexes.

Contrary to my hypothesis, no changes in insulin sensitivity in either sex regardless of diet or chemical exposure were observed after 5 and 9 weeks of exposure. Interestingly, using a similar dosage of insulin, Sims and colleagues (2013) also reported that HFD-feeding induced no changes in insulin sensitivity of male mice. Given that HFD-fed males trended towards hyperinsulinemia at 4 and 8 weeks post-initial exposure compared to their chow-fed counterparts, a decrease in insulin sensitivity was predicted. In the future, a higher dose of insulin could be utilized, closer to 1.0 U/kg (see Fraulob et al, 2010). Furthermore, sexual dimorphism in insulin sensitivity has been well established with pre-menopausal women being less susceptible to insulin resistance than men (Geer and Shen, 2000). Finally, the C57BL/6 strain of mice is not homogenous across sub-strains with respect to the development of diet-induced insulin resistance and the sub-strain employed in this experiment, C57BL/6J, does not consistently develop diet-induced insulin resistance (Fisher-Wellman et al, 2016; Gareski et al, 2009).

Taken together, these data lend support to my hypothesis that a ‘double-hit’ of TCDD exposure and HFD-feeding was more deleterious that either in isolation. In particular, my

hypothesis was correct only in female mice whereby concomitant TCDD exposure and HFD-feeding accelerated hyperglycemia after 4 weeks while inhibiting compensatory hyperinsulinemia as seen in control HFD-fed female mice.

CHAPTER 6: Discussion

Dioxin exposure is linked to a modest increase in diabetes incidence in humans; however the mechanism remains to be elucidated. My thesis sought to investigate the effects of chronic, low dose TCDD exposure in C57BL/6 mice on glucose homeostasis and β-cell function along with the role of TCDD-mediated *Cyp1a1/1a2* induction. My research demonstrated that chronic, low dose *in vivo* TCDD exposure was not sufficient to produce diabetic-like pathology in mice after 4 weeks of exposure. However, female mice were more susceptible to the metabolic disrupting effects of a 'double-hit' concurrent TCDD exposure and HFD-feeding. Importantly, male and female mice differed in their response to *ex vivo* TCDD exposure along with the role of Cyp1a1/1a2 enzymes during exposure.

Within our experimental timeframe, chronic, low dose *in vivo* TCDD exposure did not produce diabetic-like pathology in male WT C57BL/6 mice after 4 weeks of exposure. Although male mice had fasting hypoglycemia after *in vivo* TCDD exposure, my data contrasts from previous reports using one-time micromolar TCDD administration (see 1.6.3 *Effects of TCDD on Mammalian Models*) as the trend was reversing to normoglycemia at the experimental endpoint. Furthermore, this effect was not reproducible in chow-fed TCDD-exposed male mice during my 12 week 'double-hit' experiment. Given that we used a dioxin concentration of approximately 100-1000 times

lower than previously reported (Kurita et al, 2009; Novelli et al, 2005), my data indicates that male murine exposure to nanomolar quantities of dioxin does not mimic micromolar exposure with respect to diabetic-like pathology, at least within the timeframe of my experiments. In this way, chronic, low dose *in vivo* exposure to TCDD in male mice using quantities relevant to human exposure is not enough to negatively impact blood glucose homeostasis and insulin secretion on its own. That being said, a limitation of this study is the relatively short-term nature of the exposure. Lifetime exposure in humans would equate to approximately 2 years in mice and a study of this nature would not be realistic for an MSc thesis project. Regardless, these data may have implications in human toxicology whereby chronic, low dose TCDD exposure by itself may not be causal in prompting diabetic-like pathology in men. Rather, my research highlights significant differences in response to chronic, low dose TCDD exposure between sexes. In particular, my data indicates that a 'double-hit' of TCDD exposure in conjunction with another metabolic stressor such as a HFD is sufficient to at least transiently promote diabetic-like pathology in female mice.

During my 'double-hit' TCDD and HFD-feeding experiment, HFD-fed females exposed to TCDD had accelerated hyperglycemia at 4 weeks post-initial exposure compared to their HFD-fed control counterparts. This is interesting given that females did not gain weight after 12 weeks HFD-feeding nor were there any changes to insulin sensitivity due to diet and/or chemical exposure. Importantly, HFD-fed females exposed to TCDD did not develop compensatory hyperinsulinemia unlike their HFD-fed control female counterparts. A possible explanation for the hyperglycemia and lack of compensatory hyperinsulinemia in HFD-fed female mice exposed to TCDD could be a change in β-cell

glucose sensitivity or glucose uptake. In other words, β-cells of these mice may have an impaired ability to sense and/or uptake glucose and therefore are unable to mount an appropriate compensatory hyperinsulinemic response like their HFD-fed control counterparts. In line with this, a decrease in pancreatic glucose uptake following *in vivo* micromolar exposure of TCDD has been previously reported (Novelli et al, 2005), albeit it in male mice. Although Novelli and colleagues (2005) did not find differences in *Glut-2* expression of male mice, others have found decreases in glucose uptake following *in vivo* nanomolar TCDD exposure in male and female mice, rats and guinea pigs (Enan and Matsumura 1994) and in immortalized cells (Sutter et al, 2019; Tonak et al, 2007). In the future, analysis of genes associated with β-cell glucose sensitivity and uptake such as *Gck* and *Glut-2* in isolated islets from my 'double-hit' experiment is warranted. Furthermore, genes related to other aspects of insulin secretion such as cation channels (see 1.2.1 *Glucose-Stimulated Insulin Secretion*) may reveal alternative pathways to understand the phenotype observed in HFD-fed female mice exposed to TCDD. Taken together, my data is in line with human epidemiological research highlighting women as being particularly susceptible to T2D following dioxin exposure (Eskenazi et al, 2004; Warner et al, 2013).

My research revealed that following chronic, low dose *in vivo* TCDD exposure, Cyp1a1/1a2 enzymes do not play a significant role in modulating blood glucose homeostasis or insulin secretion in male mice. However, my *ex vivo* data revealed that the induction of Cyp1a1/1a2 enzymes is likely deleterious with respect to insulin secretion following a high glucose stimulus in male isolated islets. Indeed, knocking out *Cyp1a1/1a2* in male isolated islets decreased insulin secretion to levels similar to that of WT male

islets exposed to TCDD. Furthermore, during TCDD exposure, KO male islets secreted more insulin than WT male islets. In contrast to females whereby the enzyme likely plays a constitutive role that suppresses insulin secretion, I speculate that TCDD-mediated *Cyp1a1/1a2* induction in male mice may be deleterious. My *ex vivo* data from male mice is in line with the classical idea that *Cyp1a1* induction is dangerous (as described in 1.6.2 *Animal TCDD Metabolism*). Direct TCDD exposure is speculated to decrease insulin secretion in WT male mice by an AhR-mediated pathway as male mice lacking AhR are functionally immune to the effects of *in vivo* micromolar TCDD exposure (Kurita et al, 2009). Given that Cyp1a2 is thought to be the enzyme that metabolizes TCDD in rodents (Diliberto et al, 1997), unmetabolized TCDD likely persists in KO male murine islets and continues to stimulate the AhR and suppress insulin secretion. Taken together, my research suggests that TCDD-mediated *Cyp1a1/1a2* induction in male pancreatic islets is deleterious with respect to insulin secretion.

My 4 week *in vivo* exposure to TCDD using WT and KO mice revealed that Cyp1a1/1a2 enzymes may play a role in insulin sensitivity in female mice. Following chronic, low dose *in vivo* TCDD exposure, female KO mice were insulin resistant compared to control KO female mice. In line with classical ligand-mediated receptor upregulation, an increase in female KO islet insulin secretion would support insulin resistance in TCDD-exposed female KO mice. However, there was no difference in *in vivo* insulin secretion between TCDD-exposed and control KO female mice. Rather, insulin intolerance seen in my *in vivo* experiment is likely caused by changes in insulin action at target tissues associated with TCDD-mediated *Cyp1a1/1a2* induction. As previously described (Discussion 3.5), males and females differ in insulin sensitivity because of female sex hormones

potentiating insulin sensitivity. Due to the role of Cyp1a1/1a2 enzymes in the metabolism of estrogens, this effect is likely increased by the lack of estrogen metabolism following *Cyp1a1/1a2* deletion. Cyp1a1/1a2 enzymes are broadly expressed in many tissues including insulin target tissues and as a result, a global *Cyp1a1/1a2* deletion is not an ideal model to study the role of *Cyp1a1* induction in the endocrine pancreas. In the future, the use of pancreas-specific *Cyp1a1* KO model by driving Cyp1a1-deletion through the *Ins1* promoter will provide more insight into the role of the enzyme in the pancreas during TCDD exposure. This will help elucidate if insulin intolerance in TCDD-exposed female KO islets is mediated by deletion of *Cyp1a1/1a2* in insulin target tissues.

In isolated female islets, my *ex vivo* data suggests that Cyp1a1/1a2 enzymes have a constitutive role in suppressing insulin secretion. In this way, *Cyp1a1* induction following xenobiotic exposure in isolated female islets is speculated to neither be protective or deleterious. This may be the product of biochemical shunting of arachidonic acid in WT pancreatic islets as an increase in Cyp1a1 enzymes, an enzyme that hydroxylates arachidonic acid, would increase arachidonic acid metabolism. With the deletion of *Cyp1a1/1a2*, there may be a subsequent increase in arachidonic acid concentration in pancreatic islets due to their lack of metabolism. With an increase in arachidonic acid in pancreatic islets, I would predict a subsequent increase in insulin secretion due to stimulation by unmetabolized arachidonic acid (summarized in Figure 6). Arachidonic acid is known to stimulate insulin secretion (for a comprehensive review, see Robertson et al, 1986) likely through fatty acid receptors such as the GPR40, which is known to potentiate insulin secretion following a glucose stimulus (see 1.2.2 *Lipid-Stimulated Insulin Secretion*). In WT female mice, arachidonic acid is speculated to be efficiently

metabolized by constitutively expressed Cyp1a1/1a2 enzymes, thereby negating its insulin secretion-potentiating effects. This pathway may be different in females due to interaction between the AhR and the nuclear ERα (as described in Discussion 3.5). Given that the degree of *Cyp1a1* mRNA induction between sexes was comparable, the difference likely lies in the myriad of secondary messenger effector proteins associated with the AhR and female sex hormone pathways. In this way, Cyp1a1 is speculated to be a key regulatory enzyme in female pancreatic islets that modulates the degree of insulin secretion by metabolizing insulin secretion-potentiating lipids, such as arachidonic acid.

A limitation of my research is that the only gene analysis I conducted was to validate *Cyp1a1* induction in WT isolated islets exposed to TCDD and the lack thereof in islets lacking *Cyp1a1/1a2* exposed to TCDD. To address this, mRNA from isolated islets from my *ex vivo* TCDD exposure in *Cyp1a1/1a2* KO and WT isolated islets experiment (Chapter 4), as well as the 12 week *in vivo* 'double-hit' TCDD exposure and HFD-feeding experiment in WT mice (Chapter 5) will undergo whole genome analysis using TempO-Seq® (BioSpyder) in collaboration with Health Canada. By exploring genetic differences across the whole genome, I hope to understand the role of TCDD-mediated *Cyp1a1* induction in isolated islets as well as the effect of my *in vivo* 'double-hit' model. I predict that the Tempo-Seq® experiment will highlight sexual dimorphism in genes associated with insulin secretion from both sets of islets sent for analysis. Specifically, I predict that pancreatic islets from female mice lacking *Cyp1a1/1a2* will reveal constitutive differences in genes associated with insulin secretion compared to WT female mice. Furthermore, I predict that islets from WT female mice exposed to my 'double-hit' model will demonstrate differences in insulin secretion compared to chow-fed female mice exposed to TCDD and

HFD-fed control female mice. Finally, I predict that WT male pancreatic islets directly exposed to TCDD will display differences in insulin secretion genes compared to WT male control islets and male islets lacking *Cyp1a1/1a2* directly exposed to TCDD. Another limitation of my research is that the immunohistochemical analysis of pancreatic tissue derived from my 12 week 'double-hit' experiment is still preliminary. As tissue sections were not exhaustively analyzed to calculate, conclusions about the effect of diet and/or chemical treatment on endocrine cell area, total islet area, and proportion of endocrine cells in islets remain subject to change.

Taken together, my research highlights significant differences between male and female mice in two aspects. The first is that TCDD-mediated *Cyp1a1* induction in male islets is likely deleterious for insulin secretion, while Cyp1a1 may play a constitutive modulatory role in female islets. The second major finding is that female mice are more sensitive to a 'double-hit' of TCDD-exposure and HFD-feeding with respect to glucose tolerance and fail to mount a compensatory hyperinsulinemic response. With regard to human TCDD exposure, my research suggests that females may be at particularly high risk for developing diabetic-like pathology when exposed to another metabolic stressor such as a HFD.

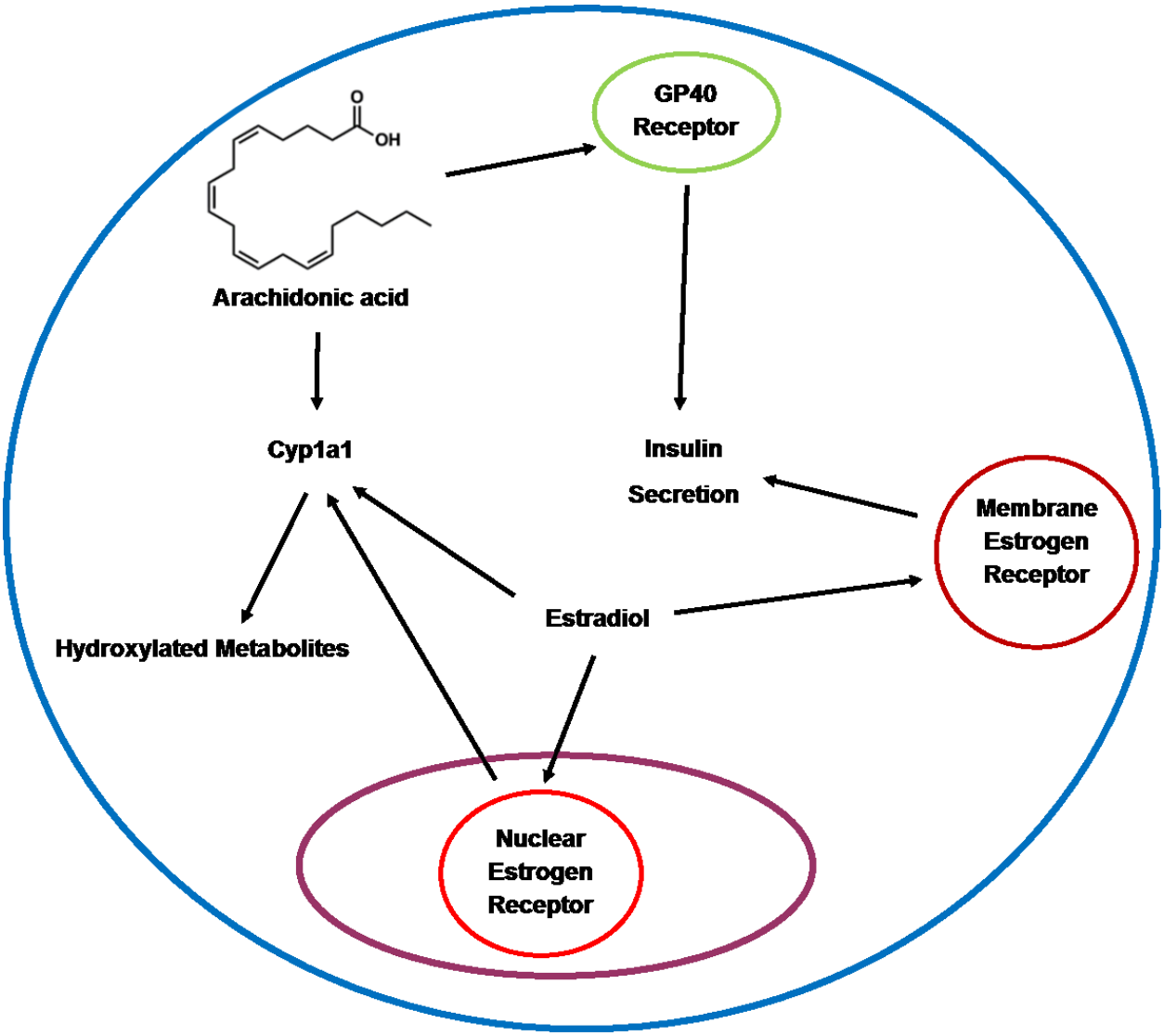

Figure 6: Proposed biochemical pathway overlap between lipid-stimulated insulin secretion, estrogen and Cyp1a1 enzyme metabolism.

CHAPTER 7: Conclusion

In line with human epidemiological data, my research reveled adult female mice as being more susceptible to metabolic disrupting effects of a 'double-hit' of chronic, low dose TCDD exposure and HFD-feeding than male mice. These data highlight the need for further research into understanding how POP exposure may impact female metabolic health.

The goal of my thesis was to understand how chronic, low dose TCDD exposure promotes diabetic pathology in C57BL/6 mice and the role of Cyp1a1/1a2 enzymes during exposure. To achieve this goal, my first aim was to determine the effect of chronic, low dose TCDD exposure in wild type and systemic *Cyp1a1/1a2* KO mice on glucose homeostasis and β-cell function. I found that chronic, low dose *in vivo* TCDD exposure had no significant effect on blood glucose homeostasis and insulin secretion or function in the presence or lack of Cyp1a1/1a2 enzymes. My second aim was to determine the effects of direct, low dose TCDD exposure in isolated pancreatic islets with and without *Cyp1a1/1a2* gene deletion. My research suggests that TCDD-mediated *Cyp1a1/1a2* induction is associated with decreased insulin secretion in WT male pancreatic islets while Cyp1a1/1a2 enzymes play a constitutive role in modulating insulin secretion in WT female mice. My third aim was to determine the effect of concurrent HFD and chronic, low dose TCDD exposure in wild type mice on glucose homeostasis and β-cell function. My data demonstrated that female mice were more susceptible to a 'double-hit' of *in vivo* TCDD exposure and HFD-feeding with respect to glucose tolerance and insulin secretion. In the future, whole genome analysis may reveal genetic differences in biochemical pathways regulating insulin secretion between male and female mice during an *in vivo*

'double-hit' and *ex vivo* TCDD exposure. Taken together, my data highlights females as particularly vulnerable to developing diabetic-like pathology following TCDD exposure, but only if exposure occurs in conjunction with another metabolic stressor such as a HFD.

Appendix

8.1 Solutions for Islet Isolation and Ex Vivo GSIS

Recipe for HBSS without Ca^{2+}

To make 1000 mL of HBSS without Ca^{2+}, 8 g of sodium chloride, 0.4 g of potassium chloride, 0.5g of sodium phosphate, 0.55g of potassium phosphate, 2.38g of (4-(2-hydroxyethyl)-1-piperazineethanesulfonic acid) (HEPES), 0.2g of magnesium chloride, and 0.9g of anhydrous dextrose were mixed in 980mL of double distilled water. The mixture was sterilized with 0.22um bottle-top filter and stored at room temperature. All chemicals were purchased from Fisher Scientific.

Recipe for HBSS with Ca^{2+}

To make 1000mL of HBSS with Ca^{2+}, 8g of sodium chloride, 0.4g of potassium chloride, 0.5g of sodium phosphate, 0.55g of potassium phosphate, 2.38g of (4-(2-hydroxyethyl)-1-piperazineethanesulfonic acid) (HEPES), 0.2g of magnesium chloride, 0.9g of anhydrous dextrose, and 0.147g of calcium chloride dihydrate were mixed in 980mL of double distilled water. Mixture was sterilized with 0.22um bottle-top filter and stored at room temperature. All chemicals were purchased from Fisher Scientific.

Recipe for KRBB

To make 1000mL of KRBB, 57.5mL of 2M sodium chloride, 5mL of 1M potassium chloride, 2g of sodium bicarbonate, 2.5mL of 1M calcium chloride, 1mL of 1M magnesium chloride, 10mL of HEPES, and 1g of bovine serum albumin were mixed in 921mL of double distilled water. The mixture was sterilized with 0.22um bottle-top filter and the KRBB solution was used immediately as BSA degrades. All chemicals were purchased from Fisher Scientific.

8.2 Solutions for Genotyping

Recipe for 11.25% Chelex

To make 11.25% Chelex, thoroughly mix 4.5g Chelex (Bio-Rad, Cat: 142-1253) in 40mL of double distilled water and store at -30°C.

Recipe for Chelex Solution

To 40mL of 11.25% Chelex, 400uL of proteinase K (Acros Organics: Cat: BP1700-100*),* 400uL of 10% Tween 20 (Acros Organics, Cat: BP337-100), 1mL of protein kinase K (0.01g in 1mL of RNase-free water, SPECIFY) were added. The Chelex solution was vortex after preparation and prior to use and stored at -30°C.

Recipe for Genotyping MasterMix-Primer Solution

To make enough MasterMix-Primer Solution for 1uL of DNA sample, 12.5uL iProof HF Master Mix (Bio-Rad, Cat: 1725310), and 1.25uL Cyp1a1 primer mixture were mixed in 10.25uL RNAse-free water (Invitrogen, Cat: 10977015).

Recipe for Genotyping Cyp1a1 Primer Mixture

Mix 10uL of each primer in 60uL of RNAse-free water. Vortex thoroughly after preparation and prior to use. Store at -30°C.

Recipe for 2% Agarose Gel

To make enough 2% agarose gel for 1 PCR run, 2g agarose (Bio-Rad, Cat: 1613101), and 10 uL of SYBR DNA gel stain (Thermo Fisher Scientific, Cat: S33102) were mixed together in 100uL of 1x Tris-acetate EDTA (TAE) buffer (SPECIFY). The mixture was placed in a conventional microwave for 1:30 minutes and cooled by running water on the sides of the container. The mixture was poured into a gel mould and bubbles that formed were removed by using a pipet tip and allowed 30 minutes to set.

Recipe for Genotyping DNA Loading Buffer

5x DNA Loading buffer (Bio-Rad, Cat: 1610767) was diluted with RNAse-free water (Invitrogen, Cat: 10977015) to make 2x and stored at room temperature.

Thermocycler Genotyping Protocol

1. 98°C, 1 minute
2. 98°C, 5 seconds
3. 63°C, 10 seconds
4. 72°C, 20 seconds
5. GOTO step 2, 34x
6. 72°C, 3 minutes
7. 4°C, infinite

8.3 Solutions of PCR

DNase MasterMix Recipe

To prepare a 2mL DNase MasterMix solution from the iScript gDNA clear cDNA Synthesis Kit (Bio-Rad, Cat: 1725035), 0.5uL iScript DNase was mixed with 1.5uL iScript DNase Buffer and kept on ice.

Recipe for 10 μM Forward/Reverse Primer Mix

To make a 10uM primer mix from stock solutions, 10uL of forward primer with 10uL of reverse primer were mixed in 80uL RNAse-free water. The mixture was vortexed thoroughly after preparation and before use. The mixture was stored at -30°C and thawed on ice when ready to use.

Recipe for qPCR MasterMix

To make 9uL of MasterMix for each reaction, 0.4uL of forward/reverse primer mix and 5uL of the corresponding Supermix (SensiFAST SYBR No-ROX, Bioline, Cat: BIO-980050; Sso Advanced Universal SYBR Green Supermix, Bio-Rad, Cat: 1725271) were mixed in 3.6uL RNAse-free water. Note, if multiple primers were being run on the same plate, separate MasterMixes for each primer set were made. The MasterMix was kept on ice until ready to use and mixed by inversion 10 times and centrifuged (1000rpm, 1 minute, room temperature) prior to use.

Reconstituting Primers for 100 μM Stock

To make a 100 μM primer stock solution, the primer was resuspended in the appropriate amount of RNase-free water.

8.4 Solution for Immunohistochemistry

Recipe for 10 mM Citrate Buffer

To make 1 L of 10 mM citrate buffer, dissolve 2.94g of sodium citrate (Fisher Scientific, Cat: S279-500) in 1 L of double distilled water. Using 1N HCl, adjust pH to 6.0 then slowly add 0.5 mL of Tween 20 (Fisher Scientific, Cat: BP337-100).

Bibliography

Aguilar-Bryan L, Bryan J (1999) Molecular biology of adenosine triphosphate-sensitive potassium channels. Endocr Rev 20(2): 101-135.

Ahrén B, Gudbjartsson T, Al-Amin AN, Mårtensson H, Myrsén-Axcrona U, Karlsson S, Mulder H, Sundler F (1999) Islet perturbations in rats fed a high-fat diet. Pancreas 18: 75-83.

Ahrén B, Simonsson E, Scheurink AJ, Mulder H, Myrsén U, Sundler F (1997) Dissociated insulinotropic sensitivity to glucose and carbachol in high-fat diet-induced insulin resistance in C57BL/6J mice. Metab Clin Exp 46: 97-106.

Allen JR, Norback DH (1973) Polychlorinated biphenyl- and triphenyl-induced gastric mucosal hyperplasia in primates. Science 179: 498-499.

Allen JR, Van Miller JP, Norback DH (1975) Tissue distribution, excretion and biological Effects of [^{14}C]tetrachlorodibenzo-*p*-dioxin in Rats. Cosmet Toxicol 13: 501-505.

American Diabetes Association (2010) Diagnosis and Classification of Diabetes Mellitus. Diabetes Care 33(1): S62-S69s.

Angrish MM, Dominici CY, Zacharewski TR (2013) TCDD-elicited effects on liver, serum, and adipose lipid composition in C57BL/6 mice. Toxicol Sci 131(1): 108-115.

Angrish MM, Mets BD, Jones AD, Zacharewski TR (2012) Dietary fat is a lipid source in 2,3,7,8-tetrachlorodibenzon-*p*-dioxin (TCDD)-elicited hepatic steatosis in C57BL/6 mice. Toxicol Sci 128(2): 377-386.

Araki E, Lipes MA, Patti ME, Brüning JC, Haag B 3rd, Johnson RS, Kahn C (1994) Alternative pathway of insulin signalling in mice with targeted disruption of the IRS-1 gene. Nature 372(6502):186-190.

Ashcroft FM, Harrison DE, Ashcroft SJ (1984) Glucose induces closure of single potassium channels in isolated rat pancreatic beta- cells. Nature 312:446–448.

Ashcroft FM, Rorsman P (1989) Electrophysiology of the pancreatic β-cell. Prog Biophys Mol Biol 54: 87–143.

Atkinson MA, Eisenbarth GS, Michels AW (2015) Type 1 diabetes. Lancet 383(9911): 69-82.

Banks YB, Birnbaum LS (1991) Absorption of 2,3,7,8-tetrachlorodibenzo-*p*-dioxin (TCDD) after low dose dermal exposure. Toxicol App Pharmacol 107: 302-310.

Bansal N (2015) Prediabetes diagnosis and treatment: A review. World J Diabetes 6(2): 296-303.

Bao S, Jacobson DA, Wohltmann M, Bohrer A, Jin W, Philipson LH, Turk J (2008) Glucose homeostasis, insulin secretion, and islet phospholipids in mice that overexpress iPLA2b in pancreatic b-cells and in iPLA2b-null mice. Am J Physiol Endocrinol Metab 294: E217–E229.

Beischlag TV, Perdew GH (2005) ER alpha-AHR-ARNT protein-protein interactions mediate estradiol-dependent transrepression of dioxin-inducible gene transcription. J Biol Chem 280(22): 21607-21611.

Bertazzi PA & di Domenica A (2003) Health consequences of the Seveso, Italy, accident. In Dioxin and Health, 2nd ed. Schecter A, Gasiewicz TA, eds. Wiley, Hoboken, NJ, USA. pp. 827-853.

Bertazzi PA, Bernucci I, Brambilla G, Consonni D, Pesatori AC (1999) The Seveso studies on early and long-term effects of dioxin exposure: A review. Environ Health Perspect 106(2): 625-633.

Brewster DW, Banks YB, Clark AM, Birnbau LS (1989) Comparative dermal absorption of 2,3,7,8-tetrachlorodibenzo-p-dioxin and the polychlorinated dibenzofurans. Toxciol Appl Pharmcol 97: 156-166.

Brewster DW, Matsumura F (1984) TCDD (2,3,7,8-tetrachlorodibenzo-p-dioxin) reduces lipoprotein lipase activity in the adipose tissue of the guinea pig. Biochem Biophys Res Commun 122: 810-817.

Briaud I, Kelpe CL, Johnson LM, Tran PO, Poitout V (2002) Differential effects of hyperlipidemia on insulin secretion in islets of langerhans from hyperglycemic versus normoglycemic rats. Diabetes 51: 662-668.

Briscoe CP, Tadayyon M, Andrews JL, Benson WG, Chambers JK, Eilert MM, Ellis C, Elshourbagy NA, Goetz AS, Minnick DT, Murdock PR, Sauls HR Jr, Shabon U, Spinage LD, Strum JC, Szekeres PG, Tan KB, Way JM, Ignar DM, Wilson S, Muir AI (2003) The orphan G protein-coupled receptor GPR40 is activated by medium and long chain fatty acids. J Biol Chem 28(278): 11303-11311.

Brunzell JD, Robertson RP, Lerner RL, Hazzard WR, Ensinck JW, Bierman EL, Porte D Jr (1976) Relationships between fasting plasma glucose levels and insulin secretion during intravenous glucose tolerance tests. J Clin Endocrinol Metab 42(2): 222-229.

Buettner R, Scholmerich J, Bollheimer LC (2007) High-fat diets: modeling the metabolic disorders of human obesity in rodents. Obesity (Silver Spring) 15: 798-808.

Buu-Hoi NP, Chanh PH, Sesque G, Azum-Gelade M, Saint-Ruf G (1972) Organs as targets of “dioxin” (2,3,7,8-tetrachlorodibenzo-p-dioxin) intoxication. Naturwissenschaften 59: 174-175.

Calvert GM, Sweeny MH, Deddens J, Wall DK (1999) Evaluation of diabetes mellitus, serum glucose, and thyroid function among United States workers exposed to 2,3,7,8-tetrachlorodibenzo-p-dioxin. Occup Environ Med 56: 270-276.

Cerf ME (2013) Beta Cell Dysfunction and Insulin Resistance. Front Endocrinol (Lausanne) 4(37): 1-12.

Chapman DE, Schiller CM (1985) Dose-related effects of 2,3,7,8-tetrachlorodibenzo-*p*-dioxin (TCDD) in C57BL/6J and DBA/2J mice. Toxicol Appl Pharmacol 78: 147-157.

Chen C, Cohrs CM, Stertmann J, Bozsak R, Speier S (2017) Human beta cell mass and function in diabetes: Recent advances in knowledge and technologies to understand disease pathogenesis. Mol Metab 6(9): 943-957.

Chobtang J, de Boer IJM, Hoogenboom RLAP, Haasnoot W, Kijlstra A, Meerburg BG (2011) The need and potential of biosensors to detect dioxins and dioxin-Like polychlorinated biphenyls along the milk, eggs and meat food chain. Sensors (Basel) 11(12): 11692-11716.

Clarke J, Flatt PR, Barnett CR (1997) Cytochrome P450 1A-like protein expressed in the islets of Langerhans and altered pancreatic β-cell secretory responsivenss. Brit J Pharmacol 121: 389-394.

Cole P, Trichopoulos D, Pastides H, Starr T, Mandel JS (2003) Dioxin and cancer: a critical review. Regul Toxicol Pharmacol 38: 378-388.

Collins JJ, Bodner K, Aylward LL, Wilken M, Swaen G, Budinksy R, Rowlands C, Bodnar C (2009) Mortality rates among workers exposed to dioxins in the manufacture of pentachlorophenol. J Occup Environ Med 51(10): 1212-1219.

Committee to Review the Health Effects in Vietnam Veterans of Exposure to Herbicides (Ninth Biennial Update); Board on the Health of Select Populations; Institute of Medicine. Veterans and Agent Orange: Update 2012. Washington (DC):

National Academies Press (US); 2014 Mar 6. 3, Exposure to the Herbicides Used in Vietnam.

Consonni D, Pesatori AC, Zocchetti C, Sindaco R, D'Oro LC, Rubagotti M, Bertazzi PA (2008) Mortality in a population exposed to dioxin after the Seveso, Italy, accident in 1976: 25 years of follow-up. Am J Epidemiol 167: 847-858.

Copps KD, White MF (2012) Regulation of insulin sensitivity by serine/threonine phosphorylation of insulin receptor substrate proteins IRS1 and IRS2. Diabetologia 55(10): 2565-2582.

Davidson HV, Peshavaria M, Hutton JC (1987) Proteolytic conversion of proinsulin into insulin. Identification of a Ca2+-dependent acidic endopeptidase in isolated insulin-secretory granules. Biochem J 246(2): 279-286.

De Tata V (2014) Association of dioxin and other persistent organic pollutants (POPs) with diabetes: Epidemiological evidence and new mechanisms of beta cell dysfunction. Int J Mol Sci 15(5): 7787-811.

Dean PM (1973) Ultrastructural morphometry of the pancreatic β-cell. Diabetologia 9(2): 115-119.

Del Prato S, Tiengo A (2001) The importance of first-phase insulin secretion: implications for the therapy of type 2 diabetes mellitus. Diabetes Metab Res Rev 17(3): 164-174.

Diliberto JJ, Burgin D, Birnbaum LS (1997) Role of CYP1A2 in hepatic sequestering of dioxin: studies using CYP1A2 knock-out mice. Biochem Biophys Res Comm 236(2): 431-433.

Durrin LK, Jones PBC, Fish JM, Galeazzi DR, Whitlock JP (1987) 2,3,7,8-Tetrachlorodibenzo-p-dioxin receptors regulate transcription of the cytrochrome P1-450 gene. J Cell Biochem 35: 153-160.

Ebner K, Brewster DW, Matsumura F (1988) Effects of 2,3,7,8-tetrachlorodibenzo-p-dioxin on serum insulin and glucose levels in the rabbit. J Environ Sci Health 23: 427-438.

Enan E, Matsumura F (1994) 2,3,7,8-Tetrachlorodibenzo-p-dioxin (TCDD)-induced changes in glucose transporter activity in guinea pigs, mice and rats in vivo and in vitro. J Biochem Toxicol 9: 97-106.

Eskenazi B, Mocarelli P, Warner M, Needham L, Patterson DG Jr, Samuels S, Turner W, Gerthoux PM, Brambilla P (2004) Relationship of serum TCDD concentrations and age at exposure of female residents of Seveso, Italy. Environ Health Perspect 112(1): 22-27.

Everett CJ, Frithsen IL, Diaz VA, Koopman RJ, Simpson WM, Mainous AG (2007) Association of polychlorinated dibenzo-p-dioxin, a polychlorinated biphenyl, and

DDT with diabetes in the 1999-2002 National Health and Nutrition Examination Survey. Environ Res 103(3): 413-418.

Fader KA, Nault R, Ammendolia DA, Harkema JR, Williams JR, Crawford RB, Kaminski NE, Potter D, Sharratt B, Zacharewski TR (2015) 2,3,7,8-Tetrachlorodibenzo-p-dioxin alters lipid metabolism and depletes immune cell populations in the jejunum of C57BL/6 mice. Toxicol Sci 148(2): 567-580.

Fader KA, Nault R, Zhang C, Kumagai K, Harkema JR, Zacharewski TR (2017) 2,3,7,8-Tetrachlorodibenzo-*p*-dioxin (TCDD)-elicited effects on bile acid homeostasis: Alterations in biosynthesis, enterohepatic circulation, and microbial metabolism. Sci Rep 7: 5921.

Fan Z, Makielski JC (1997) Anionic phospholipids activate ATP-sensitive potassium channels. J Biol Chem 272(9): 5388-5395.

Feng DD, Luo Z, Roh SG, Hernandez M, Tawadros N, Keating DJ, Chen C (2006) Reduction in voltage-gated K+ currents in primary cultured rat pancreatic beta-cells by linoleic acids. Endocrinol 147: 674–682.

Filardo EJ, Thomas P (2012) Minireview: G protein-coupled estrogen receptor-1, GPER-1: its mechanism of action and role in female reproductive cancer, renal and vascular physiology. Endocrinol 153(7): 2953-2962.

Fisher-Wellman KH, Ryan TE, Smith CD, Gilliam LAA, Lin CT, Reese LR, Torres MJ, Neufer PD (2016) A direct comparison of metabolic responses to high-fat diet in C57BL/6J and C57BL/6NJ mice. Diabetes 65: 3249-3261.

Fraulob JC, Ogg-Diamantino R, Fernandes-Santos C, Aguila MB, Mandarim-de-Lacerda CA (2010) A mouse model of metabolic syndrome: Insulin resistance, fatty liver and non-alcoholic fatty pancreas disease (NAFPD) in C57BL/6 mice fed a high fat diet. J Clin Biochem Nutr 46(3): 212-223.

Fu Z, Gilbert ER, Liu D (2013) Regulation of insulin synthesis and secretion and pancreatic beta-cell dysfunction in diabetes. Curr Diabetes Rev 9(1): 25-53.

Ganesan S, Calle R, Zawalich K, Greenwalt K, Zawalich W, Shulman GI, Rasmussen H (1992) Immunocytochemical localization of α-protein kinase C in rat pancreatic β-cells during glucose-induced insulin secretion. J Cell Biol 119: 313-324.

Ganesan S, Calle R, Zawalich K, Smallwood JI, Zawalich WS, H Rasmussen (1990) Glucose-induced translocation of protein kinase C in rat pancreatic islets. PNAS 87: 9893-9897.

Gareski TWS, Kubasiak D, Unger TJ, Li X, Panza D, Qadri A, Bedard P, Ranganath S, Gimeno R, Hahm S, Perreault M (2009) The severity of insulin resistance in C57BL/6 mice depends on genetic background and dietary fat source. Available from: ⟨http://professional.diabetes.org/Abstracts_Display.aspx?TYP=1&CID=73710⟩.

Gasiewicz TA, Holscher MA, Neal RA (1980) The effect of total parenteral nutrition on the toxicity of 2,3,7,8-tetrachlorodibenzo-p-dioxin in the rat. Appl Pharmacol 54: 69-88.

Geer EB, Shen W (2009) Gender differences in insulin resistance, body composition, and energy balance. Gend Med 6(1): 60-75.

Geusau A, Abraham K, Geissler K, Sator MO, Stingl G, Tschachler E (2001) Severe 2,3,7,8-tetrachlorodibenzo-*p*-dioxin (TCDD) intoxication: Clinical and laboratory effects. Environ Health Perspect 109(8): 865-869.

Gill S, Stevenson J, Kristiana Ika, Brown AJ (2011) Cholesterol-dependent degradation of squalene monooxygenase, a control point in cholesterol synthesis beyond HMG-CoA reductase. Cell Metab 13(3): 260-273.

Gilon P, Ravier MA, Jonas JC, Henquin JC (2002) Control mechanisms of the oscillations of insulin secretion in vitro and in vivo. Diabetes 51(1): S144-S151.

Ginsberg HN, Zhang YL, Hernandez-Ono A (2005) Regulation of plasma triglycerides in insulin resistance and diabetes. Arch Med Res 36(3): 232-240.

Giri AK (1986) Mutagenic and genotoxic effects of 2,3,7,8-tetrachlorodibenzo-*p*-dioxin, a review. Mutat Res 168: 241-248.

Golson ML, Misfeldt AA, Kopsombut UG, Petersen CP, Gannon M (2010) High fat diet regulation of β-cell proliferation and β-cell mass. Open Endocrinol J 4:10.

Gonzalez FJ, Fernandez-Salguero P (1998) The aryl hydrocarbon receptor: Studies using the AhR-null mice. Drug Metab and Dispos 26(12): 1194-1998.

Göttel M, Le Corre L, Dumont C, Schrenk D, Chagnon MC (2014) Estrogen receptor α and aryl hydrocarbon receptor cross-talk in a transfected hepatoma cell line (HepG2) exposed to 2,3,7,8-tetrachlorodibenzo-p-dioxin. Toxicol Rep 1:1029-1036.

Gu YZ, Hogenesch JB, Bradfield CA (2000) The PAS superfamily: sensors of environmental and developmental signals. Annu Rev Pharmacol Toxicol 40: 519-561.

Guengerich FP (2008) Cytochrome P450 and chemical toxicology. Chem Res Toxicol 21: 70-83.

Gupta BN, Vos JG, Moore JA, Zinkl JG, Bullock BC (1973) Pathologic effect of 2,3,7,8-tetrachlorodibenzo-p-dioxin in laboratory animals. Environ Health Perspect 5: 125-140.

Hall DD, Davare MA, Shi M, Allen ML, Weisenhaus M, McKnight GS, Hell JW (2007) Critical role of cAMP-dependent protein kinase anchoring to the L-type calcium channel Cav1.2 via A-kinase anchor protein 150 in neurons. Biochem 46(6): 1635-1646.

Hao M, Head WS, Gunawardana SC, Hasty AH, Piston DW (2007) Direct effect of cholesterol on insulin secretion. Diabetes 56(9): 2328-2338.

Henley DV, Bellone CJ, Williams DA, Ruh TS, Ruh MF (2004) Aryl hydrocarbon receptor-mediated posttranscriptional regulation of IL-1beta. Arch Biochem Biophys 422(1): 42-51.

Henriksen GL, Ketchum NS, Michalek JE, Swaby JA (1997) Serum dioxin and diabetes mellitus in veterans of Operation Ranch Hand. Epidemiology 8(3): 252-258.

Hilgemann DW, Ball R (1996) Regulation of cardiac Na^+, Ca^{2+} exchange and K_{ATP} potassium channels by PIP_2. Sci 273(5277): 956-959.

Hoffer A, Chang CY, Puga A (1996) Dioxin induces transcription of fos and jun genes by Ah receptor-dependent and -independent pathways. Toxicol Appl Pharmacol 141(1): 238-247.

Huang XF, Arvan P (1995) Intracellular transport of proinsulin in pancreatic beta-cells. Structural maturation probed by disulfide accessibility. J Biol Chem 270(35): 20417–20423.

In't Veld P, Marichal M (2010) Microscopic Anatomy of the Human Islet of Langerhans. In: The Islets of Langerhans (Islam S, ed), pp1-3, Uppsala, Sweden.

Inagami K, Koga T, Kikuchi M, Hashimoto M, Takahashi H, Wada K (1969) Experimental study of hairless mice following administration of rice oil used by a Yusho patient. Fukuoka Acta Med 60: 548-553.

International Diabetes Foundation Diabetes Atlas 7 (2015) http://www.diabetesatlas.org/atlas/atlas.html (cited April 17, 2019)

Ishida T, Kan-o S, Mutoh J, Takeda S, Ishii Y, Hashiguchi I, Akamine A, Yamada H (2005) 2,3,7,8-Tetrachlorodibenzo-p-dioxin-induced change in intestinal function and pathology: Evidence for the involvement of arylhydrocarbon receptor-mediated alteration of glucose transportation. Toxicol Appl Pharmcol 205: 89-97.

Itoh Y, Kawamata Y, Harada M, Kobayashi M, Fujii R, Fukusumi S, Ogi K, Hosoya M, Tanaka Y, Uejima H, Tanaka H, Maruyama M, Satoh R, Okubo S, Kizawa H, Komatsu H, Matsumura F, Noguchi Y, Shinohara T, Hinuma S, Fujisawa Y, Fujino M (2003) Free fatty acids regulate insulin secretion from pancreatic β-cells through GPR40. Nature 422: 173–176.

Jacobson DA, Kuznetsov A, Lopez JP, Kash S, Ammala CE, Philipson LH (2007a) Kv2.1 ablation alters glucose-induced islet electrical activity, enhancing insulin secretion. Cell Metab 6: 229–235.

Jacobson DA, Philipson LH (2007) Action potentials and insulin secretion: new insights into the role of Kv channels. Diabetes Obes Metab 9(2): 89-98.

Jacobson DA, Weber CR, Bao S, Turk J, Philipson LH (2007b) Modulation of the pancreatic islet β-cell-delayed rectifier potassium channel Kv2.1 by the polyunsaturated fatty acid arachidonate. J Biol Chem 282: 7442–7449.

Jonsson J, Carlsson L, Edlund T, Edlund H (1994) Insulin-promoter-factor 1 is required for pancreas development in mice. Nature 371: 606-609.

Joung-Soon K, Hyun-Sul L, Sung-Il C, Hae-Kwan C, Min-Kyung L (2003) Impact of Agent Orange exposure among Korean Vietnam veterans. Industrial Health, 41: 149-157.

Kang HK, Dalager NA, Needham LL, Patterson DG, Lees PS, Yates K, Matanoski GM (2006) Health status of the Army Chemical Corps Vietnam veterans who sprayed defoliant in Vietnam. Am J Ind Med 49(11): 875-884.

Karouna-Renier NK, Rao KR, Lanza JJ, Davias DA, Wilson PA (2007) Serum profiles of PCDDs and PCDFs, in individuals near Escambia Wood Treating Company Superfund site in Pensacola, FL. Chemosphere 69: 1312-1319.

Kerger BD, Scott PK, Pavuk M, Gough M, Paustenbach DJ (2012) Re-analysis of Ranch Hand study supports reverse causation between dioxin and diabetes. Crit Rev Toxicol 42(8): 669-687.

Kessova IG, DeCarli LM, Lieber CS (1998) Inducibility of cytochrome P-4502E1 and P-4501A1 in the rat pancreas. Alcohol Clin Exp Res 22(2): 501-504.

Kharat I, Saatcioglu F (1996) Antiestrogenic effects of 2,3,7,8-tetrachlorodibenzo-*p*-dioxin Are mediated by direct transcriptional interference with the liganded estrogen receptor CROSS-TALK BETWEEN ARYL HYDROCARBON- AND ESTROGEN-MEDIATED SIGNALING. J Biol Chem 271: 10533-10537.

Khattabi IE, Sharma A (2015) Proper activation of MafA is required for optimal differentiation and maturation of pancreatic β-cells. Best Pract Res Clin Endocrinol Metab 29(6): 821-831.

Kim J, Jeong JI, Kim KM, Choi I, Pratley RE, Lee YH (2014) Improved glucose tolerance with restored expression of glucose transporter 4 in C57BL/6 mice after a long period of high-fat diet feeding. Animal Cells Sys 18(3): 197-203.

Kobertz WR, Wang D, Wogan GN, Essigmann JM (1997) An intercalation inhibitor altering the target selectivity of DNA damaging agents: Synthesis of site-specific aflatoxin B1 adducts in a p53 mutational hotspot. PNAS USA 94: 9579-9584.

Kociba RJ, Keeler PA, Park CN, Gehring PJ (1979) 2,3,7,8-Tetrachlorodibenzo-*p*-dioxin (TCDD): Results of a 13-week oral toxicity study in rats. Toxicol Apply Pharmcol 35: 553-574.

Kolluri SK, Weiss C, Koff A, Gottlicher M (1999) p27Kip1 induction and inhibition of proliferation by the intracellular Ah receptor in developing thymus and hepatoma cells. Genes Dev 13: 1742–1753.

Krauter T, Ruppersberg P, Baukrowitz T (2001) Phospholipids as modulators of K_{ATP} channels: Distinct mechanisms for control of sensitivity to sulphonylureas, K^+ channel openers, and ATP. Mol Pharmacol 59(5): 1086-1093.

Kurita H, Yoshioka W, Nishimura N, Kubota N, Kadowaki T, Tohyama C (2009) Aryl hydrocarbon receptor-mediated effects of 2,3,7,8-tetrachlorodibenzo-p-dioxin on glucose-stimulated insulin secretion in mice. J Appl Toxicol 29(8): 689-694.

Lee AJ, Cai MX, Thomas PE, Conney AH, Zhu BT (2003) Characterization of the oxidative metabolites of 17beta-estradiol and estrone formed by 15 selectively expressed human cytochrome p450 isoforms. Endocrinol 144(8): 3382-3398.

Lee DH, Lee IK, Jin SH, Steffes M, Jacobs DR (2007) Association between serum concentrations of persistent organic pollutants and insulin resistance among nondiabetic adults: Results from the National Health and Nutrition Examination Survey 1999-2002. Diabetes Care 30(3): 622-628.

Lee DH, Lee IK, Song K, Steffes M, Toscano W, Baker BA, Jacobs DR (2006) A strong dose-response relation between serum concentrations of persistent organic pollutants and diabetes: Results from the National Health and Examination Survey 1999–2002. Diabetes Care 29(7): 1638–1644.

Lenzen S (2008) Oxidative stress: the vulnerable beta-cell. Biochem Soc Trans 36: 343-347.

Liu PC, Matsumura F (1995) Differential effects of 2,3,7,8-tetrachlorodibenzo-p-dioxin on the “adipose-type” and “brain-type” glucose transporters in mice. Mol Pharmcol 47(1): 65-73.

Liu PC, Matsumura F (2006) TCDD suppresses insulin-responsive glucose transporter (GLUT-4) gene expression from C/EBP nuclear transcription factors in 3T3-L1 adipocytes. J Biochem Mol Toxicol 20: 79-87.

Liu Z, Patil IY, Jiang T, Sancheti H, Walsh JP, Stiles BL, Cadenas E (2015) High-fat diet induces hepatic insulin resistance and impairment of synaptic plasticity. PLoS One 10(5): e0128274.

Lucier GW, McDaniel OS, Hook GER, Fowler BA, Sonawane BR, Faeder E (1973) TCDD-induced changes in rat liver microsomal enzymes. Environ Health Perspect 5: 199.

Maedler K, Spinas GA, Lehrmann R, Sergeev P, Weber M, Fontana A, Kaiser N, Donath MY (2001) Glucose induces β-cell apoptosis via upregulation of the Fas receptor in human islets. Diabetes 50(8): 1683-1690.

Magliano DJ, Loh VHY, Harding JL, Bottom J, JE Shaw (2014) Persistent organic pollutants and diabetes: A review of the epidemiological evidence. Diabetes & Metabolism 40: 1-14.

Malecki MT, Jhala US, Antonellis A, Fields L, Doria A, Orban T, Saad M, Warram JH, Montminy M, Krolewski AS (1999) Mutations in NEUROD1 are associated with the development of type 2 diabetes mellitus. Nat Gen 23: 323-328.

Mandal PK (2005) Dioxin: a review of its environmental effects and its aryl hydrocarbon receptor biology. J Comp Physiol B 175: 221-230.

Maris M, Robert S, Waelkns E, Derua R, Hernangomez MH, D'Hertog W, Cnop M, Mathieu C, Overbergh L (2012) Role of the saturated nonesterified fatty acid palmitate in beta cell dysfunction. J Proteome Res 12: 347-362.

Matthews J, Gustafsson JA (2006) Estrogen receptor and aryl hydrocarbon receptor signaling pathways. Nucl Recept Signal 4: e016.

McConnell EE (1980) Acute and chronic toxicity, carcinogenesis, reproduction, teratogenesis and mutagenesis in animals. Ref 20, pp 109-150.

McConnell EE, Moore JA, Dalgard DW (1978b) Toxicity of 2,3,7,8-tetrachlorodibenzo-p-dioxin in Rhesus monkeys (Macaca mulatta) following a single oral dose. Toxicol Appl Pharmacol 43: 175-187.

McConnell EE, Moore JA, Haseman JK, Harris MW (1978a) The comparative toxicity of chlorinated dibenzo-p-dioxin in mice and guinea pigs. Toxicol Apply Pharmacol 44: 335-356.

Meglasson MD, Matschinsky FM (1986) Pancreatic islet glucose metabolism and regulation of insulin secretion. Diabetes Metab Res Rev 2: 163-214.

Merchant M, Arellano L, Safe S (1990) The mechanism of action of alpha-naphthoflavone as an inhibitor of 2,3,7,8-tetrachlorodibenzo-p-dioxin-induced CYP1A1 gene expression. Arch Biochem Biophys 281(1): 84-89.

Michalek JE & Pavuk M (2008) Diabetes and cancer in veterans of Operation Ranch Hand after adjustment for calendar period, days of spraying, and time spent in Southeast Asia. J Occup Environ Med 50(3): 330-340.

Michalek JE, Akhtar FS, Kiel JL (1999) Serum dioxin, insulin, fasting glucose and sex hormone-binding globulin in veterans of Operation Ranch Hand. J Clin Endrocinol Metab 84(5): 1540-1543.

Mimura J, Fujii-Kuriyama Y (2003) Functional role of AhR in the expression of toxic effects by TCDD. Biochimica et Biophysica Acta 1619: 263-268.

Nagao M, Asai A, Sugihara H, Oikawa S (2015) Fat intake and the development of type 2 diabetes. Endo J 62(7): 561-572.

Nagashima H, Matsumura F (2002) 2,3,7,8-Tetrachlorodibenzo-p-dioxin (TCDD)-induced down-regulation of glucose transporting activities in mouse 3T3-L1 preadipocyte. J Environ Sci Health 37: 1-14.

National Toxicology Program (2006) NTP technical report on the toxicology and carcinogenesis studies of 2,3,7,8-tetrachlorodibenzo-*p*-dioxin (TCDD) (CAS No. 1746–01–6) in female Harlan Sprague-Dawley rats (Gavage Studies). Natl Toxicol Program Tech Rep Ser, 521: 4–232.

Naya FJ, Huang DP, Qiu Y, Mutoh H, DeMayo FJ, Leiter AB, Tsai MJ (1997) Diabetes, defective pancreatic morphogenesis, and abnormal enteroendocrine differentiation in BETA2/NeuroD-deficient mice. Genes & Dev 11: 2323-2334.

Neel, BA, Sargis, RM (2011) The paradox of progress: Environmental disruption of metabolism and the diabetes epidemic. Diabetes 60(7): 1838–1848.

Neuberger M, Landvoigt W, Derntl F (1991) Blood levels of 2,3,7,8-tetrachlorodibenzo-*p*-dioxin in chemical workers after chloracne and in comparison groups. Int Arch Occ Environ Health, 63(5): 325-327.

Nov O, Shapiro H, Ovadia H, Tarnovscki T, Dvir I, Shemesh E, Kovsan J, Shelef I, Carmi Y, Voronov E, Apte RN, Lewis E, Haim Y, Konrad D, Bashan N, Rudich A (2013) Interleukin-1β regulates fat-liver crosstalk in obesity by auto-paracrine modulation of adipose tissue inflammation and expandability. PLoS One 8(1): e53626.

Novelli M, Piaggi S, De Tata V (2005) 2,3,7,8-Tetrachlorodibenzo-*p*-dioxin-induced impairment of glucose-stimulated insulin secretion in isolated rat pancreatic islets. Toxicol Lett 156: 307-314.

Ohlsson H, Karlsson K, Edlund T (1993) IPF1, a homeodomain-containing transactivator of the insulin gene. EMBO J 12(11): 4251-4259.

Oliveira RB, Maschio DA, Carvalho CP, Collares-Buzato CB (2015) Influence of gender and time diet exposure on endocrine pancreas remodeling in response to high fat diet-induced metabolic disturbances in mice. Ann Anat 200: 88-97.

Olofsson CS, Salehi A, Holm C, Rorsman P (2003) Palmitate increases L-type Ca2+ currents and the size of the readily releasable granule pool in mouse pancreatic β-cells. J Physiol 557(3): 935-948.

Olsen H, Enan E, Matsumura F (1998) 2,3,7,8-Tetrachlorodibenzo-*p*-dioxin mechanism of action to reduce lipoprotein lipase activity in the 3T3-L1 preadipocyte cell line. J Biochem Mol Toxicol 12: 29-39.

Orci L, Ravazzola M, Amherdt M, Madsen O, Perrelet A, Vassalli JD, Anderson RG (1986) Conversion of proinsulin to insulin occurs coordinately with acidification of maturing secretory vesicles. J Cell Biol 103(6 Pt 1): 2273-2281.

Orci L, Ravazzola M, Baetens D, Inman L, Amherdt M, Pederson RG, Newgard CB, Johnson JH, Unger RH (1990) Evidence that downregulation of β-cell glucose transporters in non-insulin dependent diabetes may be the cause of diabetic hyperglycemia. PNAS 87: 9953-9957.

Parhofer KG (2015) Interaction between glucose and lipid metabolism: More than diabetic dyslipidemia. Diabetes Metab J 39(5): 353-362.

Patzelt C, Labrecque AD, Duguid JR, Carroll RJ, Keim PS, Heinrikson RL, Steiner DF (1978) Detection and kinetic behavior of preproinsulin in pancreatic islets. PNAS 75(3):1260–1264.

Pfeifer MA, Halter JB, Porte D (1981) Insulin secretion in diabetes mellitus. Am J Med 70(3):579-588.

Piaggi S, Novelli M, Martino L, Masini M, Raggi C, Orciuolo E, Masiello P, Casini A, De Tata V (2007) Cell death and impairment of glucose-stimulated insulin secretion induced by 2,3,7,8-tetrachlorodibenzo-*p*-dioxin (TCDD) in the beta-cell line INS-1E. Toxicol Appl Pharmacol 220(3): 333-340.

Piper WN, Rose JQ, Gehring PJ (1973) Excretion and tissue distribution of 2,3,7,8-tetrachlorodibenzon-*p*-dioxin in the rat. Environ Health Perspect 5: 241.

Pirke JL, Wolfe WH, Patterson DG, Needham LL, Michalek JE, Miner JC, Peterson MR, Phillips DL (1989) Estimates of the half-life of 2,3,7,8-tetrachlorodibenzo-*p*-dioxin in Vietnam veterans of operation ranch hand. J Toxicol Environ Health 27: 165-171.

Poiger H, Buser HR, Weber H, Zweifel U, Schlater Ch (1982) Structure elucidation of mammalian TCDD-metabolites. Experientia 38: 484-486.

Poiger H, Schlatter C (1986) Pharmacokinetics of 2,3,7,8-TCDD in man. Chemosphere 15(9-12): 1489-1496.

Poland A, Glover E (1974) Comparison of 2,3,7,8-tetrachlorodibenzo-*p*-dioxin, a potent inducer of aryl hydrocarbon receptor hydroxylase, with 3-methylcholanthrene. Mol Pharmcol 10: 349-359.

Poland A, Knutson JC (1982) 2,3,7,8-Tetrachlorodibenzo-*p*-dioxin and related halogenated aromatic hydrocarbons: examination of the mechanism of toxicity. Ann Rev Pharmacol Toxicol 22: 517-554.

Rhodes CJ, Halban PA (1987) Newly synthesized proinsulin/insulin and stored insulin are released from pancreatic B cells predominantly via a regulated, rather than a constitutive, pathway. J Cell Biol 105(1): 145-153.

Robertson RP (1986) Arachidonic acid metabolite regulation of insulin secretion. Diabetes Metab Rev 2(3-4): 261-296.

Rorsman P, Renström E (2003) Insulin granule dynamics in pancreatic beta cells. Diabetologia 46(8): 1029-1045.

Rose JQ, Ramsey JC, Wentzler TH, Hummel RA, Gehring PJ (1976) The fate of 2,3,7,8-tetrachlorodibenzo-*p*-dioxin following single and repeated oral doses to the rat. Toxicol Appl Pharmacol 36: 209-226.

Rosenbaum T, Castanares DT, Lopez-Vaides HE, Hiriart M (2002) Nerve growth factor increases L-type calcium current in pancreatic beta-cells in culture. J Membr Biol 186: 177–184.

Rosenbaum T, Sanchez-Soto MC, Hiriart M (2001) Nerve growth factor increases insulin secretion and barium current in pancreatic beta-cells. Diabetes 50: 1755–1762.

Salehi A, Flodgren E, Nilsson NE, Jimenez-Feltstrom J, Miyazaki J, Owman C, Olde B (2005) Free fatty acid receptor 1 (FFA(1)R/GPR40) and its involvement in fatty-acid-stimulated insulin secretion. Cell Tissue Res 322: 207–215.

Sander M, Neubuser A, Kalamaras J, Ee HC, Martin GR, German MS (1997) Genetic analysis reveals that PAX-6 is required for normal transcription of pancreatic genes and islet development. Genes & Dev 11: 1662-1673.

Sang L, Dick IE, Yue DT (2016) Protein kinase A modulation of $CaV_{1.4}$ calcium channels. Nat Commun 7: 12239.

Sawahata T, Olson JR, Neal RA (1982) Identification of 2,3,7,8-tetrachlorodibenzo-*p*-dioxin (TCDD) formed on incubation with isolated rat hepatocytes. Biochem Biophys Res Comms 105(1): 341-346.

Schaffer AE, Taylor BL, Benthuysen JR, Liu J, Thorel F, Yuan W, Jiao Y, Kaestner KH, Herrera PL, Magnuson MA, May CL, Sander M (2013) Nkx6.1 controls a gene regulatory network required for establishing and maintaining pancreatic Beta cell identity. PLoS Genet 9(1): e1003274.

Schisler JC, Jensen PB, Taylor DG, Becker TC, Knop FK, Takekawa S, German M, Weir GC, Lu D, Mirmira RG, Newgard CB (2005) The Nkx6.1 homeodomain transcription factor suppresses glucagon expression and regulates glucose-stimulated insulin secretion in islet beta cells. PNAS 102(20): 7297-7302.

Seefeld MD, Corbett SW, Keesey RE, Peterson RE (1984) Characterization of the wasting syndrome in rats treated with 2,3,7,8-tetrachlorodibenzo-p-dioxin. Toxicol Appl Pharmacol 73: 311-322.

Shapiro H, Shachar S, Sekler I, Hershfinkel M, Walker MD (2005) Role of GPR40 in fatty acid action on the beta cell line INS-1E. Biochem Biophys Res Commun 335(1): 97-104.

Sharma G, Prossnitz ER (2011) Mechanisms of estradiol-induced insulin secretion by the G protein-coupled estrogen receptor GPR30/GPER in pancreatic beta-cells. Endocrinol 152(8):3030-3039.

Shiao MS, Liao BY, Long M, Yu HS (2008) Adaptive evolution of the unsulin two-gene system in mouse. Genetics 178(3): 1683-1691.

Sims EK, Hatanaka M, Morris DL, Tersey SA, Kono T, Chaudry ZZ, Day KH, Moss DR, Stull ND, Mirmira RG, Evans-Molina C (2013) Divergent compensatory responses to high-fat diet between C57BL6/J and C57BLKS/J inbred mouse strains. Am J Physiol Endocrinol Metab 305(12): E1495-1511.

Smith GD, Pangborn WA, Blessing RH (2003) The structure of T6 human insulin at 1. 0 A resolution. Acta Crystallogr D Biol Crystallogr 59(3): 474–482.

Son DS, Rozman KK (2002) 2,3,7,8-Tetrachlorodibenzo-*p*-dioxin (TCDD) induces plasminogen activator inhibitor-1 through aryl hydrocarbon receptor-mediated pathway in mouse hepatoma cell lines. Arch Toxicol 76: 404-413.

Sorg O, Zennegg M, Schmid P, Fedosyuk R, Valikhnovskyi R, Gaide O, Kniazevych V, Saurat S-H (2009) 2,3,7,8-tetrachlorodibenzo-*p*-dioxin (TCDD) poisoning in Victor Yushchenko: identification and measurement of TCDD metabolites. Lancet 374: 1179-1185.

Staffers DA, Ferrer J, Clarke WL, Habener JF (1997) Early-onset type-II diabetes mellitus (MODY4) linked to IPF1. Nat Gen 17: 138-139.

Stansfeld PJ, Hopkinson R, Ashcroft FM, Sansom MSP (2009) PIP2-binding site in Kir channels: Definition by multiscale biomolecular simulations. Biochem 48(46): 10926-10933.

Steenland K, Piacitelli L, Deddens J, Fingerhut M, Chang LI (1999) Cancer, heart disease, diabetes in workers exposed to 2,3,7,8-tetrachlorodibenzo-*p*-dioxin. J Natl Cancer Inst 91: 779-786.

Straub SG, Sharp GW (2002) Glucose-stimulated signalling pathways in biphasic insulin secretion. Diabetes Metab Res Rev 18: 451–463.

Sutter CH, Olesen KM, Bhuju J, Guo Z, Sutter TR (2019) AhR regulates metabolic reprogramming to promote SIRT1-dependent keratinocyte differentiation. J Invest Dermatol 139(4): 818-826.

Swift LL, Gasiewicz TA, Dunn GD, Soule PD, Neal RA (1981) Characterization of hyperlipidemia in guinea pigs induced by 2,3,7,8-tetrachlorodibenzon-*p*-dioxin. Toxicol Appl Pharmacol 59: 489-499.

Taylor BL, Liu FF, Sander M (2013a) Nkx6.1 is essential for maintaining the functional state of pancreatic beta cells. Cell Rep 4(6): 1262-1275.

Taylor KW, Novak RF, Anderson HA, Birnbaum LS, Blystone C, DeVito M, Jacobs D, Kohrle J, Lee DH, Rylander L, Rignell-Hydbom A, Toernero-Velez R, Turyk ME, Boyles AL, Thayer KA, Lind L (2013b) Evaluation of the association between persistent organic pollutants (POPs) and diabetes in epidemiological studies: A National Toxicology Program workshop review. Environ Health Perspect 121: 774-783.

Thorens B, Weir GC, Leahy JL, Lodish HF, Bonner-Weir S (1990) Reduced expression of the liver/beta cell glucose transporter isoform in glucose-insensitive pancreatic beta cells of diabetic rats. PNAS USA 87: 6492–6496.

Tonack S, Kind K, Thompson JG, Wobus AM, Fischer B, Santos AN (2007) Dioxin affects glucose transport via the arylhydrocarbon receptor signal cascade in pluripotent embryonic carcinoma cells. Endocrinol 148(12): 5902-5912.

United States and Canada. Great Lakes Water Quality Agreement, 1972. http://www.on.ec.gc.ca/glwqa

Valera A, Solanes G, Fernandez-Alvarez J, Pujol A, Ferrer J, Asins A (1994) Expression of GLUT-2 antisense RNA in beta-cells of transgenic mice leads to diabetes. J Biol Chem 269-28543-28546.

Vena J, Boffetta P, Becher H, Benn T, Bueno-de-Mesquita HB, Coggon D, Colin D, Flesch-Janys D, Green L, Kauppinen T, Littorin M, Lynge E, Matthews JD, Neuberger M, Pearce N, Pesatori AC, Saracci R, Steenland K, Kogevinas M (1998) Exposure to dioxin and nonneoplastic mortality in the expanded IARC international cohort study of phenoxy herbicide and chlorophenol production workers and sprayers. Environ Health Perspect 106: 645-653.

Vos JG, Faith RE, Lust MI (1980) Immune alterations. Ref 20 pp 241-266.

Walsh AA, Szklarz GD, Scott EE (2013) Human cytochrome P450 1A1 structure and utility in understanding drug and xenobiotic metabolism. J Biol Chem 288(18):12932-12943.

Wang SL, Yang CY, Tsai PC, Guo LY (2008) Increased risk of diabetes and polychlorinated biphenyls and dioxins. Diabetes Care 31: 1574-1579.

Warner M, Mocarelli P, Brambilla P, Wesselink A, Samuels S, Signorini S, Eskenazi B (2013). Diabetes, metabolic syndrome, and obesity in relation to serum dioxin concentrations. The Seveso women's health study. Environ Health Prospect 121: 906-911.

Watson ML, Macrae K, Marley AE, Hundal HS (2011) Chronic effects of palmitate overload on nutrient-induced insulin secretion and autocrine signalling in pancreatic MIN6 beta-cells. PLoS One 6(10): e25975.

Winzell MS, Ahrén B (2004) The high-fat diet-fed mouse: a model for studying mechanisms and treatment of impaired glucose tolerance and type 2 diabetes. Diabetes 53(3): S124-129.

Wiser O, Trus M, Hernandez A, Renstrom E, Barg S, Rorsman P, Atlas D (1999) The voltage sensitive LC-type Ca2+ channel is functionally coupled to the exocytotic machinery. PNAS 96: 248–253.

Withers DJ1 Gutierrez JS, Towery H, Burks DJ, Ren JM, Previs S, Zhang Y, Bernal D, Pons S, Shulman GI, Bonner-Weir S, White MF (1998) Disruption of IRS-2 causes type 2 diabetes in mice. Nature 391(6670): 900-904.

Wu D, Nishimura N, Kuo V, Fiehn O, Shahbaz S, Winkle LV, Matsumura F, Vogel C (2011) Activation of aryl hydrocarbon receptor induces vascular inflammation and promotes atherosclerosis in ApoE-/- mice. Aterioscler Thromb Vasc Biol 31(6): 1260-1267.

Wu Y, Ding Y, Tanaka Y, Zhang W (2014) Risk factors contributing to type 2 diabetes and recent advances in the treatment and prevention. Int J Med Sci 11(11): 1185-1200.

Yang SN, Larsson O, Branstrom R, Bertorello AM, Leibiger B, Leibiger IB, Moede T, Kohler M, Meister B, Berggren PO (1999) Syntaxin 1 interacts with the LD subtype of voltage-gated Ca2+ channels in pancreatic b cells. PNAS 96:10164–10169.

Yang SN, Shi Y, Yang G, Li Y, Yu J, Berggren PO (2014) Ionic mechanisms in pancreatic β cell signaling. Cell Mol Life Sci 71: 4149-4177.

Yang Y, Smith DL Jr, Keating KD, Allison DB, Nagy TR (2014) Variations in body weight, food intake and body composition after long-term high-fat diet feeding in C57BL/6J mice. Obesity (Silver Spring) 22(10): 2147-2155.

Yasuda T, Kajimoto Y, Fujitani Y, Watada H, Yamamoto S, Watarai T, Umayahara Y, Matsuhisa M, Gorogawa S, Kuwayama Y, Tano Y, Yamasaki Y, Hori M (2002) PAX6 mutation as a genetic factor common to aniridia and glucose intolerance. Diabetes 51(1): 224-230.

Yokoi N, Kanamori M, Horikawa Y, Takeda J, Sanke T, Furuta H, Nanjo K, Mori H, Kasuga M, Hara K, Kadowaki T, Tanizawa Y, Oka Y, Iwami Y, Ohgawara H, Yamada Y, Seino Y, Yano H, Cox NJ, Seino S (2006) Association studies of variants in the genes involved in pancreatic beta-cell function in type 2 diabetes in Japanese subjects. Diabetes 55(8): 2379-2386.

Zaher H, Fernandez-Salquero PM, Letterio J, Sheikh MS, Fornace AJ, Roberts AB, Gonzalez FJ (1998) The involvement of aryl hydrocarbon receptor in the activation of transforming growth factor-beta and apoptosis. Mol Pharmacol 54(2): 313-321.

Zawalich WS, Zawalich KC (1996) Regulation of insulin secretion by phospholipase C. Am Physiol Soc 271(3): E409-E416.

Zhang C, Moriguchi T, Kajihara M, Esaki R, Harada A, Shimohata H, Oishi H, Hamada M, Morito N, Hasegawa K, Kudo T, Engel JD, Yamamoto M, Takahashi S (2005) MafA is a key regulator of glucose-stimulated insulin secretion. Mol Cell Bio 25(12): 4969-4976.

Zhao L, Guo M, Matsuoka T, Hagman DK, Parazzoli SD, Poitout V, Stein R (2005) The islet β cell-enriched MafA activator is a key regulator of insulin gene transcription. J Biol Chem 280: 11887-11894.

Supplemental Data

Supplemental Table 1: Detailed ANOVA values for Figure 3.1

	Female BW Ordinary Two-way ANOVA					
Fig 3.1A	ANOVA table	SS (Type III)	DF	MS	F (DFn, DFd)	P value
	Interaction	1.692	24	0.07049	F (24, 117) = 0.06041	P>0.9999
	Time	130	8	16.25	F (8, 117) = 13.93	P<0.0001
	Group (Treatment/Genotype)	17.82	3	5.939	F (3, 117) = 5.09	P=0.0024
	Residual	136.5	117	1.167		

	Female BW AUC Ordinary One-way ANOVA					
Fig 3.1B	ANOVA table	SS	DF	MS	F (DFn, DFd)	P value
	Treatment (between columns)	987	3	329	F (3, 13) = 0.7368	P=0.5486
	Residual (within columns)	5804	13	446.5		
	Total	6791	16			

	Female BG Ordinary Two-way ANOVA					
Fig 3.1C	ANOVA table	SS (Type III)	DF	MS	F (DFn, DFd)	P value
	Interaction	18.51	12	1.543	F (12, 65) = 1.116	P=0.3628
	Time	16.21	4	4.052	F (4, 65) = 2.932	P=0.0272
	Group (Treatment/Genotype)	7.577	3	2.526	F (3, 65) = 1.828	P=0.1509
	Residual	89.82	65	1.382		

	Female BG AUC Ordinary One-way ANOVA					
Fig 3.1D	ANOVA table	SS	DF	MS	F (DFn, DFd)	P value
	Treatment (between columns)	660.7	3	220.2	F (3, 13) = 3.297	P=0.0547
	Residual (within columns)	868.5	13	66.81		
	Total	1529	16			

	Male BW Ordinary Two-way ANOVA					
Fig 3.1E	ANOVA table	SS (Type III)	DF	MS	F (DFn, DFd)	P value
	Interaction	5.911	24	0.2463	F (24, 126) = 0.2671	P=0.9998
	Time	360.7	8	45.09	F (8, 126) = 48.89	P<0.0001
	Group (Treatment/Genotype)	59.05	3	19.68	F (3, 126) = 21.34	P<0.0001
	Residual	116.2	126	0.9222		

	Male BW AUC Ordinary One-way ANOVA					
Fig 3.1F	ANOVA table	SS	DF	MS	F (DFn, DFd)	P value
	Treatment (between columns)	3733	3	1244	F (3, 14) = 3.36	P=0.0493
	Residual (within columns)	5185	14	370.3		
	Total	8918	17			

	Male BG Ordinary Two-way ANOVA					
Fig 3.1G	ANOVA table	SS (Type III)	DF	MS	F (DFn, DFd)	P value
	Interaction	16.07	12	1.339	F (12, 70) = 0.9779	P=0.4782
	Time	26.18	4	6.546	F (4, 70) = 4.781	P=0.0018
	Group (Treatment/Genotype)	22.67	3	7.555	F (3, 70) = 5.518	P=0.0018
	Residual	95.85	70	1.369		

	Male BG AUC Ordinary One-way ANOVA					
Fig 3.1H	ANOVA table	SS	DF	MS	F (DFn, DFd)	P value
	Treatment (between columns)	1792	3	597.5	F (3, 14) = 5.865	P=0.0082
	Residual (within columns)	1426	14	101.9		
	Total	3219	17			

Supplemental Table 2: Detailed ANOVA values for Figure 3.2

	Female ITT Repeated Measures Two-way ANOVA					
Fig 3.2A	ANOVA table	SS	DF	MS	F (DFn, DFd)	P value
	Interaction	16.11	18	0.8949	F (18, 72) = 1.331	P=0.1955
	Time	231.3	6	38.55	F (6, 72) = 57.32	P<0.0001
	Group (Treatment/Genotype)	27.35	3	9.117	F (3, 12) = 3.089	P=0.0679
	Subjects (matching)	35.42	12	2.952	F (12, 72) = 4.39	P<0.0001
	Residual	48.42	72	0.6725		

	Female ITT AUC Ordinary One-way ANOVA					
	ANOVA table	SS	DF	MS	F (DFn, DFd)	P value
Fig 3.2B	Treatment (between columns)	89666	3	29889	F (3, 12) = 3.465	P=0.0509
	Residual (within columns)	103501	12	8625		
	Total	193166	15			

	Male ITT Repeated Measures Two-way ANOVA					
	ANOVA table	SS	DF	MS	F (DFn, DFd)	P value
Fig 3.2C	Interaction	10.89	18	0.6048	F (18, 66) = 0.6608	P=0.8360
	Time	182.3	6	30.38	F (6, 66) = 33.19	P<0.0001
	Group (Treatment/Genotype)	14.93	3	4.977	F (3, 11) = 1.662	P=0.2321
	Subjects (matching)	32.94	11	2.995	F (11, 66) = 3.272	P=0.0013
	Residual	60.41	66	0.9153		

	Male ITT AUC Ordinary One-way ANOVA					
	ANOVA table	SS	DF	MS	F (DFn, DFd)	P value
Fig 3.2D	Treatment (between columns)	37751	3	12584	F (3, 11) = 1.064	P=0.4039
	Residual (within columns)	130156	11	11832		
	Total	167907	14			

	Female GTT Repeated Measures Two-way ANOVA					
	ANOVA table	SS	DF	MS	F (DFn, DFd)	P value
Fig 3.2E	Interaction	59.23	15	3.948	F (15, 55) = 1.037	P=0.4337
	Time	1651	5	330.2	F (5, 55) = 86.73	P<0.0001
	Group (Treatment/Genotype)	78.47	3	26.16	F (3, 11) = 1.047	P=0.4101
	Subjects (matching)	274.7	11	24.97	F (11, 55) = 6.56	P<0.0001
	Residual	209.4	55	3.807		

	Female GTT AUC Ordinary One-way ANOVA					
	ANOVA table	SS	DF	MS	F (DFn, DFd)	P value
Fig 3.2F	Treatment (between columns)	238109	3	79370	F (3, 11) = 1.23	P=0.3452
	Residual (within columns)	709901	11	64536		
	Total	948010	14			

	Male GTT Repeated Measures Two-way ANOVA					
	ANOVA table	SS	DF	MS	F (DFn, DFd)	P value
Fig 3.2G	Interaction	86.72	15	5.781	F (15, 70) = 1.268	P=0.2460
	Time	2950	5	589.9	F (5, 70) = 129.4	P<0.0001
	Group (Treatment/Genotype)	242.9	3	80.95	F (3, 14) = 1.974	P=0.1643
	Subjects (matching)	574.2	14	41.01	F (14, 70) = 8.993	P<0.0001
	Residual	319.2	70	4.56		

	Male GTT AUC Ordinary One-way ANOVA					
	ANOVA table	SS	DF	MS	F (DFn, DFd)	P value
Fig 3.2H	Treatment (between columns)	764256	3	254752	F (3, 14) = 1.964	P=0.1658
	Residual (within columns)	2E+06	14	129701		
	Total	3E+06	17			

	Female GSIS Repeated Measures Two-way ANOVA					
	ANOVA table	SS	DF	MS	F (DFn, DFd)	P value
Fig 3.2I	Interaction	0.1986	9	0.02206	F (9, 36) = 1.024	P=0.4397
	Time	1.016	3	0.3386	F (3, 36) = 15.72	P<0.0001
	Group (Treatment/Genotype)	0.2215	3	0.07384	F (3, 12) = 2.909	P=0.0782
	Subjects (matching)	0.3046	12	0.02539	F (12, 36) = 1.179	P=0.3341
	Residual	0.7753	36	0.02154		

	Female GSIS AUC Ordinary One-way ANOVA					
	ANOVA table	SS	DF	MS	F (DFn, DFd)	P value
Fig 3.2J	Treatment (between columns)	178	3	59.33	F (3, 12) = 1.863	P=0.1897
	Residual (within columns)	382.2	12	31.85		
	Total	560.2	15			

	Male GSIS Repeated Measures Two-way ANOVA					
	ANOVA table	SS	DF	MS	F (DFn, DFd)	P value
Fig 3.2K	Interaction	0.7794	9	0.0866	F (9, 42) = 1.355	P=0.2390
	Time	2.279	3	0.7595	F (3, 42) = 11.89	P<0.0001
	Group (Treatment/Genotype)	0.8641	3	0.288	F (3, 14) = 1.445	P=0.2720
	Subjects (matching)	2.791	14	0.1994	F (14, 42) = 3.12	P=0.0022
	Residual	2.684	42	0.0639		

	Male GSIS AUC Ordinary One-way ANOVA					
	ANOVA table	SS	DF	MS	F (DFn, DFd)	P value
Fig 3.2L	Treatment (between columns)	767.9	3	256	F (3, 14) = 1.078	P=0.3904
	Residual (within columns)	3325	14	237.5		
	Total	4093	17			

Supplemental Table 3: Detailed ANOVA values for Figure 4.1

	Female *Ex Vivo* Total Insulin Ordinary One-way ANOVA					
	ANOVA table	SS	DF	MS	F (DFn, DFd)	P value
Fig 4.1A	Treatment (between columns)	74.51	3	24.84	F (3, 20) = 1.032	P=0.3997
	Residual (within columns)	481.3	20	24.07		
	Total	555.8	23			

	Female *Ex Vivo* GSIS Repeated Measures Two-way ANOVA					
Fig 4.1B	ANOVA table	SS	DF	MS	F (DFn, DFd)	P value
	Interaction	22.06	3	7.353	F (3, 20) = 2.787	P=0.0672
	Time	43.21	1	43.21	F (1, 20) = 16.38	P=0.0006
	Genotype	30.67	3	10.22	F (3, 20) = 3.187	P=0.0460
	Subjects (matching)	64.16	20	3.208	F (20, 20) = 1.216	P=0.3332
	Residual	52.77	20	2.639		

	Female *Cyp1a1* mRNA Expression Ordinary One-way ANOVA					
Fig 4.1C	ANOVA table	SS	DF	MS	F (DFn, DFd)	P value
	Treatment (between columns)	116.6	3	38.88	F (3, 14) = 20.19	P<0.0001
	Residual (within columns)	26.97	14	1.926		
	Total	143.6	17			

	Male *Ex Vivo* GSIS Repeated Measures Two-way ANOVA					
Fig 4.1D	ANOVA table	SS	DF	MS	F (DFn, DFd)	P value
	Interaction	5.381	3	1.794	F (3, 17) = 3.605	P=0.0351
	Time	30.13	1	30.13	F (1, 17) = 60.56	P<0.0001
	Genotype	4.909	3	1.636	F (3, 17) = 3.258	P=0.0474
	Subjects (matching)	8.538	17	0.502	F (17, 17) = 1.009	P=0.4924
	Residual	8.458	17	0.498		

	Male *Ex Vivo* Total Insulin Ordinary One-way ANOVA					
Fig 4.1F	ANOVA table	SS	DF	MS	F (DFn, DFd)	P value
	Treatment (between columns)	97.37	3	32.46	F (3, 18) = 0.6085	P=0.6181
	Residual (within columns)	960.1	18	53.34		
	Total	1057	21			

	Male *Cyp1a1* mRNA Expression Ordinary One-way ANOVA					
Fig 4.1E	ANOVA table	SS	DF	MS	F (DFn, DFd)	P value
	Treatment (between columns)	74.15	3	24.72	F (3, 14) = 34.1	P<0.0001
	Residual (within columns)	10.15	14	0.725		
	Total	84.3	17			

Supplemental Table 4: Detailed ANOVA values for Figure 5.2

	Female BW Ordinary Two-way ANOVA					
Fig 5.2A	ANOVA table	SS (Type III)	DF	MS	F (DFn, DFd)	P value
	Interaction	82.15	81	1.014	F (81, 922) = 0.6642	P=0.9896
	Time	2748	27	101.8	F (27, 922) = 66.65	P<0.0001
	Group (Treatment/Diet)	28.53	3	9.51	F (3, 922) = 6.228	P=0.0003
	Residual	1408	922	1.527		

	Female BW AUC Ordinary One-way ANOVA					
Fig 5.2B	ANOVA table	SS	DF	MS	F (DFn, DFd)	P value
	Treatment (between columns)	8789	3	2930	F (3, 33) = 0.4303	P=0.7326
	Residual (within columns)	224652	33	6808		
	Total	233441	36			

	Female BG Ordinary Two-way ANOVA					
Fig 5.2C	ANOVA table	SS (Type III)	DF	MS	F (DFn, DFd)	P value
	Interaction	60.58	39	1.553	F (39, 455) = 0.896	P=0.6522
	Time	83.5	13	6.423	F (13, 455) = 3.705	P<0.0001
	Group (Treatment/Diet)	82.17	3	27.39	F (3, 455) = 15.8	P<0.0001
	Residual	788.8	455	1.734		

	Female BG AUC Ordinary One-way ANOVA					
Fig 5.2D	ANOVA table	SS	DF	MS	F (DFn, DFd)	P value
	Treatment (between columns)	44971	3	14990	F (3, 33) = 9.146	P=0.0002
	Residual (within columns)	54089	33	1639		
	Total	99060	36			

	Male BW Ordinary Two-way ANOVA					
Fig 5.2E	ANOVA table	SS (Type III)	DF	MS	F (DFn, DFd)	P value
	Interaction	307.5	78	3.942	F (78, 806) = 1.088	P=0.2890
	Time	7123	26	274	F (26, 806) = 75.64	P<0.0001
	Group (Treatment/Diet)	605.1	3	201.7	F (3, 806) = 55.69	P<0.0001
	Residual	2919	806	3.622		

	Male BW AUC Ordinary One-way ANOVA					
Fig 5.2F	ANOVA table	SS	DF	MS	F (DFn, DFd)	P value
	Treatment (between columns)	229710	3	76570	F (3, 30) = 3.154	P=0.0392
	Residual (within columns)	728313	30	24277		
	Total	958022	33			

	Male BG Ordinary Two-way ANOVA					
Fig 5.2G	ANOVA table	SS (Type III)	DF	MS	F (DFn, DFd)	P value
	Interaction	82.53	39	2.116	F (39, 430) = 1.391	P=0.0639
	Time	163.4	13	12.57	F (13, 430) = 8.259	P<0.0001
	Group (Treatment/Diet)	39.94	3	13.31	F (3, 430) = 8.749	P<0.0001
	Residual	654.3	430	1.522		

	Male BG AUC Ordinary One-way ANOVA					
Fig 5.2H	ANOVA table	SS	DF	MS	F (DFn, DFd)	P value
	Treatment (between columns)	33756	3	11252	F (3, 31) = 7.011	P=0.0010
	Residual (within columns)	49749	31	1605		
	Total	83505	34			

Supplemental Table 5: Detailed ANOVA values for Figure 5.3

	Female GTT (Week 4) Repeated Measures Two-way ANOVA					
Fig 5.3A	ANOVA table	SS	DF	MS	F (DFn, DFd)	P value
	Interaction	150.9	12	12.58	F (12, 108) = 2.122	P=0.0210
	Time	3295	4	823.7	F (4, 108) = 139	P<0.0001
	Group (Treatment/Diet)	395.6	3	131.9	F (3, 27) = 4.554	P=0.0105
	Subjects (matching)	781.9	27	28.96	F (27, 108) = 4.886	P<0.0001
	Residual	640.1	108	5.927		

	Female GSIS (Week 4) AUC Ordinary One-way ANOVA					
Fig 5.3C	ANOVA table	SS	DF	MS	F (DFn, DFd)	P value
	Treatment (between columns)	449.3	3	149.8	F (3, 24) = 1.825	P=0.1695
	Residual (within columns)	1970	24	82.07		
	Total	2419	27			

	Male GTT (Week 4) Repeated Measures Two-way ANOVA					
Fig 5.3D	ANOVA table	SS	DF	MS	F (DFn, DFd)	P value
	Interaction	164.1	12	13.67	F (12, 104) = 1.532	P=0.1243
	Time	5604	4	1401	F (4, 104) = 157	P<0.0001
	Group (Treatment/Diet)	525.6	3	175.2	F (3, 26) = 4.058	P=0.0172
	Subjects (matching)	1122	26	43.17	F (26, 104) = 4.838	P<0.0001
	Residual	928	104	8.923		

	Male GSIS (Week 4) AUC Ordinary One-way ANOVA					
Fig 5.3F	ANOVA table	SS	DF	MS	F (DFn, DFd)	P value
	Treatment (between columns)	1882	3	627.4	F (3, 19) = 3.678	P=0.0304
	Residual (within columns)	3241	19	170.6		
	Total	5123	22			

	Female GTT (Week 8) Repeated Measures Two-way ANOVA					
Fig 5.3G	ANOVA table	SS	DF	MS	F (DFn, DFd)	P value
	Interaction	199.4	12	16.61	F (12, 108) = 2.698	P=0.0032
	Time	3052	4	763.1	F (4, 108) = 123.9	P<0.0001
	Group (Treatment/Diet)	589.5	3	196.5	F (3, 27) = 6.01	P=0.0028
	Subjects (matching)	882.7	27	32.69	F (27, 108) = 5.309	P<0.0001
	Residual	665.1	108	6.158		

	Female GSIS (Week 8) AUC Ordinary One-way ANOVA					
Fig 5.3I	ANOVA table	SS	DF	MS	F (DFn, DFd)	P value
	Treatment (between columns)	1182	3	393.9	F (3, 25) = 11.71	P<0.0001
	Residual (within columns)	840.8	25	33.63		
	Total	2023	28			

	Male GTT (Week 8) Repeated Measures Two-way ANOVA					
Fig 5.3J	ANOVA table	SS	DF	MS	F (DFn, DFd)	P value
	Interaction	211.5	12	17.62	F (12, 108) = 2.359	P=0.0098
	Time	7280	4	1820	F (4, 108) = 243.6	P<0.0001
	Group (Treatment/Diet)	510	3	170	F (3, 27) = 4.358	P=0.0126
	Subjects (matching)	1053	27	39.01	F (27, 108) = 5.221	P<0.0001
	Residual	806.9	108	7.472		

	Male GSIS 2 AUC Ordinary One-way ANOVA					
Fig 5.3L	ANOVA table	SS	DF	MS	F (DFn, DFd)	P value
	Treatment (between columns)	3152	3	1051	F (3, 17) = 4.705	P=0.0144
	Residual (within columns)	3797	17	223.4		
	Total	6950	20			

Supplemental Table 6: Detailed ANOVA values for Figure 5.4

	Female % Beta-Cell Area Ordinary One-way ANOVA					
Fig 5.4A	ANOVA table	SS	DF	MS	F (DFn, DFd)	P value
	Treatment (between columns)	126.8	3	42.26	F (3, 12) = 0.5427	P=0.6622
	Residual (within columns)	934.5	12	77.87		
	Total	1061	15			

	Female % Alpha-Cell Area Ordinary One-way ANOVA					
Fig 5.4B	ANOVA table	SS	DF	MS	F (DFn, DFd)	P value
	Treatment (between columns)	126.8	3	42.26	F (3, 12) = 0.5427	P=0.6622
	Residual (within columns)	934.5	12	77.87		
	Total	1061	15			

	Female % Delta-Cell Area Ordinary One-way ANOVA					
Fig 5.4C	ANOVA table	SS	DF	MS	F (DFn, DFd)	P value
	Treatment (between columns)	94.69	3	31.56	F (3, 12) = 0.673	P=0.5849
	Residual (within columns)	562.8	12	46.9		
	Total	657.5	15			

	Female Total Islet Area Ordinary One-way ANOVA					
Fig 5.4D	ANOVA table	SS	DF	MS	F (DFn, DFd)	P value
	Treatment (between columns)	2026704	3	675568	F (3, 12) = 0.1756	P=0.9108
	Residual (within columns)	46161362	12	3846780		
	Total	48188066	15			

	Female Beta-Alpha Ratio Ordinary One-way ANOVA					
Fig 5.4E	ANOVA table	SS	DF	MS	F (DFn, DFd)	P value
	Treatment (between columns)	3.775	3	1.258	F (3, 12) = 0.3088	P=0.8187
	Residual (within columns)	48.9	12	4.075		
	Total	52.68	15			

	Female Beta-Delta Ratio Ordinary One-way ANOVA					
Fig 5.4F	ANOVA table	SS	DF	MS	F (DFn, DFd)	P value
	Treatment (between columns)	12.67	3	4.224	F (3, 12) = 1.086	P=0.3921
	Residual (within columns)	46.66	12	3.888		
	Total	59.33	15			

	Male % Beta-Cell Area Ordinary One-way ANOVA					
Fig 5.4G	ANOVA table	SS	DF	MS	F (DFn, DFd)	P value
	Treatment (between columns)	63.07	3	21.02	F (3, 13) = 0.9242	P=0.4566
	Residual (within columns)	295.7	13	22.75		
	Total	358.8	16			

	Male % Alpha-Cell Area Ordinary One-way ANOVA					
Fig 5.4H	ANOVA table	SS	DF	MS	F (DFn, DFd)	P value
	Treatment (between columns)	63.07	3	21.02	F (3, 13) = 0.9242	P=0.4566
	Residual (within columns)	295.7	13	22.75		
	Total	358.8	16			

	Male % Delta-Cell Area Ordinary One-way ANOVA					
Fig 5.4I	ANOVA table	SS	DF	MS	F (DFn, DFd)	P value
	Treatment (between columns)	303.5	3	101.2	F (3, 13) = 1.819	P=0.1934
	Residual (within columns)	723.1	13	55.62		
	Total	1027	16			

	Male Total Islet Area Ordinary One-way ANOVA					
Fig 5.4J	ANOVA table	SS	DF	MS	F (DFn, DFd)	P value
	Treatment (between columns)	20022736	3	6674245	F (3, 12) = 4.111	P=0.0320
	Residual (within columns)	19482849	12	1623571		
	Total	39505585	15			

	Male Beta-Alpha Ratio Ordinary One-way ANOVA					
Fig 5.4K	ANOVA table	SS	DF	MS	F (DFn, DFd)	P value
	Treatment (between columns)	20.69	3	6.896	F (3, 13) = 0.4074	P=0.7503
	Residual (within columns)	220.1	13	16.93		
	Total	240.8	16			

	Male Beta-Delta Ratio Ordinary One-way ANOVA					
Fig 5.4L	ANOVA table	SS	DF	MS	F (DFn, DFd)	P value
	Treatment (between columns)	117.1	3	39.05	F (3, 13) = 2.439	P=0.1110
	Residual (within columns)	208.1	13	16.01		
	Total	325.3	16			

Supplemental Table 7: Detailed ANOVA values for Figure 5.6

	Female ITT (Week 5) Raw Repeated Measures Two-way ANOVA					
	ANOVA table	SS	DF	MS	F (DFn, DFd)	P value
Fig 5.6A	Interaction	8.247	12	0.6873	F (12, 96) = 0.9873	P=0.4667
	Time	15.64	4	3.911	F (4, 96) = 5.619	P=0.0004
	Group (Treatment/Diet)	34.56	3	11.52	F (3, 24) = 5.556	P=0.0048
	Subjects (matching)	49.75	24	2.073	F (24, 96) = 2.978	P<0.0001
	Residual	66.83	96	0.6961		

	Female ITT 1 Normalized Repeated Measures Two-way ANOVA					
	ANOVA table	SS	DF	MS	F (DFn, DFd)	P value
Fig 5.6B	Interaction	0.08635	12	0.007196	F (12, 96) = 0.8246	P=0.6248
	Time	0.1544	4	0.0386	F (4, 96) = 4.423	P=0.0025
	Group (Treatment/Diet)	0.1688	3	0.05625	F (3, 24) = 1.227	P=0.3216
	Subjects (matching)	1.1	24	0.04585	F (24, 96) = 5.255	P<0.0001
	Residual	0.8377	96	0.008726		

	Female ITT (Week 5) Raw AUC Ordinary One-way ANOVA					
	ANOVA table	SS	DF	MS	F (DFn, DFd)	P value
Fig 5.6C	Treatment (between columns)	49512	3	16504	F (3, 24) = 4.187	P=0.0162
	Residual (within columns)	94608	24	3942		
	Total	144121	27			

	Male ITT (Week 5) Raw Repeated Measures Two-way ANOVA					
	ANOVA table	SS	DF	MS	F (DFn, DFd)	P value
Fig 5.6D	Interaction	7.606	12	0.6338	F (12, 104) = 0.5359	P=0.8868
	Time	20.76	4	5.19	F (4, 104) = 4.388	P=0.0026
	Group (Treatment/Diet)	18.46	3	6.155	F (3, 26) = 1.274	P=0.3039
	Subjects (matching)	125.6	26	4.83	F (26, 104) = 4.084	P<0.0001
	Residual	123	104	1.183		

	Male ITT (Week 5) Normalized Repeated Measures Two-way ANOVA					
	ANOVA table	SS	DF	MS	F (DFn, DFd)	P value
Fig 5.6E	Interaction	0.05817	12	0.004847	F (12, 104) = 0.4608	P=0.9330
	Time	0.173	4	0.04325	F (4, 104) = 4.111	P=0.0039
	Group (Treatment/Diet)	0.05671	3	0.0189	F (3, 26) = 0.5337	P=0.6633
	Subjects (matching)	0.9209	26	0.03542	F (26, 104) = 3.367	P<0.0001
	Residual	1.094	104	0.01052		

	Male ITT (Week 5) Raw AUC Ordinary One-way ANOVA					
Fig 5.6F	ANOVA table	SS	DF	MS	F (DFn, DFd)	P value
	Treatment (between columns)	26946	3	8982	F (3, 26) = 0.9021	P=0.4535
	Residual (within columns)	258886	26	9957		
	Total	285831	29			

	Female ITT (Week 9) Raw Repeated Measures Two-way ANOVA					
Fig 5.6G	ANOVA table	SS	DF	MS	F (DFn, DFd)	P value
	Interaction	26.2	12	2.184	F (12, 104) = 3.336	P=0.0004
	Time	35.54	4	8.886	F (4, 104) = 13.58	P<0.0001
	Group (Treatment/Diet)	41.05	3	13.68	F (3, 26) = 1.662	P=0.1995
	Subjects (matching)	214	26	8.231	F (26, 104) = 12.58	P<0.0001
	Residual	68.07	104	0.6545		

	Female ITT (Week 9) Normalized Repeated Measures Two-way ANOVA					
Fig 5.6H	ANOVA table	SS	DF	MS	F (DFn, DFd)	P value
	Interaction	0.3411	12	0.02842	F (12, 104) = 3.133	P=0.0008
	Time	0.4484	4	0.1121	F (4, 104) = 12.36	P<0.0001
	Group (Treatment/Diet)	0.2439	3	0.08129	F (3, 26) = 1.825	P=0.1674
	Subjects (matching)	1.158	26	0.04455	F (26, 104) = 4.912	P<0.0001
	Residual	0.9433	104	0.009071		

	Female ITT (Week 9) Raw AUC Ordinary One-way ANOVA					
Fig 5.6I	ANOVA table	SS	DF	MS	F (DFn, DFd)	P value
	Treatment (between columns)	74304	3	24768	F (3, 26) = 1.659	P=0.2001
	Residual (within columns)	388063	26	14926		
	Total	462367	29			

	Male ITT (Week 9) Raw Repeated Measures Two-way ANOVA					
Fig 5.6J	ANOVA table	SS	DF	MS	F (DFn, DFd)	P value
	Interaction	20.2	12	1.684	F (12, 96) = 2.172	P=0.0190
	Time	48.86	4	12.21	F (4, 96) = 15.76	P<0.0001
	Group (Treatment/Diet)	23.42	3	7.808	F (3, 24) = 1.8	P=0.1742
	Subjects (matching)	104.1	24	4.338	F (24, 96) = 5.596	P<0.0001
	Residual	74.43	96	0.7753		

	Male ITT (Week 9) Normalized Repeated Measures Two-way ANOVA					
Fig 5.6K	ANOVA table	SS	DF	MS	F (DFn, DFd)	P value
	Interaction	0.1491	12	0.01243	F (12, 96) = 1.92	P=0.0411
	Time	0.3468	4	0.08669	F (4, 96) = 13.39	P<0.0001
	Group (Treatment/Diet)	0.3585	3	0.1195	F (3, 24) = 2.879	P=0.0570
	Subjects (matching)	0.9963	24	0.04151	F (24, 96) = 6.413	P<0.0001
	Residual	0.6214	96	0.006473		

	Male ITT (Week 9) Raw AUC Ordinary One-way ANOVA					
	ANOVA table	SS	DF	MS	F (DFn, DFd)	P value
Fig 5.6L	Treatment (between columns)	29080	3	9693	F (3, 24) = 1.152	P=0.3485
	Residual (within columns)	201949	24	8415		
	Total	231029	27			

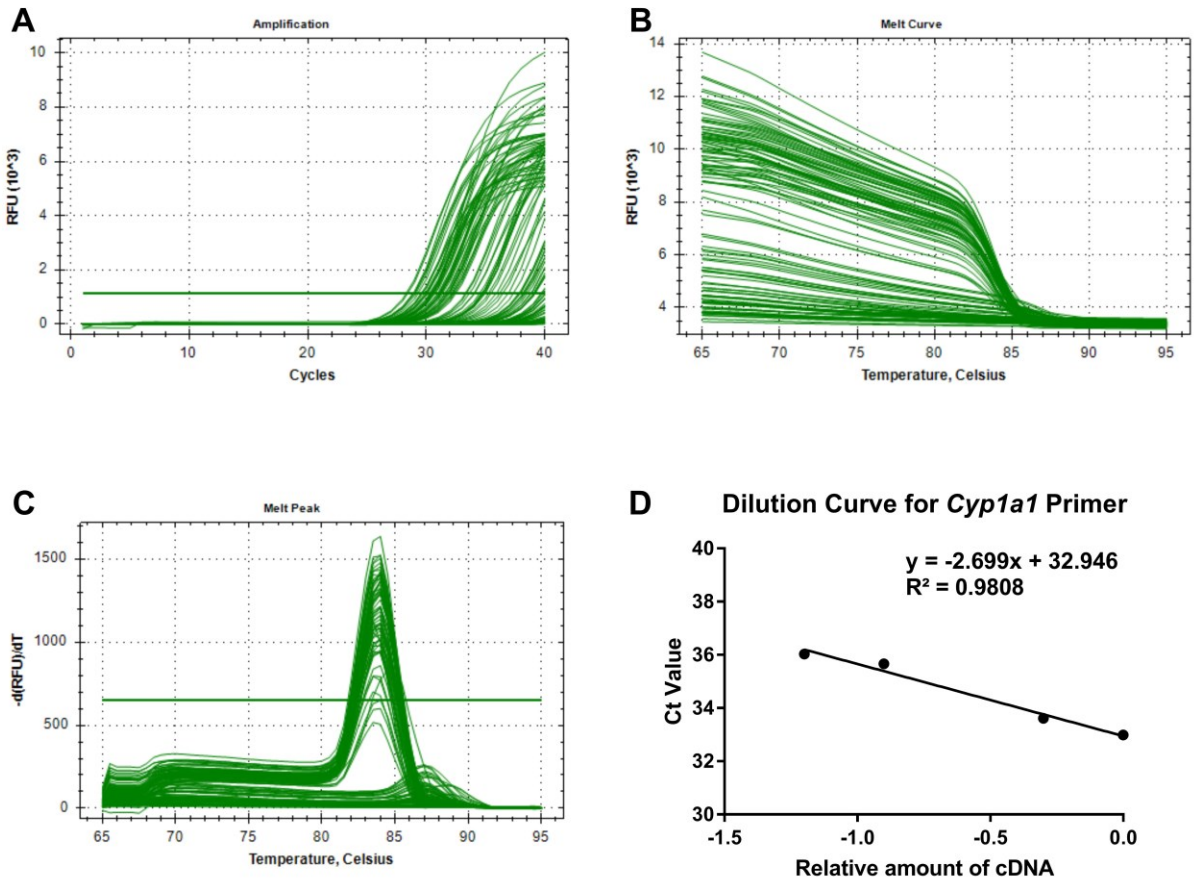

Supplemental Figure 1: Validation of *Cyp1a1* primer. **A)** Amplification curve. **B)** Melt curve. **C)** Melt peak. **D)** Dilution curve.